DEPARTMENT OF THE NAVY
NAVAL SHIP RESEARCH AND DEVELOPMENT CENTER
Washington, D.C. 20034

A METHOD FOR PREDICTING THE STATIC AERODYNAMIC CHARACTERISTICS OF TYPICAL MISSILE CONFIGURATIONS FOR ANGLES OF ATTACK TO 180 DEGREES

Bernard F. Saffell, Jr.
Millard L. Howard
and
Eugene N. Brooks, Jr.

Approved for public release; distribution unlimited
AVIATION AND SURFACE EFFECTS DEPARTMENT
Research and Development Report

March 1971

Report 3645
Aero Report 1168

SUMMARY

A method for predicting the static, longitudinal aerodynamic characteristics of typical missile configurations at zero roll angle (i.e., in a plus configuration) has been developed and programmed for use on the IBM 7090 digital computer. It can be applied throughout the subsonic, transonic, and supersonic speed regimes to slender bodies of revolution or to nose-cylinder body combinations with low aspect-ratio lifting surfaces. The aerodynamic characteristics can be computed for missile configurations operating at angles of attack up to 180 degrees. The effect of control surface deflections for all modes of aerodynamic control are taken into account by this method. The method is based on well-known linear, nonlinear crossflow and slender body theories with empirical modifications to provide the high angle of attack capability. Comparisons of the theory with experimental data are presented to demonstrate the accuracy of the method.

TABLE OF CONTENTS

LIST OF FIGURES

LIST OF TABLES

NOMENCLATURE

AR	exposed aspect ratio
b	semispan of an aerodynamic surface including the body radius, feet
C_D	total drag coefficient
C_{D_b}	base drag coefficient
C_{D_c}	crossflow drag coefficient
C_{D_f}	friction drag coefficient
C_{D_i}	induced drag coefficient
C_{D_o}	total zero-lift drag coefficient
C_{D_P}	pressure drag coefficient
C_{D_V}	wave drag coefficient
C_f	incompressible skin-friction coefficient
C_{f_c}	compressible skin-friction coefficient
$C_{D_{FP}}$	drag of a flat plate normal to the flow
C_L	total lift coefficient
C_{L_α}	lift curve slope, per radian
C_m	total longitudinal pitching moment coefficient
C_r	root-chord of an aerodynamic surface, feet
C_t	tip-chord of an aerodynamic surface, feet
d	diameter of the body at any station, feet
d_B	base diameter of the body, feet
d_N	diameter of the nose at the nose-body juncture, feet
f	spanwise location of the vortex which emanates from the forward surface, feet
h_A	height of the trailing vortex above the body centerline at the aft surface center of pressure, feet
i	downwash interference constant

NOMENCLATURE

(continued)

$(k_2 - k_1)$	apparent mass factor
K	linear lift interference factor due to angle of attack
K'	linear lift interference factor due to control surface deflection
l_B	total length of the body, feet
l_N	length of the nose, feet
l_{REF}	arbitrary reference length, usually the maximum body diameter, feet
l_T	distance from the tip of the nose to the intersection of the tail leading edge with the body, feet
l_W	distance from the tip of the nose to the intersection of the wing leading edge with the body, feet
M	free-stream Mach number
m	cotangent of the leading edge sweep angle
r	radius of the body at any station, feet
Re	Reynolds number
S_B	base area of the body, $(\text{feet})^2$
S_F	exposed planform area of one pair of forward lifting surfaces, $(\text{feet})^2$
S_N	body cross-sectional area at the nose, body juncture, $(\text{feet})^2$
S_P	planform area of the body, $(\text{feet})^2$
S_s	surface area of the body, $(\text{feet})^2$
S_T	exposed planform area of one pair of tail surfaces, $(\text{feet})^2$
S_T'	planform area of one pair of tail surfaces as obtained by extending the leading and trailing edges to the centerline of the body, $(\text{feet})^2$. See Figure 2.

NOMENCLATURE

(continued)

S_W	exposed planform area of one pair of wings, $(\text{feet})^2$
S_W'	planform area of one pair of wings as obtained by extending the leading and trailing edges to the centerline of the body, $(\text{feet})^2$. See Figure 2.
V_B	volume of the body, $(\text{feet})^3$
X_{CG}	distance from the nose to the missile center of gravity, $(\text{feet})^2$
$\overline{X}$	distance to the surface center of pressure as measured from the intersection of the leading edge of the aerodynamic surface with the body, feet
X_{CP}	distance from the nose to the center of pressure location, feet
X_h	distance from the intersection of the panel leading edge and the body to the hinge line, feet
X_p	distance from the nose to the centroid of the body planform area, feet
α	missile angle of attack, degrees
β	compressibility factor, $\sqrt{M^2-1}$
δ	control surface deflection, degrees (See Figure 1 for sign conventions)
ΔC_D	component of the induced drag coefficient
ΔC_{D_o}	increment of wave drag for the transonic speed regime
η	ratio of the drag coefficient of a circular cylinder of finite length to that of infinite length
Θ_N	conical nose semi-vortex angle, degrees
λ	lifting surface taper ratio, C_t/C_r
Λ	leading edge sweep angle, degrees
$\Lambda_{c/4}$	sweep angle of the quarter chord line, degrees

NOMENCLATURE

(continued)

SUBSCRIPTS

A	aft lifting surface, alone
B	body alone
BT	body in the presence of the tail
BT - α	body in the presence of the tail due to angle of attack
BT - δ	body in the presence of the tail due to control surface deflection
BW	body in the presence of the wing
BW - α	body in the presence of the wing due to angle of attack
F	forward surface alone
FB	forward surface in the presence of the body
N	nose
T	tail alone
T - α	tail alone due to angle of attack
T - δ	tail alone due to control surface deflection
TB	tail in the presence of the body
TB - α	tail in the presence of the body due to angle of attack
TB - δ	tail in the presence of the body due to control surface deflection
TV	tail, nonlinear component
W	wing alone
WB	wing in the presence of the body
WB - α	wing in the presence of the body due to angle of attack
WV	wing, nonlinear component

The control surface is defined as the tail regardless of the mode of control; the fixed surface is defined as the wing (see Figure 1).

INTRODUCTION

Increasing maneuverability requirements of missiles indicated a need for predicting the aerodynamic characteristics, including lift, drag, and pitching moment, of missile configurations to angles of attack of 90 degrees and higher. A study showed that existing methods for computing these aerodynamic characteristics are based on a number of different theories all of which are applicable only to small angles of attack. To fulfill the high angle of attack requirements, a method for determining the aerodynamic characteristics of low aspect-ratio configurations at zero roll angles operating at angles of attack up to 180 degrees has been developed. The method is applicable throughout the subsonic, transonic, and supersonic speed regimes up to $\beta \cdot AR \tilde{=} 10.0$, and accounts for control surface deflections.

The method is composed of well-known linear, nonlinear crossflow, and slender body theories which have been modified to provide the required high angle of attack capability. These theories can be applied to slender bodies of revolution or nose-cylinder bodies with canard, wing, or tail controls (Figure 1).

This report describes the methods developed and the computer program which has been written for use on the IBM 7090 digital computer. The description of the method is divided into three parts: lift, drag, and pitching moment. For the sake of clarity, the description of the method is kept to a minimum, without lengthy justification and description of the techniques employed. The reader is referred to the references for detailed descriptions of the various theories. The description of the computer program consists of a brief discussion of the main program and subroutines and complete instructions required for use of the program. Comparisons of theoretical results with experimental data are presented for angles of attack up to 90 degrees over the entire speed range to demonstrate the accuracy of the theories. Some data for a missile configuration at 180 degrees angle of attack is available and is compared with the theoretical results.

LIFT CHARACTERISTICS

The total lift on the missile is the sum of the body lift, the lift due to the aerodynamic surfaces, and the interference lift between the forward and aft surfaces. The lift on the body and aerodynamic surfaces is composed of two components: linear lift including the effects of the body-lifting surface interaction and nonlinear crossflow lift. In general, the crossflow lift component is caused by flow separation which occurs at angle of attack, while the interference component is the lift-loss on the aft lifting surface due to downwash from the forward surface (Reference 1).

Allen, References 2 and 3, developed a method for predicting the total lift on bodies of revolution at angles of attack. This method includes the linear or potential flow component and two nonlinear components: the viscous crossflow force and the viscous axial force. Because the contribution of the axial force component to the body lift is small, it is usually neglected. Allen's expression for the body lift is

$$C_{L_B} = (k_2 - k_1)\left(\frac{S_B}{S_{REF}}\right) \sin 2\alpha \cos\frac{\alpha}{2} + \eta C_{dc}\left(\frac{S_P}{S_{REF}}\right)\sin^2\alpha \cos\alpha - C_{D_{o_B}} \cos^2\alpha \sin\alpha \qquad (1)$$

where the first term is the linear contribution and the second term is the nonlinear contribution. The apparent mass factor, $k_2 - k_1$, and the drag ratio, η, can be obtained from Figure 3, while the crossflow drag coefficient, C_{dc}, is obtained from Figure 4. Comparisons of theory with experimental data for numerous bodies of revolution over a wide range of Mach numbers and angles of attack are presented in Reference 3. It should be noted that although this expression for the lift is independent of the nose shape, good agreement with experiment is indicated in Reference 4 for a body with an unusual shape.

The linear lift characteristics of low aspect-ratio lifting surfaces whose cross-sections are thin and symmetrical are generally a function of speed, planform area, and aspect-ratio. When the diameter of the missile body is of the same order of magnitude as the span of the

lifting surfaces, the effects of body-wing and body-tail interactions are significant. Hence, the linear lift of the aerodynamic surfaces is composed of two components: the lift on the surface in the presence of the body, and the added lift on the body due to the presence of a surface. Most low aspect-ratio missile configurations exhibit a nonlinear dependence of lift on angle of attack, especially at the higher angles. One primary cause of this is the crossflow lift component which is due to lateral flow separation and the formation of free vortices on the upper surface. This nonlinear dependence is analyzed in References 1 and 5 and summarized by Eaton in Reference 6.

The expression for the total wing lift based on an arbitrary reference area is

$$C_{L_W} = C_{L_{WB-\alpha}} + C_{L_{BW-\alpha}} + C_{L_{WV}} \tag{2}$$

In order to provide high angle of attack capability, it is necessary to modify both the linear and nonlinear theories. The lift on the wing in the presence of the body, as presented in Reference 2, is a linear function of angle of attack and can be expressed as

$$C_{L_{WB-\alpha}} = K_{WB}\, C_{L_{\alpha_W}} \left(\frac{S_W}{S_{REF}}\right) \alpha \tag{3}$$

Since the lift force does not vary linearly with angle of attack at high angles, Equation (3) is modified such that the linear lift becomes a function of sin α as shown below

$$C_{L_{WB-\alpha}} = K_{WB}\, C_{L_{\alpha_W}} \left(\frac{S_W}{S_{REF}}\right) \sin \alpha \tag{4}$$

This component of the linear lift is modified further to satisfy the end condition of zero lift at 90 degrees angle of attack. The resulting expression for the linear wing lift in the pressure of a body is

$$C_{L_{WB-\alpha}} = K_{WB}\, C_{L_{\alpha_W}} \left(\frac{S_W}{S_{REF}}\right) \sin\alpha \cos\alpha \qquad (5)$$

It is important to note that for small angles of attack the modified theory should be very close to the method of Reference 1 since sin $\alpha \cong \alpha$ and cos $\alpha \cong 1$. Similarly, the additional lift on the body due to the presence of the wing is

$$C_{L_{BW-\alpha}} = K_{BW}\, C_{L_{\alpha_W}} \left(\frac{S_W}{S_{REF}}\right) \sin\alpha \cos\alpha \qquad (6)$$

The parameters, K_{WB} and K_{BW}, are determined from Figure 5. $C_{L_{\alpha_W}}$ is obtained from Figure 6 by multiplying $\frac{C_{L_{\alpha_W}}}{AR}$ by the aspect-ratio if AR < 1.0. When the aspect ratio is greater than one, the lift-curve slope is obtained from the following equation

$$C_{L_{\alpha_W}} = \left(\frac{1}{AR^{(AR-1)/AR}}\right)\left(\frac{C_{L_{\alpha_W}}}{AR}\right) AR \qquad (7)$$

where $\left(\frac{C_{L_{\alpha_W}}}{AR}\right)$ is obtained from Figure 6. The first term of Equation (7) is an empirical modification of the lift curve slope for a lifting surface with aspect-ratio greater than 1.

The nonlinear wing lift from Reference 6 is

$$C_{L_{WV}} = C_{dc} \sin^2\alpha \left(\frac{S_W}{S_{REF}}\right) \tag{8}$$

This expression is modified to satisfy the aforementioned end condition with the result being

$$C_{L_{WV}} = C_{dc} \sin^2\alpha \left(\frac{S_W}{S_{REF}}\right) \cos\alpha \tag{9}$$

where C_{dc} is obtained from Figure 7. It should be noted that the cross-flow drag coefficient is not appreciably affected by Mach number, (References 6 and 7); hence, C_{dc} is presented independent of Mach number.

The total tail lift is computed basically the same as the wing lift except for the lift due to deflection of the control surfaces. The tail lift is expressed as

$$C_{L_T} = C_{L_{TB-\alpha}} + C_{L_{BT-\alpha}} + C_{L_{TB-\delta}} + C_{L_{BT-\delta}} + C_{L_{TV}} \tag{10}$$

where $C_{L_{TB-\alpha}}$ and $C_{L_{BT-\alpha}}$ are obtained by applying Equations (5) and (6) to the tail surface. The other three components are:

$$C_{L_{TB-\delta}} = K_{TB}' C_{L_{\alpha_T}} \sin\delta \left(\frac{S_T}{S_{REF}}\right) \cos(\alpha + \delta) \tag{11}$$

$$C_{L_{BT-\delta}} = K_{BT}' C_{L_{\alpha_T}} \sin\delta \left(\frac{S_T}{S_{REF}}\right) \cos(\alpha + \delta) \tag{12}$$

$$C_{L_{TV}} = C_{dc} \sin^2(\alpha + \delta) \left(\frac{S_T}{S_{REF}}\right) \cos(\alpha + \delta) \tag{13}$$

The parameters, K_{BT}' and K_{TB}', are obtained from Figure 5, while C_{dc} and $C_{L_{\alpha_T}}$ are obtained as specified for the wing. Notice that the nonlinear lift is based on the local angle of attack, $(\alpha + \delta)$, of the control surface.

The lift-loss on the aft surface due to downwash from the forward surface is obtained from the method presented in Reference 1 and discussed in Reference 7. Since the method for computing this component of the total lift on the missile is both complex and lengthy, only the equations necessary to compute the lift-loss are presented. The reader is referred to Reference 1 for a detailed discussion of the assumptions and technique used in deriving the method. It is noted that the nomenclature used to describe the lifting surfaces is changed from wing and tail to forward and aft surfaces. This is necessary because the control surface, whether it be wing, canard, or tail type of control, is designated the tail and because the aft surface, regardless of the mode of control, is the one which is affected by downwash.

This method is valid for the entire speed range. The lift-loss due to downwash is

$$C_{L_i} = \frac{C_{L_{\alpha_F}} C_{L_{\alpha_A}} \left[K_{FB} \sin \alpha + K_{FB}' \sin \delta_F\right] i(b - r)_A S_F}{2\pi(AR)_A (f_F - r_F) S_{REF}} \tag{14}$$

This equation is obtained from line-vortex theory assuming only one trailing vortex per forward panel exists (see Figure 8). The lateral location, f_F', and the vertical location, h_A, of the vortex are required for use in Equation (14) and to compute the interference factor, i. The lateral location of the vortex on the forward surface expressed as a fraction of the exposed semispan of this surface is

$$\left(\frac{f - r}{b - r}\right)_F = \frac{\frac{\pi}{4} - \frac{\pi}{4}(r/b)_F^2 - (r/b)_F + \frac{\left[1 + (r/b)_F^2\right]^2}{2\left[1 - (r/b)_F^2\right]} \sin^{-1}\left[\frac{1 - (r/b)_F^2}{1 + (r/b)_F^2}\right]}{2\left[1 - (r/b)_F\right]} \tag{15}$$

For convenience, the right hand side of this equation is defined as A'. Isolating f_F results in the following expression

$$f_F = A'(b - r)_F + r_F \tag{16}$$

where f_F is the spanwise location of the vortex at the forward surface. Since the lateral location of the vortex with respect to the body axis is unchanged, the subscript may be dropped and Equation (16) may be written as

$$f = A'(b - r)_F + r_F \tag{17}$$

The vertical location of the vortex, h_A, is measured normal to the body axis at the center of pressure of the aft surface. The expression for h_A is

$$h_A = -(C_r - X_h)_F \sin \delta_F + \left[l_A + (\bar{X}_{CP})_A - l_F - (C_r)_F\right] \sin \alpha \tag{18}$$

Note that the vertical location of the vortex is a function of both angle of attack and the deflection angle of the forward surface. The interference factor, i, is given by

$$i = \left(\frac{2}{1+\lambda}\right)\left[L\left(\lambda, \frac{r}{b}, \frac{f}{b}, \frac{h}{b}\right) - L\left(\lambda, \frac{r}{b}, \frac{-f}{b}, \frac{h}{b}\right) - L\left(\lambda, \frac{r}{b}, \frac{f_i}{b}, \frac{h_i}{b}\right) + L\left(\lambda, \frac{r}{b}, \frac{-f_i}{b}, \frac{h_i}{b}\right)\right] \tag{19}$$

where

$$L\left(\lambda, \frac{r}{b}, \frac{f}{b}, \frac{h}{b}\right) = \left\{\frac{(b - r\lambda) - f(1 - \lambda)}{2(b - r)} \ln\left(\frac{h^2+(f - b)^2}{h^2+(f-r)^2}\right) - \left(\frac{1 - \lambda}{b - r}\right)\left[(b - r) + h\tan^{-1}\left(\frac{f - r}{h}\right) - h\tan^{-1}\left(\frac{f - r}{h}\right)\right]\right\} \tag{20}$$

and

$$f_i = \frac{fr^2}{f^2 + h^2} \quad , \quad h_i = \frac{hr^2}{f^2 + h^2} \tag{21}$$

Hence, once the location of the vortex is determined and the position of the image vortices, f_i and h_i, is determined from Equation (21), the interference factor can be computed from Equations (19) and (20). The lift-loss due to interference can then be calculated.

The total lift based on an arbitrary reference area is obtained by adding the components

$$C_L = C_{L_B} + C_{L_W} + C_{L_T} + C_{L_i} \tag{22}$$

where C_{L_i}, a lift-loss, will be a negative quantity. The other three components include both linear and nonlinear contributions.

DRAG CHARACTERISTICS

The total aerodynamic drag acting on a missile is the sum of the zero-lift drag, the induced drag due to angle of attack and/or control surface deflection, and the base pressure drag. It is well-known that the selection of the proper technique for computing the zero-lift drag is determined by the operating speed of the missile. Hence, the methods employed to compute the zero-lift drag of a missile are described for three speed regimes. These speed regimes and their associated limits are defined as follows:

1. Subsonic -- $M < 0.8$
2. Transonic -- $0.8 \leq M \leq 1.2$
3. Supersonic -- $M > 1.2$

The description of C_{D_o} calculations for these speed regimes is followed by a description of the method used to compute the induced drag due to angle of attack and/or tail deflection. The last section presents the total drag.

1. Subsonic Region

The zero-lift drag for subsonic speeds can be expressed as

$$C_{D_o} = C_{D_{o_W}} + C_{D_{o_T}} + C_{D_{o_B}} \tag{23}$$

where each of the components is composed of skin-friction drag and pressure-drag. The pressure drag at subsonic speeds is usually small compared to the drag due to skin friction. Since the flow around high speed missiles of the type being considered here is primarily turbulent, the methods employed are developed assuming the existence of fully turbulent boundary layers.

The zero-lift drag of the body based on an arbitrary reference area is obtained from Section 4.2.3.1 of Reference 9 and can be expressed as

$$C_{D_{o_B}} = 1.02\, C_{f_B} \left[1 + \frac{1.5}{\left(l_B/d_B\right)^{3/2}} + \frac{7}{\left(l_B/d_B\right)^{3}} \right] \frac{S_s}{S_{REF}} \tag{24}$$

where C_f, the skin-friction coefficient, is determined using Figure 9.

The wing zero-lift drag as presented in Section 4.1.5.1 of Reference 9 is

$$C_{D_{o_W}} = 8.0\, C_{f_W} \left[1 + 2(t/c) + 100(t/c)^4 \right] \frac{S_W'}{S_{REF}} \tag{25}$$

The factor of 8.0 is included to account for the total wetted area of the surfaces and for the existence of four wings. The tail zero-lift drag, $C_{D_{o_T}}$, can be obtained by using the tail thickness-to-chord ratio and the total tail area, S_T', in Equation (25).

These three components, based on the same arbitrary reference area, are added as indicated by Equation (23) to give the total subsonic zero-lift drag.

2. Transonic Region

The body drag in the transonic speed regime is composed of compressible skin-friction drag, subsonic pressure drag, and transonic wave drag and is obtained using the techniques presented in Section 4.2.3.1 of Reference 9. The compressible skin-friction drag is obtained using the following equation:

$$C_{D_{f_B}} = 1.02\, C_{f_c} \frac{S_s}{S_{REF}} \tag{26}$$

where C_{f_c} is a function of both Reynolds number and Mach number and can be determined from Figures 9 and 10. The subsonic pressure drag as extracted from Equation (24) is

$$C_{D_{P_B}} = 1.02\, C_{f_B} \left[\frac{1.5}{(l_B/d_B)^{3/2}} + \frac{7}{(l_B/d_B)^3} \right] \frac{S_s}{S_{REF}} \tag{27}$$

The transonic pressure drag is computed using Equation (27) up to a Mach number of 1.0 and then it is decreased linearly from its value at 1.0 to zero at M=1.2.

The transonic wave drag of the body is obtained from Figure 11 which presents the wave drag as a function of the nose fineness ratio and Mach number. This figure was constructed from experimental data presented in Reference 10 and by using the curves of wave drag for bodies of revolution as shown in Reference 11 and reproduced here in Figure 12.

The total transonic body zero-lift drag is obtained form the following expression:

$$C_{D_{o_B}} = C_{D_{f_B}} + C_{D_{P_B}} + C_{D_{V_B}} \frac{S_N}{S_{REF}} \tag{28}$$

Experimental results show little increase in the viscous drag of the aerodynamic surfaces from the subsonic to the transonic regime and therefore, the skin-friction drag for the subsonic region is also used in the transonic regime. It may be expressed as follows:

$$C_{D_{o_W}} = 8\, C_{f_W} \left[1 + 2\left(\frac{t}{c}\right) \right] \tag{29}$$

To this wing transonic skin-friction drag is added a drag increment, $\Delta C_{D_{o_W}}$, which is the transonic wave drag of the wing surfaces. Figure 13 expresses this component as a function of thickness-to-chord ratio, $\frac{t}{c}$, aspect-ratio, and Mach number for rectangular surfaces. For surfaces having swept leading edges, $\Delta C_{D_{o_W}}$ is obtained as for rectangular surfaces and then adjusted to account for the sweep angle using the following equation:

$$\Delta C_{D_{o_W}} = \Delta C'_{D_{o_W}} \left[\cos \Lambda_{c/4} \right]^{2.5} \tag{30}$$

The Mach number used in Figure 13 to obtain $\Delta C'_{D_{o_W}}$ for swept lifting surfaces is

$$M' = M \left[\cos \Lambda_{c/4} \right]^{1/2} \tag{31}$$

This component of the drag due to the aerodynamic surfaces must be computed for both the wings and tails. The tail contribution is determined in the same manner as the wing contribution above using tail parameters.

The total transonic zero-lift drag is the sum of these components as shown below:

$$C_{D_o} = \left(C_{D_{o_W}} + \Delta C_{D_{o_W}}\right) \frac{S_W'}{S_{REF}} + \left(\Delta C_{D_{o_T}} + C_{D_{o_T}}\right) \frac{S_T'}{S_{REF}} + C_{D_{o_B}} \qquad (32)$$

3. Supersonic Region

A simple empirical method for computing the zero-lift drag for the supersonic speed regime has been developed by assuming a parabolic variation of C_{D_o} with Mach number between 1.2 and 3.0. The resulting equation which is used to compute the zero-lift drag of a missile for Mach numbers greater than 1.2 is

$$C_{D_o} = \left[\frac{C_{D_o}'' - C_{D_o}'}{\sqrt{3} - \sqrt{1.2}}\right] \sqrt{M} + \left[\frac{C_{D_o}'' - C_{D_o}'}{1 - \sqrt{3}/\sqrt{1.2}}\right] + C_{D_o}' \qquad (33)$$

where C_{D_o}' and C_{D_o}'' are the values of the total zero-lift drag at Mach numbers 1.2 and 3.0 respectively. It should be noted that although C_{D_o} for Mach numbers greater than 3.0 can be determined from Equation (33), existing hypersonic flow theories would probably provide a more accurate estimate of the zero lift drag.

In order to utilize Equation (33) for determining the variation of C_{D_o} with Mach number, C_{D_o}' and C_{D_o}'' must be specified. C_{D_o}' is determined by using the techniques described in the previous section for the transonic flow regime. Since the magnitude of the supersonic wave drag is heavily dependent on the nose shape of the missile, C_{D_o}'' is determined using one of two methods; the selection of the proper method depends on the missile forebody shape.

In the first method, which is for blunted ogives, pointed ogives, and blunted cones, the supersonic zero-lift drag is a function of Mach number and nose fineness ratio. Since C_{D_o}'' is the zero-lift drag at M=3.0, it remains to define its variation with nose fineness ratio. Hoerner, Reference 12, indicates the zero-lift drag for body-fin configurations with slender (high fineness ratio) nose shapes generally peaks at a Mach number of 1.0 to 1.2 and then decreases to approximately its subsonic value plus the transonic wave drag of the lifting surfaces at M=3.0. Similar configurations with blunted nose shapes of low fineness ratio reach a peak at about the same Mach number, but decrease very little as the Mach number is increased. Using these trends as an indication of the effect of fineness ratio on the variation of zero-lift drag with Mach number for the supersonic speed regime, C_{D_o}'' for the aforementioned nose shapes is specified as follows:

a) For $(l/d)_N \leq 0.5$, $\quad C_{D_o}'' = C_{D_o}'$

b) For $(l/d)_N \geq 8.0$, $\quad C_{D_o}'' = C_{D_o}\Big/_{M=0.8} + \left(\Delta C_{D_{o_W}} \frac{S_W'}{S_{REF}} + \Delta C_{D_{o_T}} \frac{S_T'}{S_{REF}}\right)$

where $C_{D_o}\Big/_{M=0.8}$ is determined utilizing subsonic flow theory and $\Delta C_{D_{o_W}}$ and $\Delta C_{D_{o_T}}$ are the transonic wing and tail wave drag. The variation of the forebody wave drag as a function of Mach number is presented in Figure 12 and was used to construct Figure 14 which is utilized with the following equation:

$$C_{D_o}'' = K_1 C_{D_o}' \tag{34}$$

to compute C_{D_o}'' for nose fineness ratios between 0.5 and 8.0.

In the second method, which is for pointed conical noses, C_{D_o}'' is determined from the following equation:

$$C_{D_o}'' = C_{D_o}\Big/_{M=0.8} + \left(\Delta C_{D_{o_W}} \frac{S_W'}{S_{REF}} + \Delta C_{D_{o_T}} \frac{S_T'}{S_{REF}}\right) + C_{D_{V_N}} \qquad (35)$$

where the first two terms are obtained in the same manner described above. The forebody wave drag, which for this type of nose is a function of Mach number and the cone semivertex angle, is obtained from Figure 15.

Once C_{D_o}'' is determined, Equation (30) can be used to compute the zero-lift drag at any Mach number between 1.2 and 3.0. The complete zero-lift drag curve of a missile can now be determined.

4. Induced Drag

The induced drag due to angle of attack and/or tail surface deflection is composed of four drag increments as shown below:

$$C_{D_i} = \Delta C_{D_{B-\alpha}} + \Delta C_{D_{W-\alpha}} + \Delta C_{D_{T-\alpha}} + \Delta C_{D_{T-\delta}} \qquad (36)$$

The drag increment for the body is obtained using a method presented in Reference 3, while the induced drag due to the wing and tail is obtained from the drag of an equivalent flat plate normal to the flow. The induced drag on a body of revolution at angle of attack can be expressed as follows:

$$\Delta C_{D_{B-\alpha}} = (k_2 - k_1)\left(\frac{S_b}{S_{REF}}\right)\sin^2\alpha + \eta C_{dc}\left(\frac{S_p}{S_{REF}}\right)\sin^3\alpha \qquad (37)$$

The wing induced drag based on an arbitrary reference area is obtained from

$$\Delta C_{D_{W-\alpha}} = C_{D_{FP}} \left(\frac{S_W \sin \alpha}{S_{REF}} \right) \tag{38}$$

where $C_{D_{FP}}$ is the drag of a flat plate normal to the flow field, and is determined from Figure 16. The drag curve shown in Figure 16 has been constructed using the three-dimensional subsonic drag coefficient for a flat plate normal to the flow (Reference 13) and the variation of the drag coefficient with Mach number for the two-dimensional flat plate (Reference 12). The equivalent flat plate area of the wing is taken as the projection of the wing area on the normal plane, $S_W \sin \alpha$. Similarly, the drag increment of the tail surface at angle of attack is

$$\Delta C_{D_{T-\alpha}} = C_{D_{FP}} \left(\frac{S_T \sin \alpha}{S_{REF}} \right) \tag{39}$$

The drag increment due to deflection of the tail surface cannot be obtained directly since the drag increment is not a linear function of local angle of attack. The total drag increment for the tail surface can be expressed as

$$\Delta C_{D_{T-\alpha}} + \Delta C_{D_{T-\delta}} = C_{D_{FP}} \left[\frac{S_T \sin(\alpha + \delta)}{S_{REF}} \right] \tag{40}$$

where $(\alpha + \delta)$ is the local tail angle of attack. It now becomes a simple matter to obtain the drag increment due to the deflection of the control surface by taking the difference between Equations (39) and (40). Thus

$$\Delta C_{D_{T-\delta}} = \left(\Delta C_{D_{T-\alpha}} + \Delta C_{D_{T-\delta}} \right) - \Delta C_{D_{T-\alpha}} \tag{41}$$

6. Total Drag

The total drag can be expressed as follows:

$$C_D = C_{D_o} + C_{D_i} \tag{42}$$

where C_{D_i} is determined using Equation (36) and C_{D_o} is obtained from Equation (23), (32), or (33) depending on the speed of the missile. Base pressure drag is not included in Equation (42).

PITCHING MOMENT CHARACTERISTICS

The total pitching moment acting on the missile is the sum of the moments due to the lift and drag forces acting on the body, wings, and tails. Most methods for computing the pitching moment (References 1, 6, and 9) consider only the moment due to lift. This is valid only for small angles of attack. If large angles of attack are to be considered, the moment must include the drag contribution. In general, the body longitudinal pitching moment is determined directly; while the other components are determined only after the centers of pressure of the wing and tail surfaces are specified.

The body-alone pitching moment about its center of gravity is obtained from the method of Allen, References 2 and 3. The expression is

$$C_{m_B} = (k_2 - k_1)\left(\frac{V_B - S_B\left(l_B - X_{CG}\right)}{S_{REF}\, l_{REF}}\right)\sin 2\alpha \cos\frac{\alpha}{2} + \eta C_{dc}\left(\frac{S_P}{S_{REF}}\right)\left(\frac{X_{CG} - X_P}{l_{REF}}\right)\sin^2\alpha \qquad (43)$$

where $(k_2 - k_1)$, C_{dc}, and η are determined from Figures 3 and 4. This moment coefficient, C_{m_B}, is based on an arbitrary reference length and area.

As noted above, the center of pressure locations for the wing and tail surfaces must be specified before their pitching moments can be determined. It must be remembered that the linear lift of the aerodynamic surfaces is composed of two components: the lift on the surface in the presence of the missile body and the additional lift on the body due to the presence of a lifting surface. This means that in order to determine the linear pitching moment caused by the lifting surfaces, it is necessary to specify the center of pressure location for each of these linear components.

The center of pressure of the lift on the wing in the presence of the body as measured from the junction of the wing leading edge and the

body is obtained using Figure 17. The reference point is transferred to the nose by using the following equation

$$X_{WB} = \left(\frac{\overline{X}}{C_r}\right)_{WB} \left(C_r\right)_W + l_W \tag{44}$$

where $\left(\frac{\overline{X}}{C_r}\right)_{WB}$ is obtained from Figure 17a for subsonic speeds and from Figure 17b for supersonic speeds.

The center of pressure of the additional lift on the body in the presence of the wing is obtained using Figure 18 if the flow is subsonic, and either Figure 19 or 20 if the flow is supersonic. For the case of supersonic flow, Figure 19 is used if

$$\beta AR\ (1 + \lambda)\left(1 + \frac{1}{m\beta}\right) \leq 4.0$$

and Figure 20 is used if the above quantity is greater than 4.0. The center of pressure, $\overline{X}_{BW}$, as obtained from the aforementioned figures, is referred to the nose by using the following equation.

$$\left(X_{CP}\right)_{BW} = \left(\frac{\overline{X}}{C_r}\right)_{BW} \left(C_r\right)_W + l_W \tag{45}$$

The location of both centers of pressure for the tails, $\left(X_{CP}\right)_{TB}$ and $\left(X_{CP}\right)_{BT}$, can also be obtained from the above procedure.

The centers of pressure for a given lifting surface are combined to obtain a single average center of pressure location for each set of aerodynamic surfaces. For example, the average center of pressure of the wings is obtained by computing the total pitching moment due to the wings and dividing by the wing normal force. The pitching moment about the

nose of the body due to the wing is

$$C_{m_W} = \left[\left(C_{L_{WB}} + C_{L_{WV}} + C_{L_i}\right)\cos\alpha + \Delta C_{D_{W-\alpha}} \sin\alpha\right]\left[\left(X_{CP}\right)_{WB}/l_{REF}\right] + \left[C_{L_{BW}}\cos\alpha\right]\left[\left(X_{CP}\right)_{BW}/l_{REF}\right] \tag{46}$$

where all of the above terms have been previously defined. The average wing center of pressure as measured from the nose of the body can now be defined as

$$\left(X_{CP}\right)_W = \frac{C_{mW}\, l_{REF}}{\left(C_{L_W} + C_{L_i}\right)\cos\alpha + \Delta C_{D_{W-\alpha}} \sin\alpha} \tag{47}$$

Similarly, the tail pitching moment and center of pressure including the effect of surface deflection can be expressed as

$$C_{m_T} = \left[\left(C_{L_{TB-\alpha}} + C_{L_{TV}} + C_{L_i}\right)\cos\alpha + C_{L_{TB-\delta}} + \left(\Delta C_{D_{T-\alpha}} + \Delta C_{D_{T-\delta}}\right)\sin\alpha\right]\left[\left(X_{CP}\right)_{TB}/l_{REF}\right] + \left[C_{L_{BT-\alpha}}\cos\alpha + C_{L_{BT-\delta}}\right]\left[\left(X_{CP}\right)_{BT}/l_{REF}\right] \tag{48}$$

$$\left(X_{CP}\right)_T = \frac{C_{mT}\, l_{REF}}{\left(C_{L_{T-\alpha}} + C_{L_i}\right)\cos\alpha + C_{L_{T-\delta}} + \left(\Delta C_{D_{T-\alpha}} + \Delta C_{D_{T-\delta}}\right)\sin\alpha} \tag{49}$$

where

$$C_{L_{T-\alpha}} = C_{L_{TB-\alpha}} + C_{L_{BT-\alpha}} + C_{L_{TV}}$$

and

$$C_{L_{T-\delta}} = C_{L_{TB-\delta}} + C_{L_{BT-\delta}}$$

The total longitudinal pitching moment of the missile about the missile's center of gravity may be expressed as

$$C_m = C_{m_B} + C_{m_W}\left[\frac{X_{CG} - \left(X_{CP}\right)_W}{\left(X_{CP}\right)_W}\right] + C_{m_T}\left[\frac{X_{CG} - \left(X_{CP}\right)_T}{\left(X_{CP}\right)_T}\right] \qquad (50)$$

COMPUTER PROGRAM DESCRIPTION

The method presented herein for obtaining the static aerodynamic characteristics of a missile has been programmed for use on the IBM 7090 computer and other compatible digital computers. The program, Table 1, is written in Fortran II and requires only the geometric characteristics of the missile and its flight conditions as inputs. The output consists of the static longitudinal aerodynamic characteristics in coefficient form, the center-of-pressure location for the body, wings, and tails, the lift-curve slope for each set of lifting surfaces, and the components of the lift and normal force coefficients. The force components referred to are the body, wing, and tail lift and normal force coefficients and the coefficient representing the lift-loss due to downwash. The aerodynamic characteristics are output in both the stability and body axis systems (Figure 21). Provision has been made for a third lifting surface to account for the possibility of using strakes in combination with two other sets of lifting surfaces (Figure 1).

The program itself consists of a main program and three subroutines--GEOSUB, CLASUB, and CATSUB. The first subroutine performs some initial geometric computations, determines the nose wave drag constant (Figure 14), and obtains the Reynolds number per foot based on the altitude input to the program. Subroutine CLASUB determines the lift-curve slope of the lifting surfaces from curve fits employed to represent the curves presented in Figure 6. The last subroutine, CATSUB, obtains the body-wing and body-tail interference factors, computes the center of pressure location as a function of the root chord of the lifting surfaces, and determines the crossflow drag coefficient for the lifting surfaces.

The program computes the static force and moment coefficients for typical missile configurations at specified angles of attack, control surface deflection angles and Mach numbers. The angle of attack range is -180° to $+180^\circ$, and any control surface deflection within this range may be used. The Mach number is limited to 3.0 only because the drag prediction methods are valid up to this particular Mach number. The program can be used for configurations at $M > 3.0$; however, the drag predictions above this limit should be used with caution. The computer

program can be used to obtain build-up information; that is, the aerodynamic characteristics of the missile body alone, the body-wing configuration, and the body-tail configuration. This information may be obtained by simply setting the appropriate parameters to zero.

The inputs to the computer program with their FORTRAN symbols are presented in Table 2. The format for preparing the input cards is presented in Table 3. It should be noted that if a configuration does not have a control surface, e.g. a body alone configuration, the number of control surface deflection angles should be set at one and the deflection angle, itself, would be 0.0 degrees. Cards 11 and 12 are used only when the number of angles of attack require their use. The output variables are defined in Table 4. There is no limit to the number of data decks which may be stacked together and run at the same time.

COMPARISON OF THEORY WITH EXPERIMENTAL DATA

Numerous comparisons of theory with experiment have been made in order to establish and verify the accuracy of the method. Figure 22 presents the configurations used for comparison. Configuration 1 is a strake-tail configuration. Figure 23 presents the comparison between the experimental data and the theoretical results obtained from the method described herein. The theoretical lift and drag are within 15 percent of the experimental data for M = 0.7. The deviation for M = 1.1 does increase to about 25 percent. However, it should be noted that the accuracy of the method to 30 degrees is good. The method also predicts the center of pressure location very satisfactorily.

Configuration 2 is a wing-controlled vehicle. Comparisons are presented in Figure 24 for Mach numbers of 1.12 and 2.16 and for wing deflection angles of 0 and -10 degrees. Although high angle of attack data is not available for this configuration, it appears that the comparatively high theoretical lift shown by Configuration 1 may be more pronounced for Configuration 2. This trend is seen by the decrease in the slope of the experimental lift data at 25 to 30 degrees angle of attack, Figure 24. The comparison with the wing deflected down 10 degrees appeared to be good.

Data for Configuration 3 is presented in Figure 25. Configuration 4 was tested by the Cornell Aeronautical Laboratory to 180 degrees angle of attack, Reference 14. Comparison of theory with experimental data is presented in Figure 26.

CONCLUSIONS

A method for predicting the static, longitudinal aerodynamic characteristics of low aspect-ratio missiles operating at angles of attack to 180 degrees has been developed. The method is valid for a wide speed range and considers control surface deflections. A computer program, written to facilitate use of the method, has been described. Results obtained using the method have been compared with wind tunnel data and acceptable agreement has been demonstrated.

REFERENCES

1. Pitts, William C., Jack N. Nielsen and George E. Kaattari. Lift and Center of Pressure of Wing-Body-Tail Combinations at Subsonic, Transonic and Supersonic Speeds. Wash., 1957. 70 p. incl. illus. (National Advisory Committee for Aeronautics. Rpt. 1307)

2. Allen, H. Julian. Estimation of the Forces and Moments Acting on Inclined Bodies of Revolution of High Fineness Ratio. Wash., D.C. Nov 1949. 27 p. incl. illus. (National Advisory Committee for Aeronautics. RM A9I26)

3. Allen, H. Julian and Edward W. Perkins. Characteristics of Flow Over Inclined Bodies of Revolution. Wash., D.C., Mar 1951. 47 p. incl. illus. (National Advisory Committee for Aeronautics. RM A50L07)

4. Jorgensen, Leland H. and Stuart L. Treon. Measured and Estimated Aerodynamic Characteristics for a Model of a Rocket Booster at Mach Numbers From 0.6 to 4.0 and at Angles of Attack From 0° to 180°. Wash., D.C., Sep 1961. 76 p. incl. illus. (National Aeronautics and Space Administration. Tech. Memo. X-580)

5. Flax, A. H. and H. P. Lawrence. The Aerodynamics of Low-Aspect-Ratio Wings and Wing-Body Combinations. Buffalo, Sep 1951. [66] l. incl. illus. (Cornell Aeronautical Lab., Inc. Rpt. CAL-37) (Also in Proceedings of Third Anglo-American Aeronautical Conference, Brighton, Eng., 3-14 Sep 1951. London, Royal Aeronautical Society, 1952)

6. Eaton, Peter T. A Method for Predicting the Static Aerodynamic Characteristics of Low-Aspect Ratio Configurations. Wash., D.C. Jun 1966. 90 p. incl. illus. (Naval Ship Research and Development Center. Rpt. 2216. Aero Rpt. 1112) (AD 647234)

7. Gersten, K. Calculation of Non-Linear Aerodynamic Stability Derivatives of Aeroplanes. Paris [1962] 20 p. incl. illus. (Advisory Group for Aerospace Research and Development. Rpt. 342) (Deutsche Forschungsanstalt für Luft - und Raumfahrt. Bericht 143)

8. Frantz, Gerald E. Lift Curve Slopes of Low Aspect Ratio Wings at Transonic Speeds. Columbus, Ohio, Jun 1963. 32 l. incl. illus. (North American Aviation, Inc. Applied Mechanics Tech. Note AM-TN-2-63)

9. Douglas Aircraft Co., Inc. USAF Stability and Control DATCOM. Rev. W-P AFB, Jul 1963. ^{2}v. (loose-leaf)

10. Stoney, William E., Jr. Collection of Zero-Lift Drag Data on Bodies of Revolution From Free-Flight Investigations. Wash., 1961. 188 p. incl. illus. (National Aeronautics & Space Administration. Tech. Rpt. R-100. Formerly NACA TN 4201)

11. Royal Aeronautical Society. Data Sheets: Aerodynamics. Vol. 4. London, Aug. 1964.

12. Hoerner, Sighard F. Fluid Dynamic Drag. [2d. ed.] Midland Park, N. J., 1965.

13. Dommasch, David O., Sydney S. Sherby and Thomas F. Connolly. Airplane Aerodynamics. 3rd ed. New York, Pitman [1961] 600 p.

14. Beil, W. J. and others. Major Developments for the Jet Vane Controlled Bomber Defense Missile. Buffalo, Mar 1955. 226 l. incl. illus. (Cornell Aeronautical Lab., Inc. Rpt. BE-753-S-24. Contract AF33(038)22346)

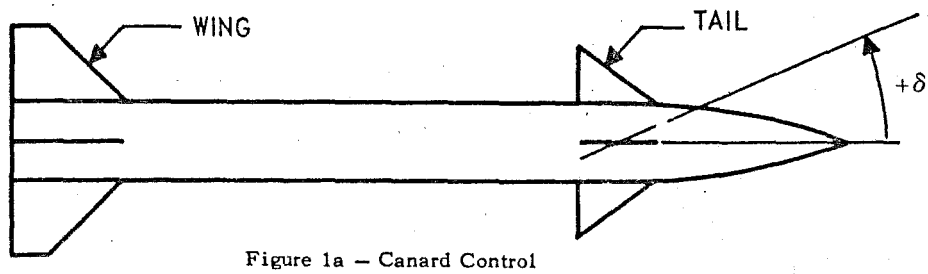

Figure 1a – Canard Control

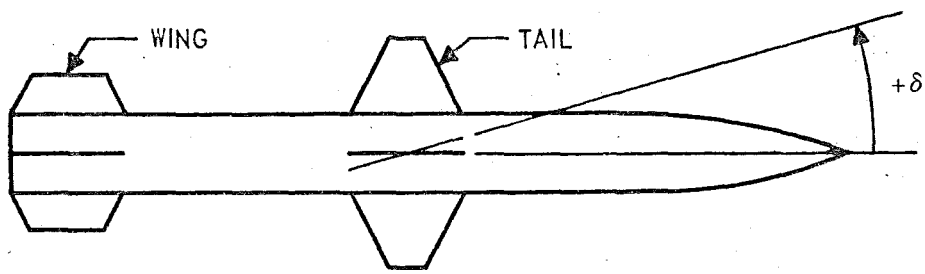

Figure 1b – Wing Control

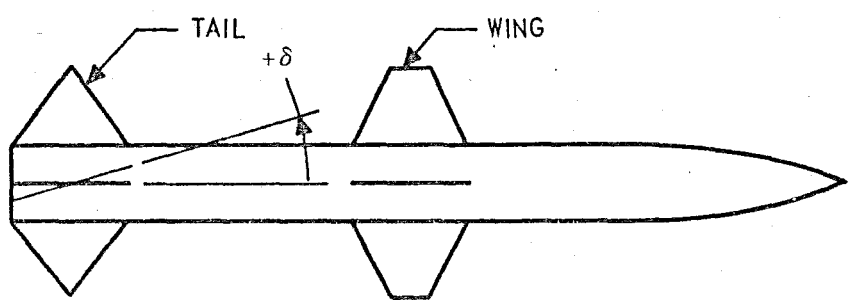

Figure 1c – Tail Control

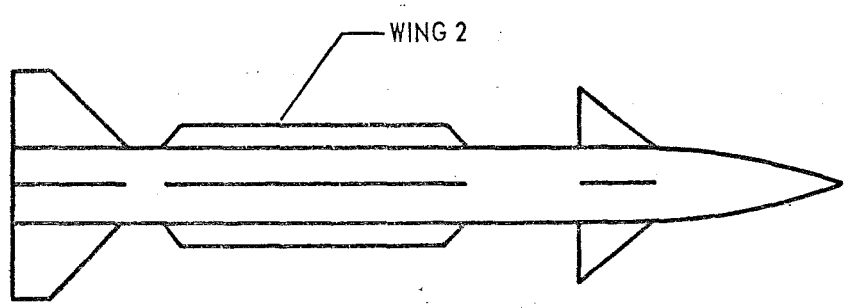

Figure 1d – Three Surfaces – Any Mode of Control

Figure 1 – Typical Missile Configurations

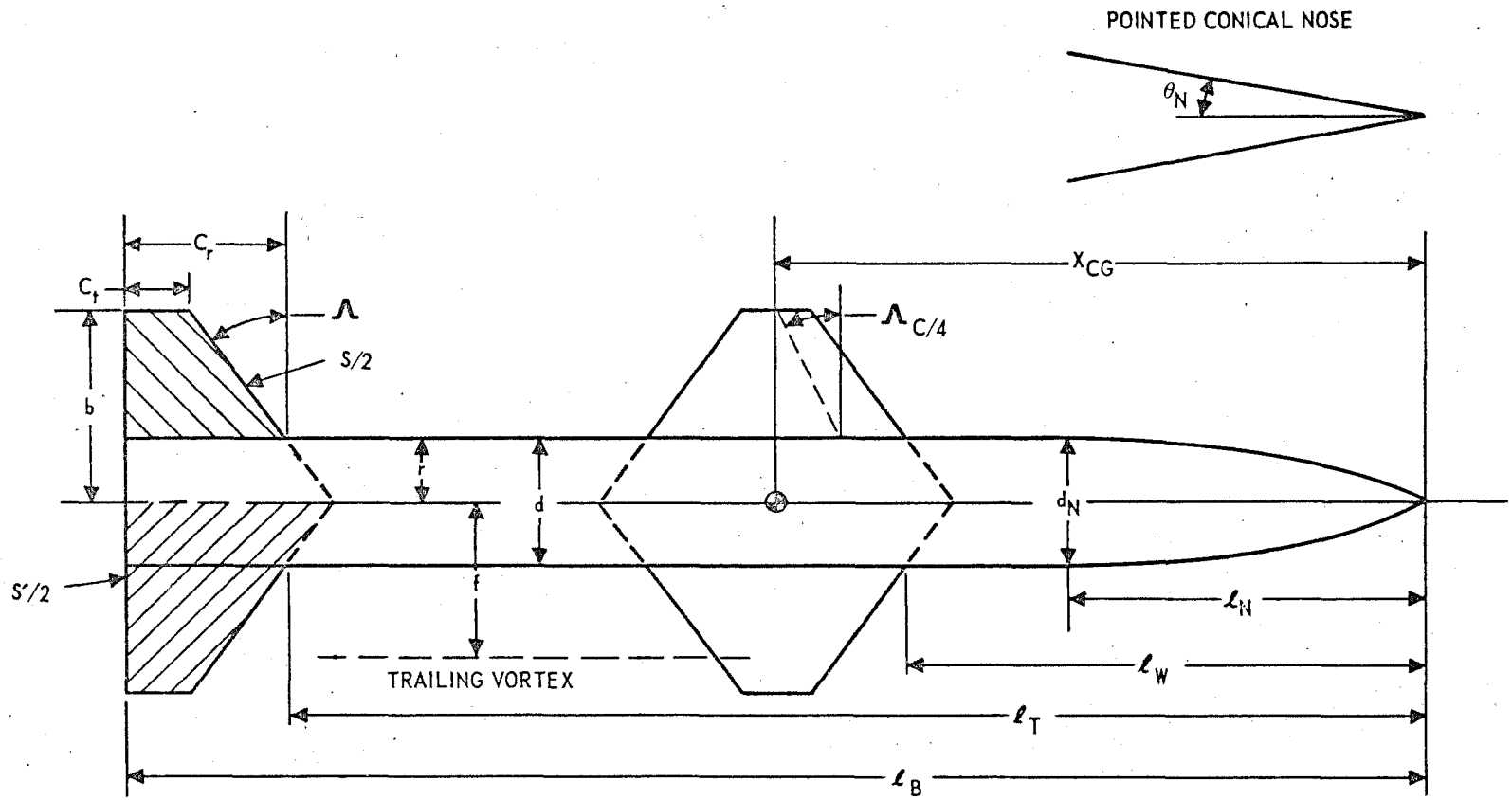

Figure 2 – General Geometric Characteristics

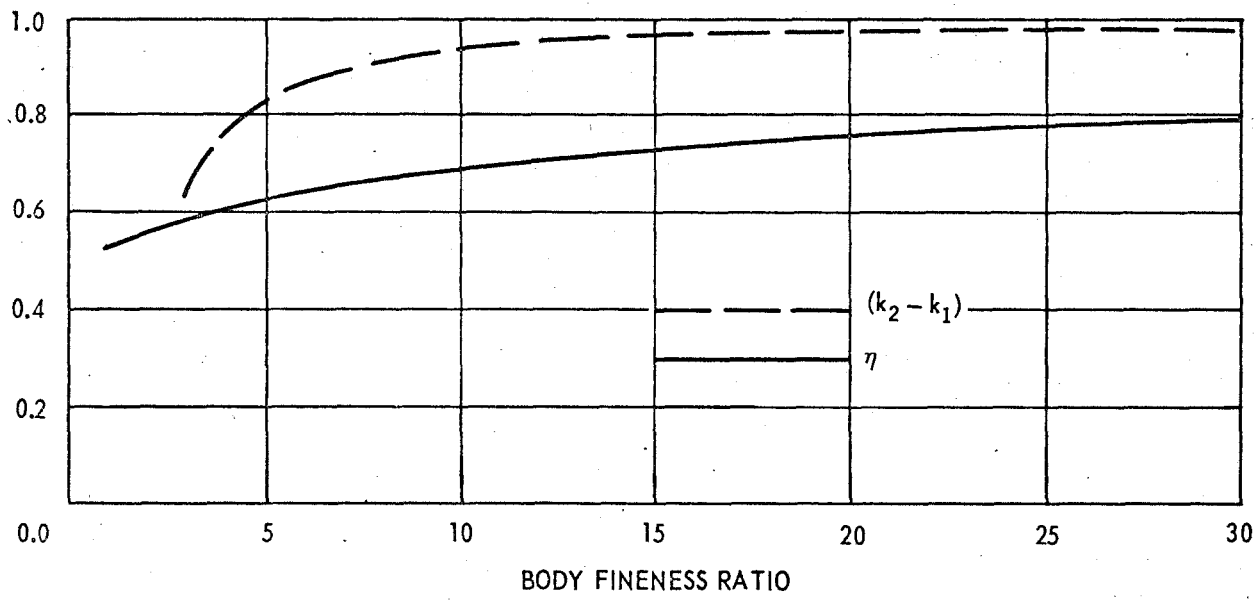

Figure 3 – Parameters Used to Compute Body Normal Force and Pitching Moment (from Reference 3)

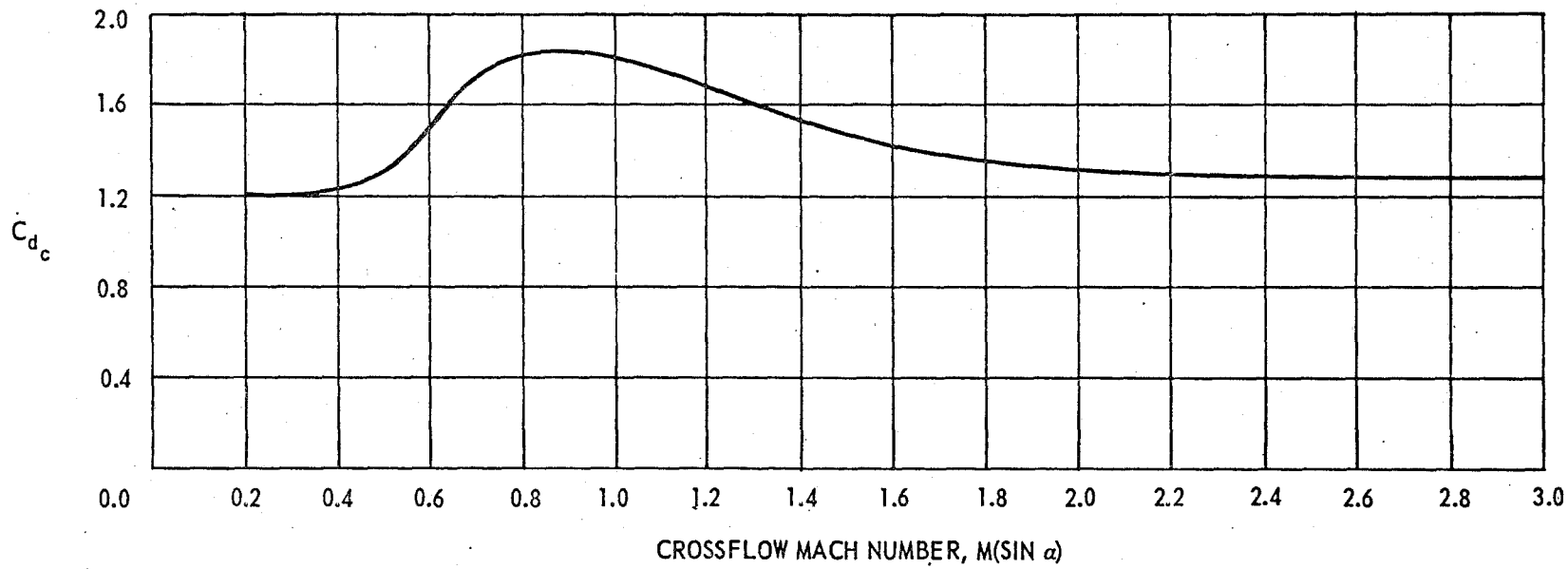

Figure 4 – Crossflow Drag Coefficient as a Function of Mach Number (from Reference 3)

Figure 5 – Linear Lift Interference Factors (from Reference 7)

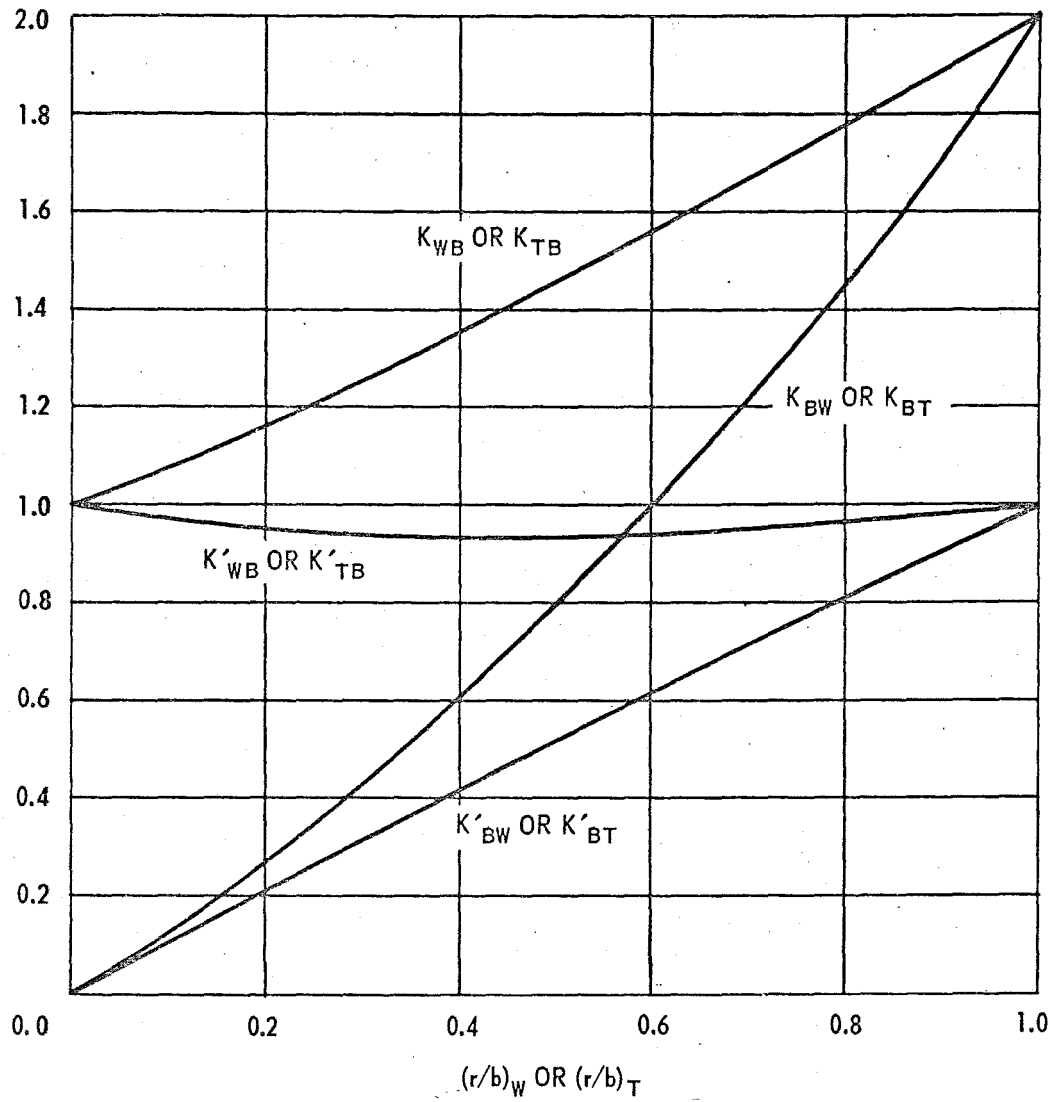

Figure 5a – $(\beta AR)(1+\lambda)(1/m\beta+1) \leq 4$

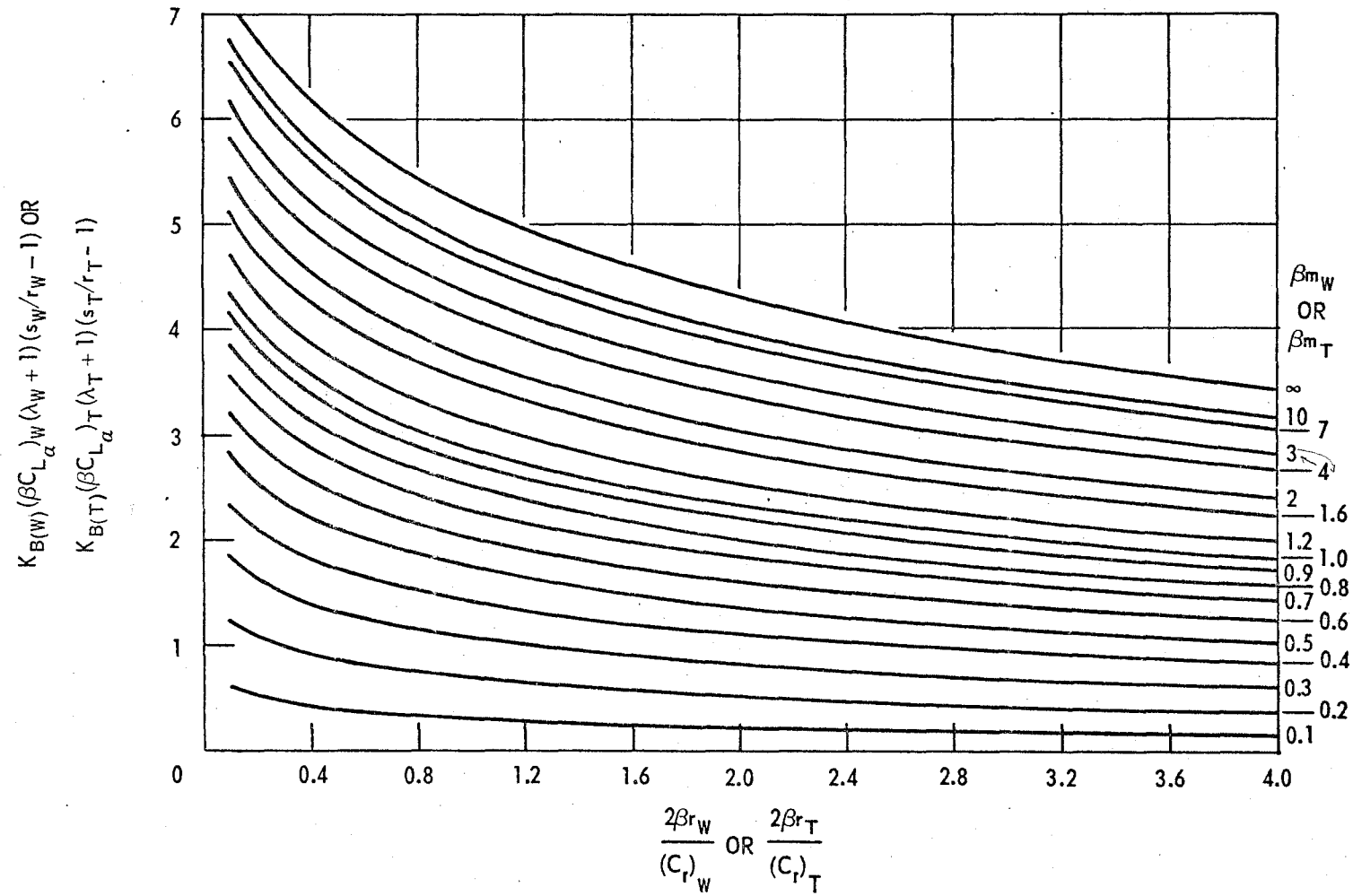

Figure 5b – $(\beta AR)(1 + \lambda)(1/m\beta + 1) > 4$; with Afterbody

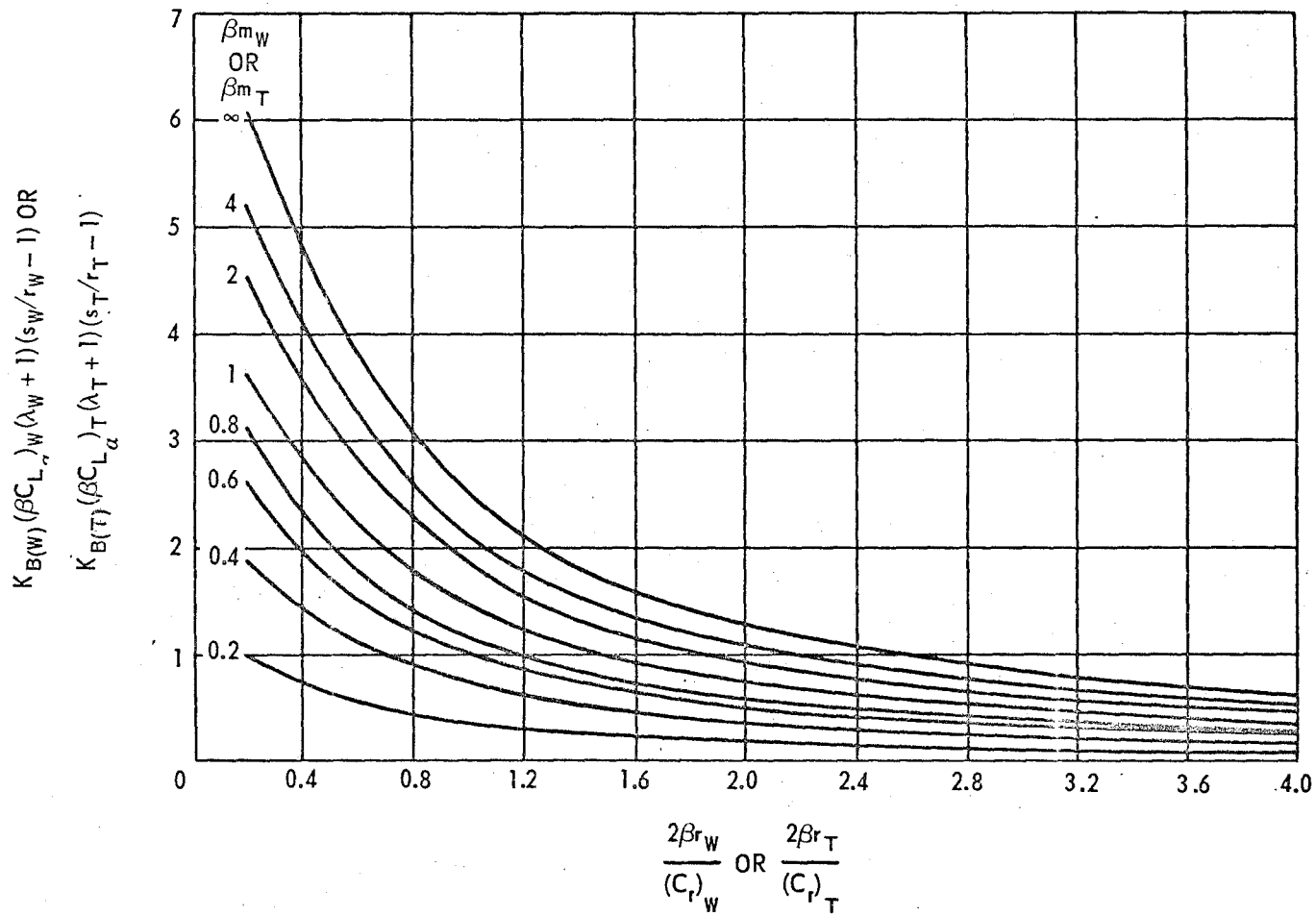

Figure 5c – $(\beta AR)(1 + \lambda)(1/m\beta + 1) > 4$; No Afterbody

Figure 6 – Lift Curve Slope for Wings and Tails (from Reference 8)

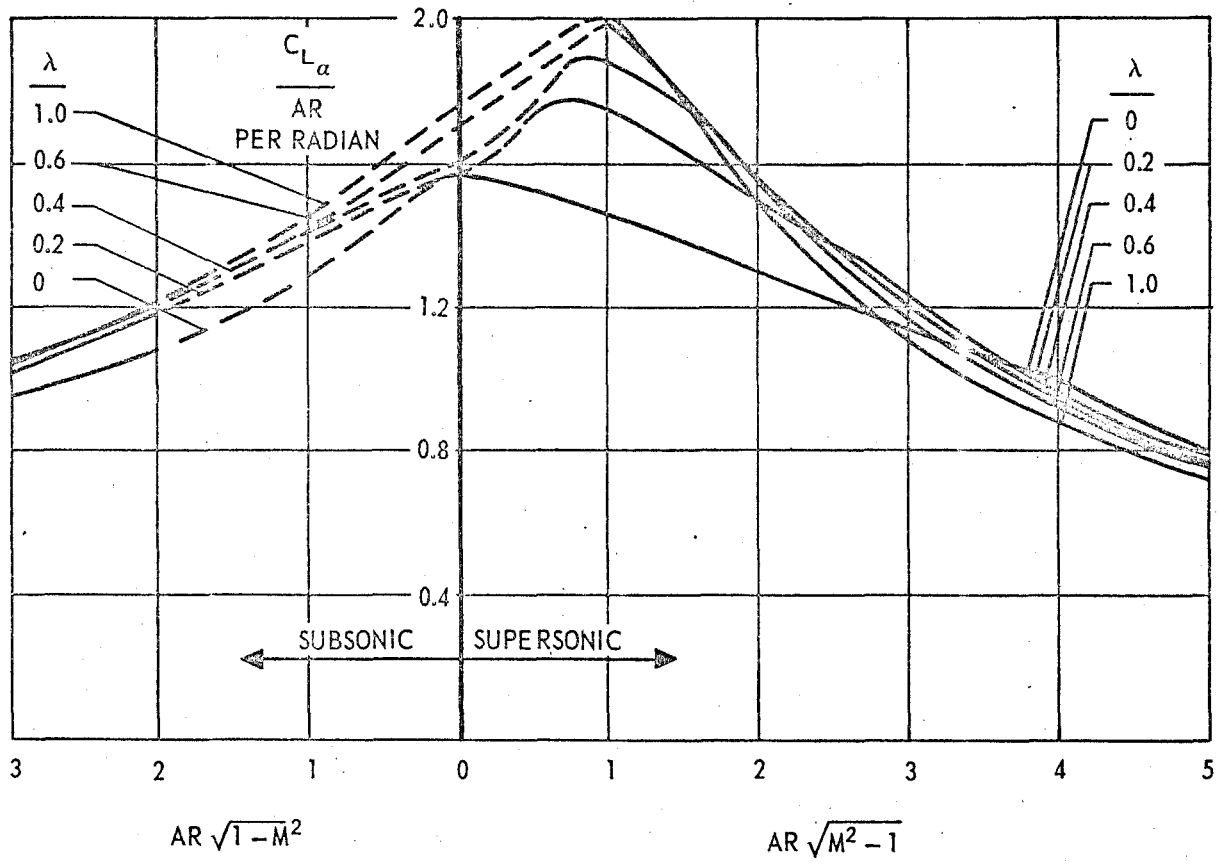

Figure 6a – Unswept Trailing Edge

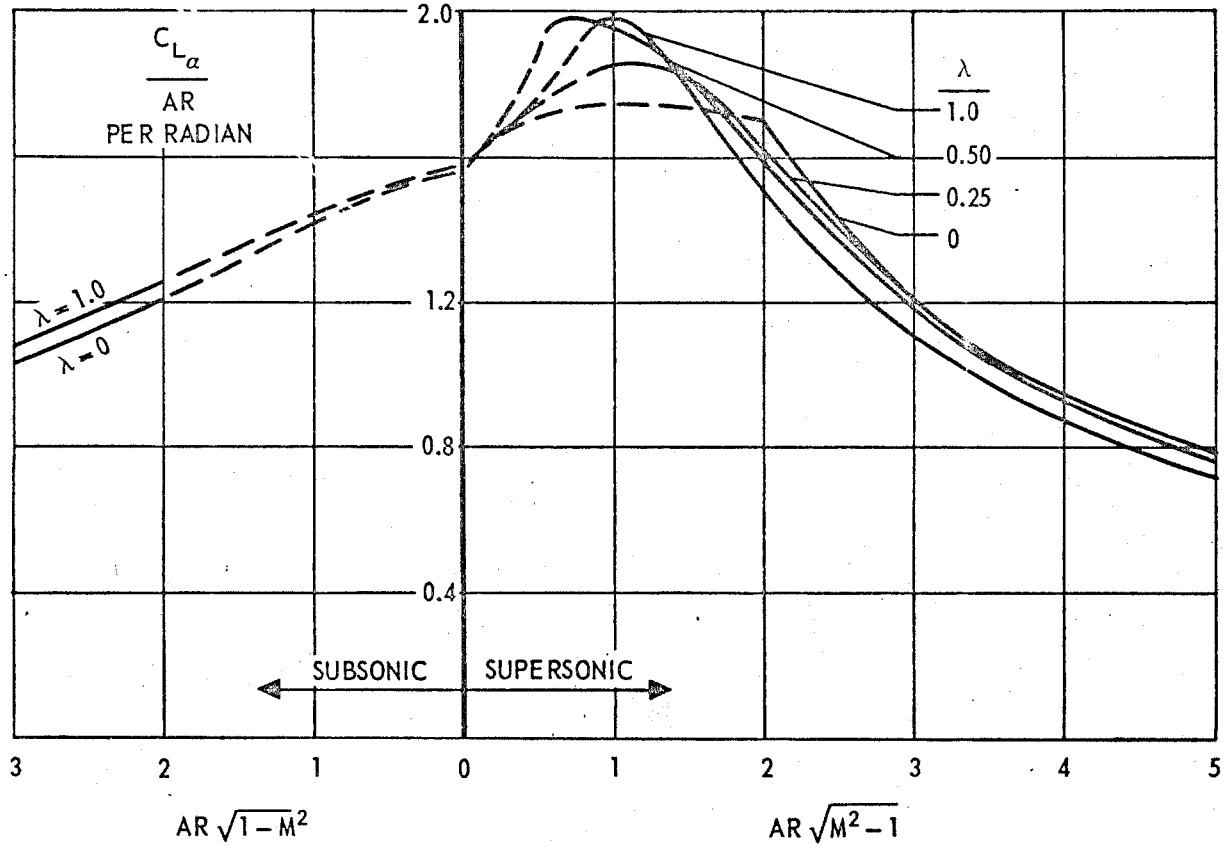

Figure 6b — Unswept Mid Chord

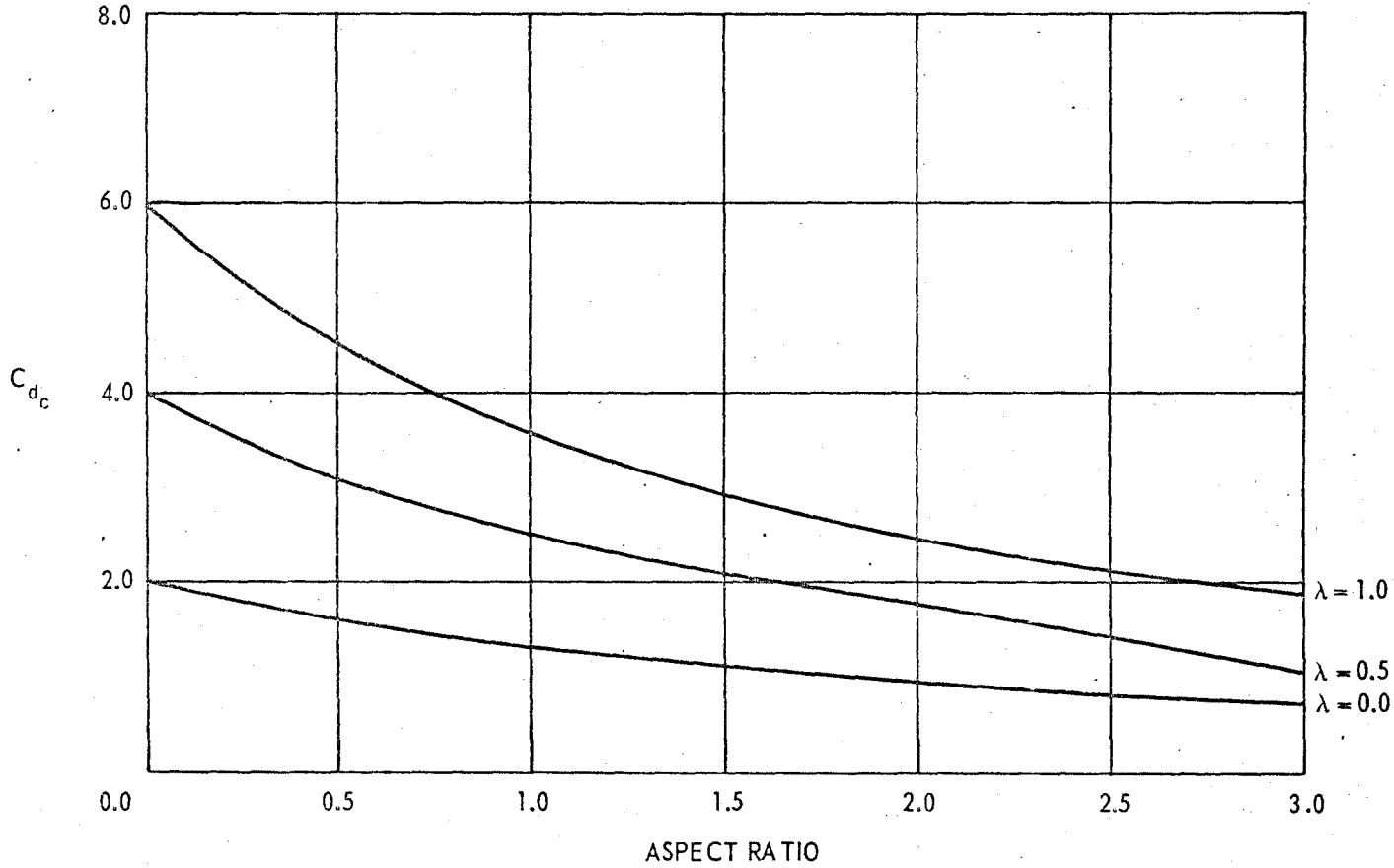

Figure 7 – Crossflow Drag Coefficient for Wings and Tails as a Function of Aspect Ratio and Taper Ratio

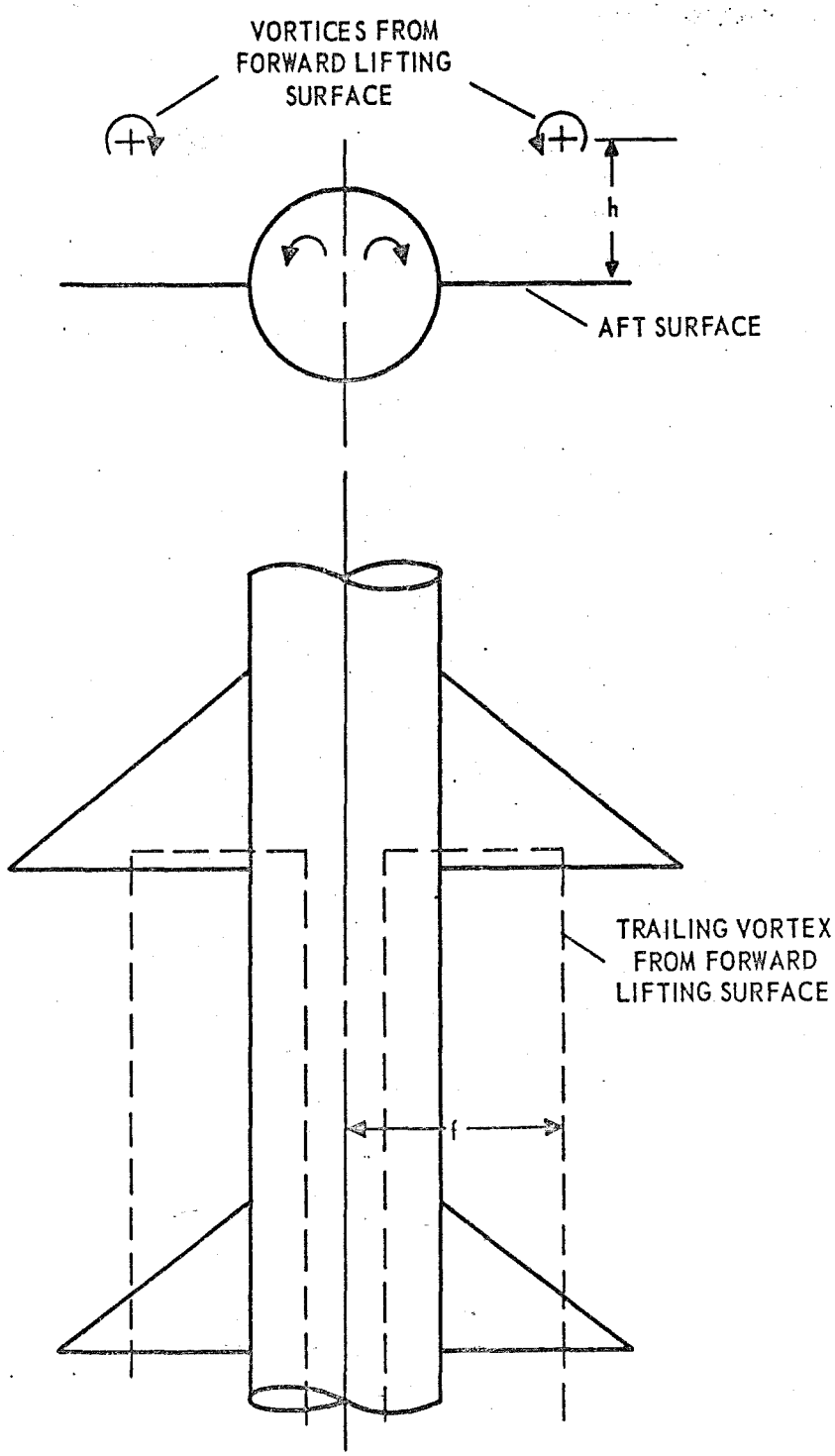

Figure 8 – Vortex Model Used to Determine the Lift Loss due to Downwash (from Reference 1)

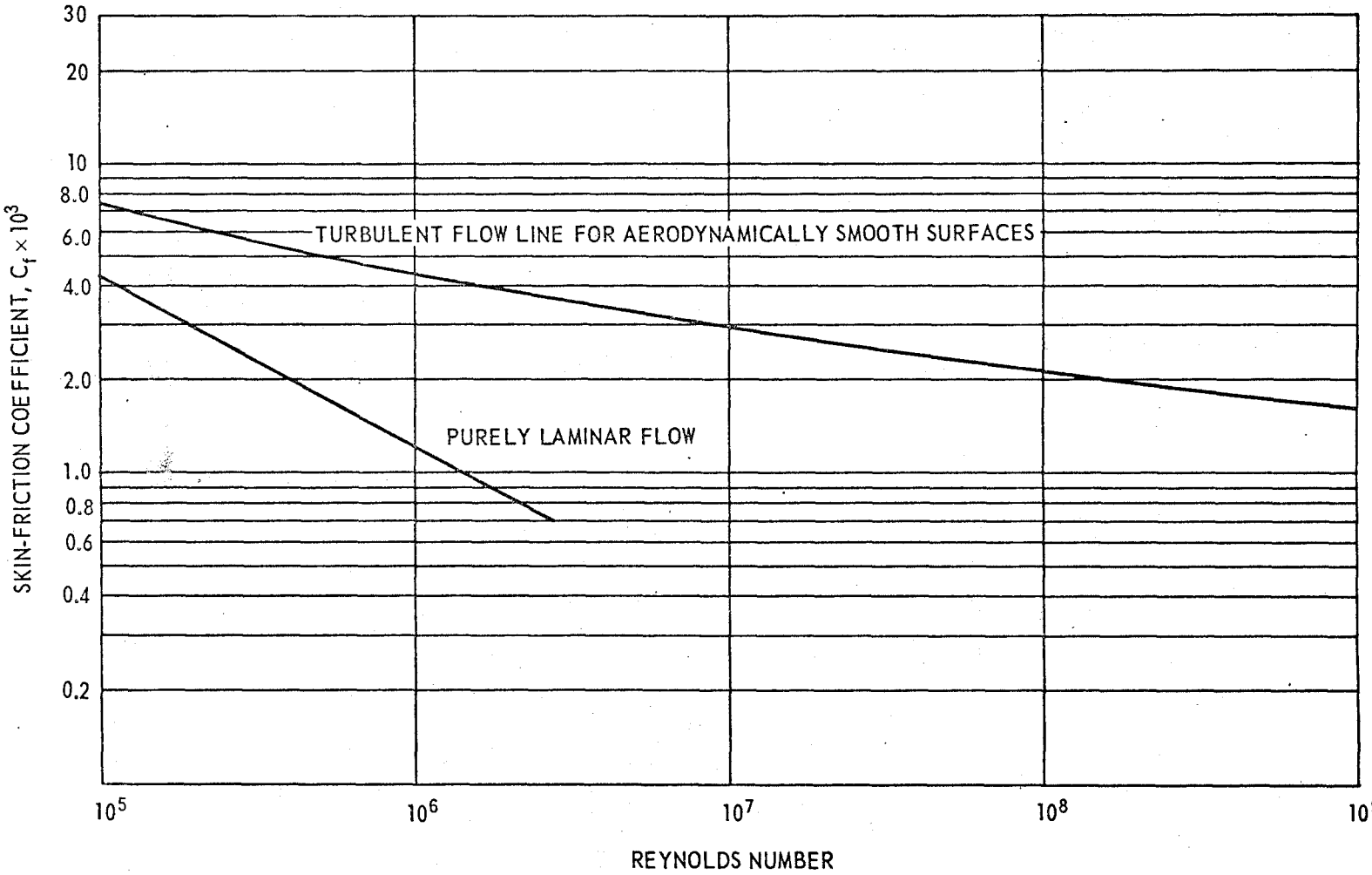

Figure 9 – Incompressible Skin Friction Coefficient (from Reference 9)

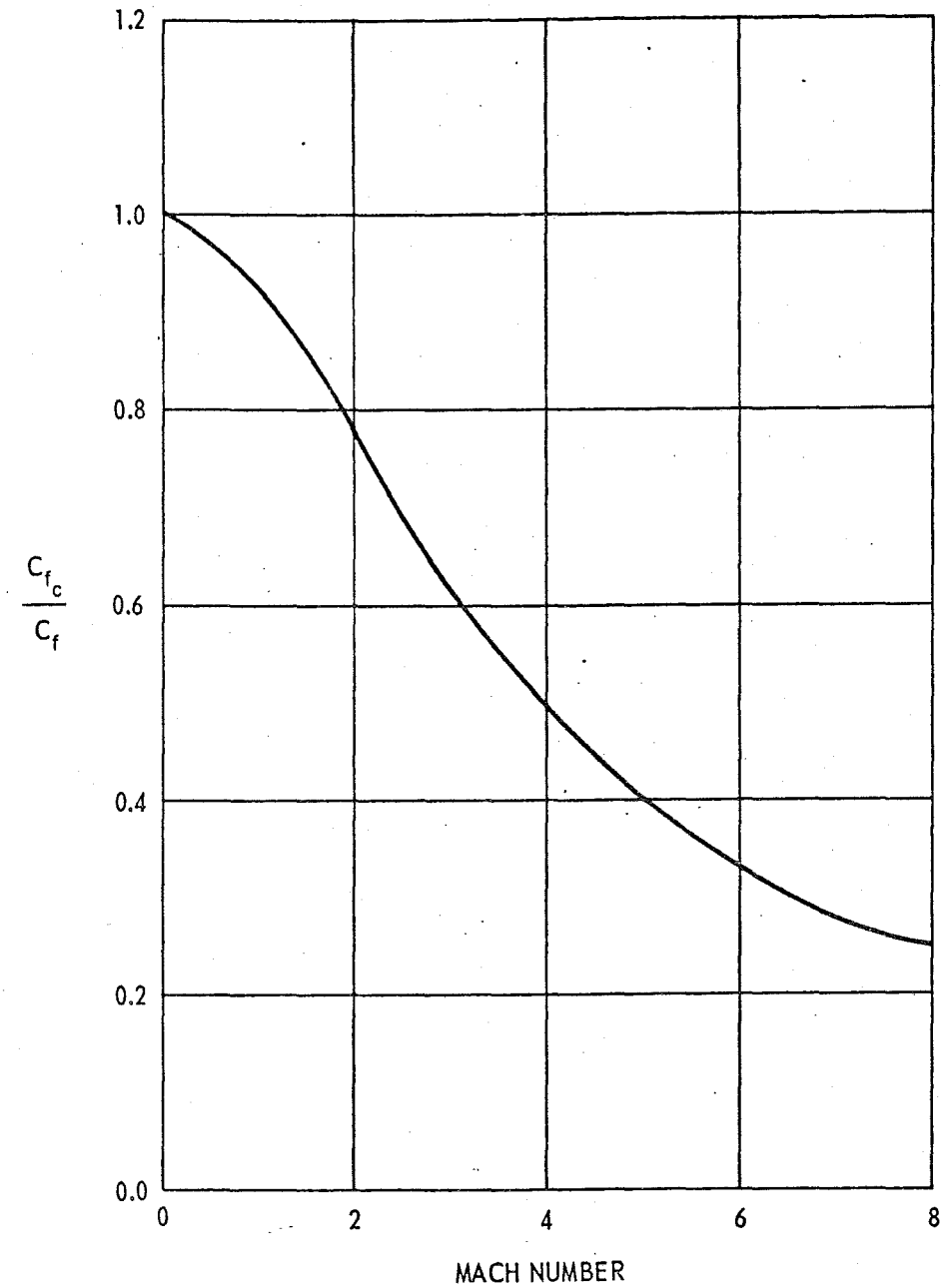

Figure 10 – Compressibility Effect on Turbulent Skin Friction (from Reference 9)

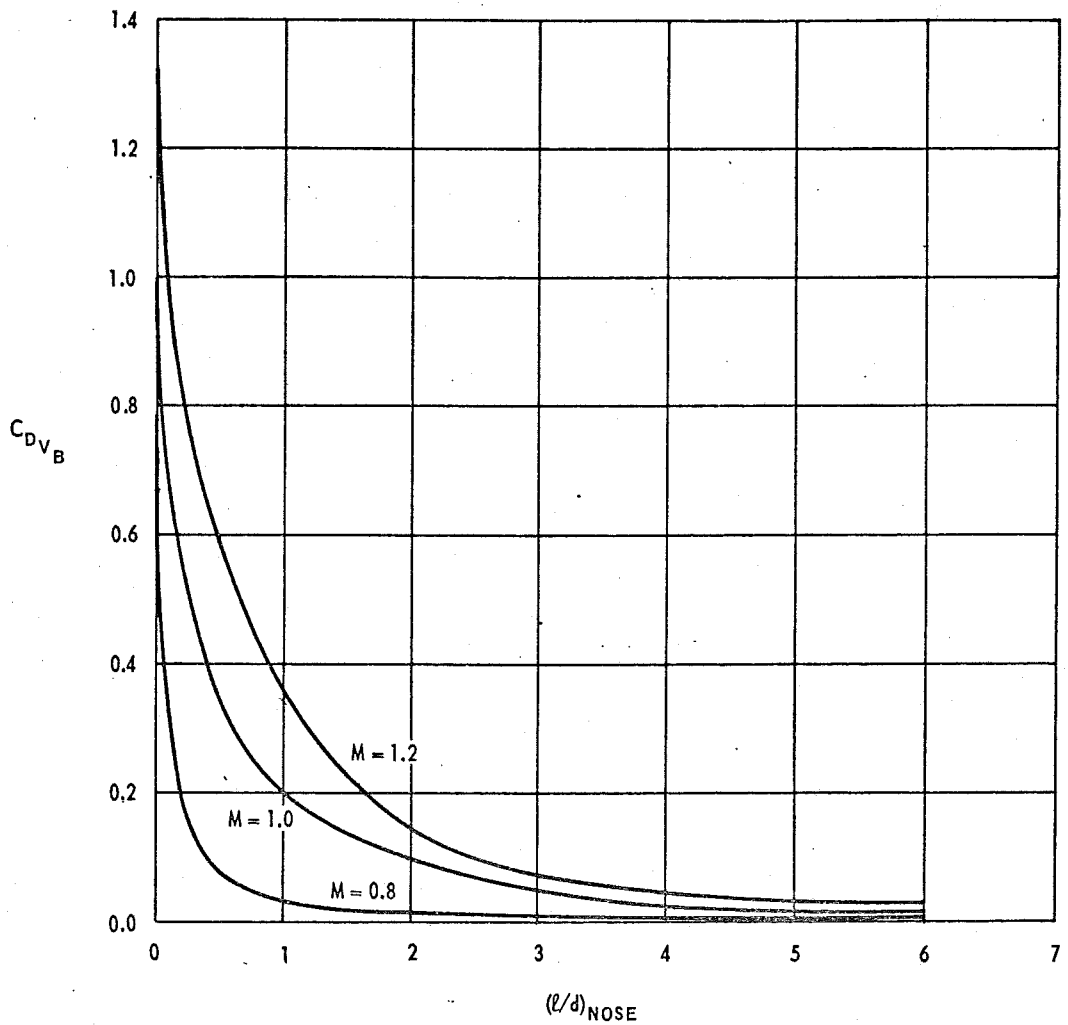

Figure 11 – Transonic Wave Drag for Ogival and Blunted Conical Forebodies

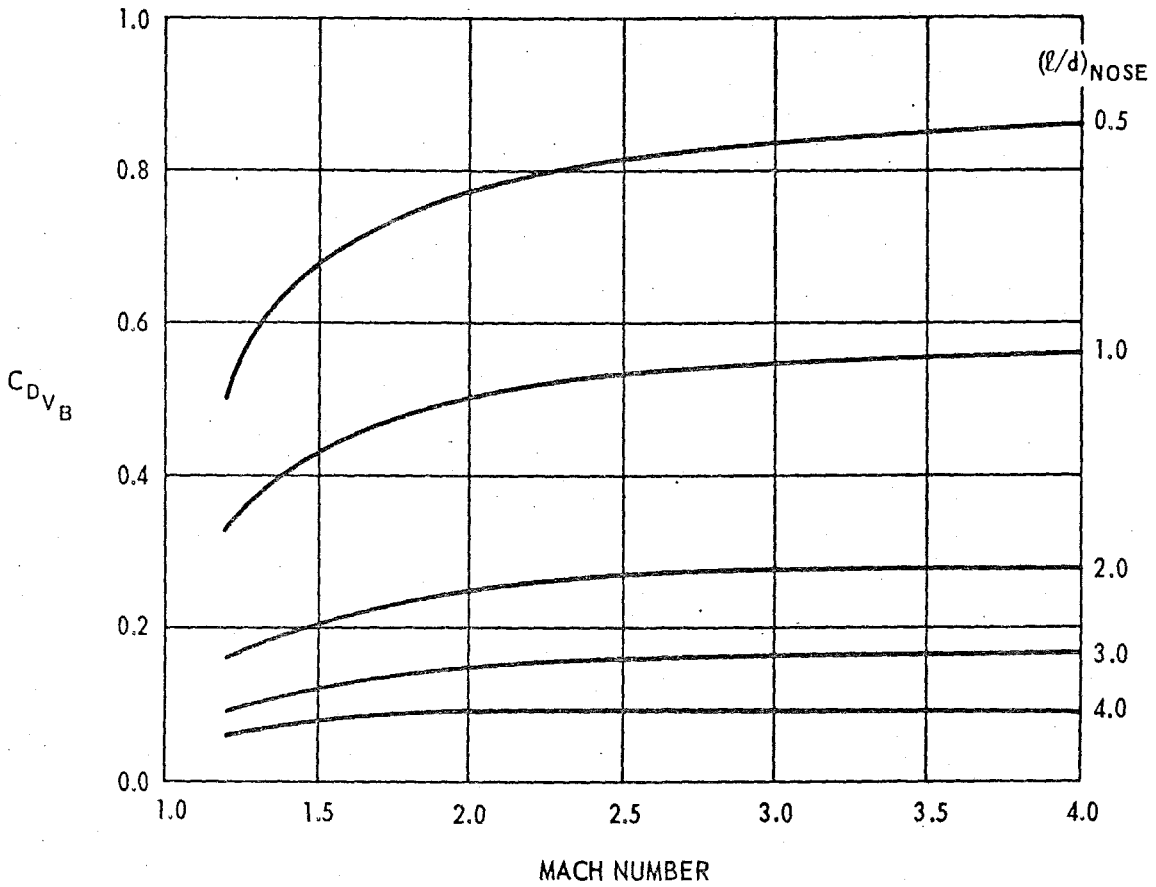

Figure 12 – External Wave Drag of Blunt Forebodies (from Reference 11)

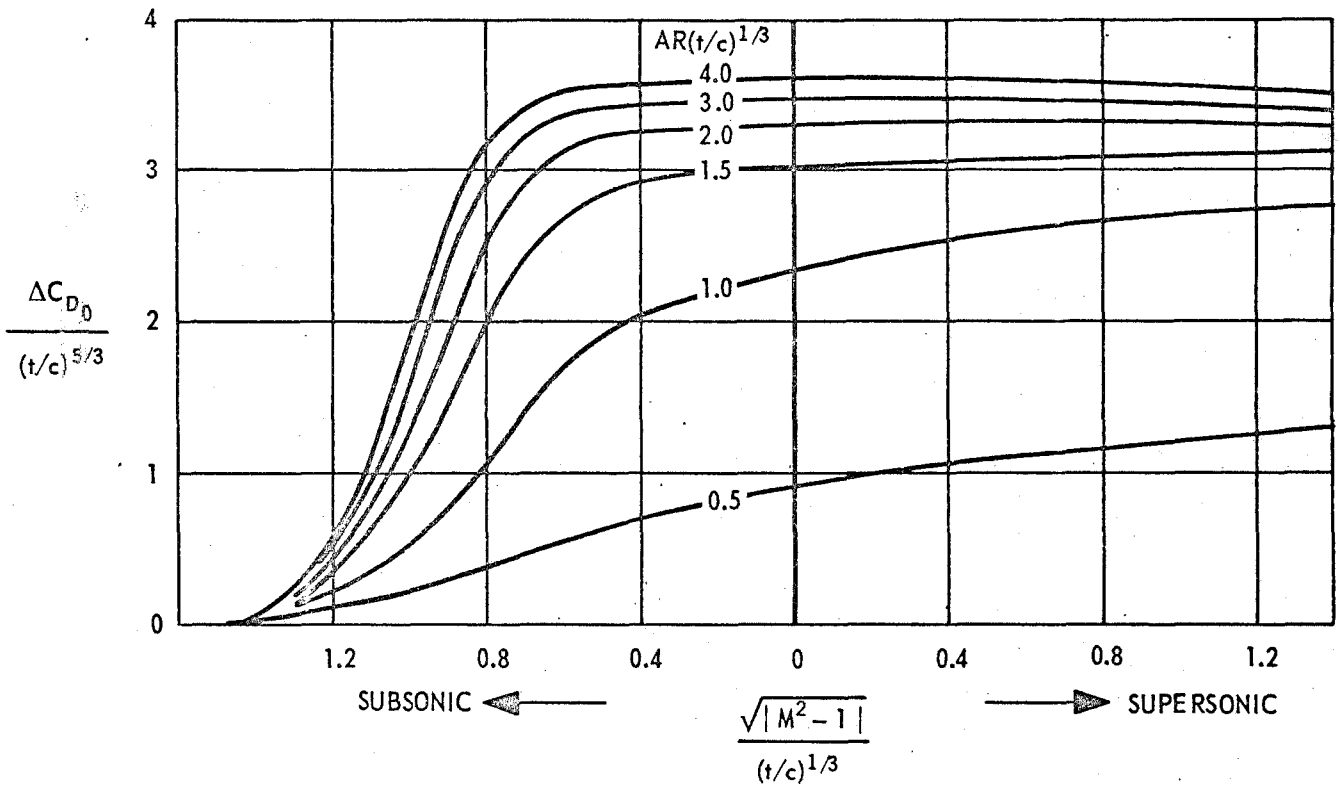

Figure 13:– Transonic Zero-Lift Wing Wave Drag for Unswept Wings (from Reference 9)

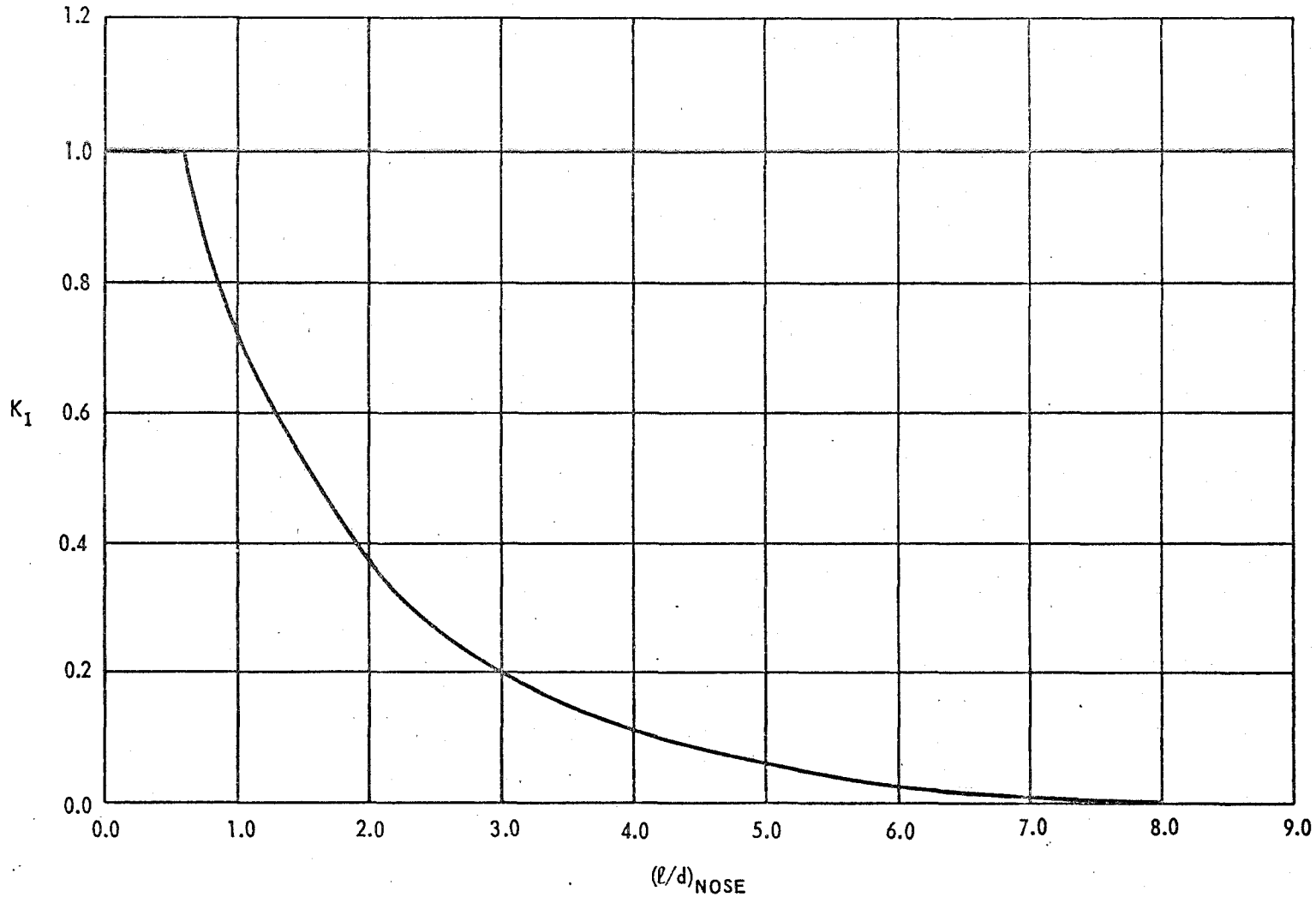

Figure 14 – Ratio of Wave Drag for Noses of Various Fineness Ratios to the Wave Drag for a Hemispherical Nose

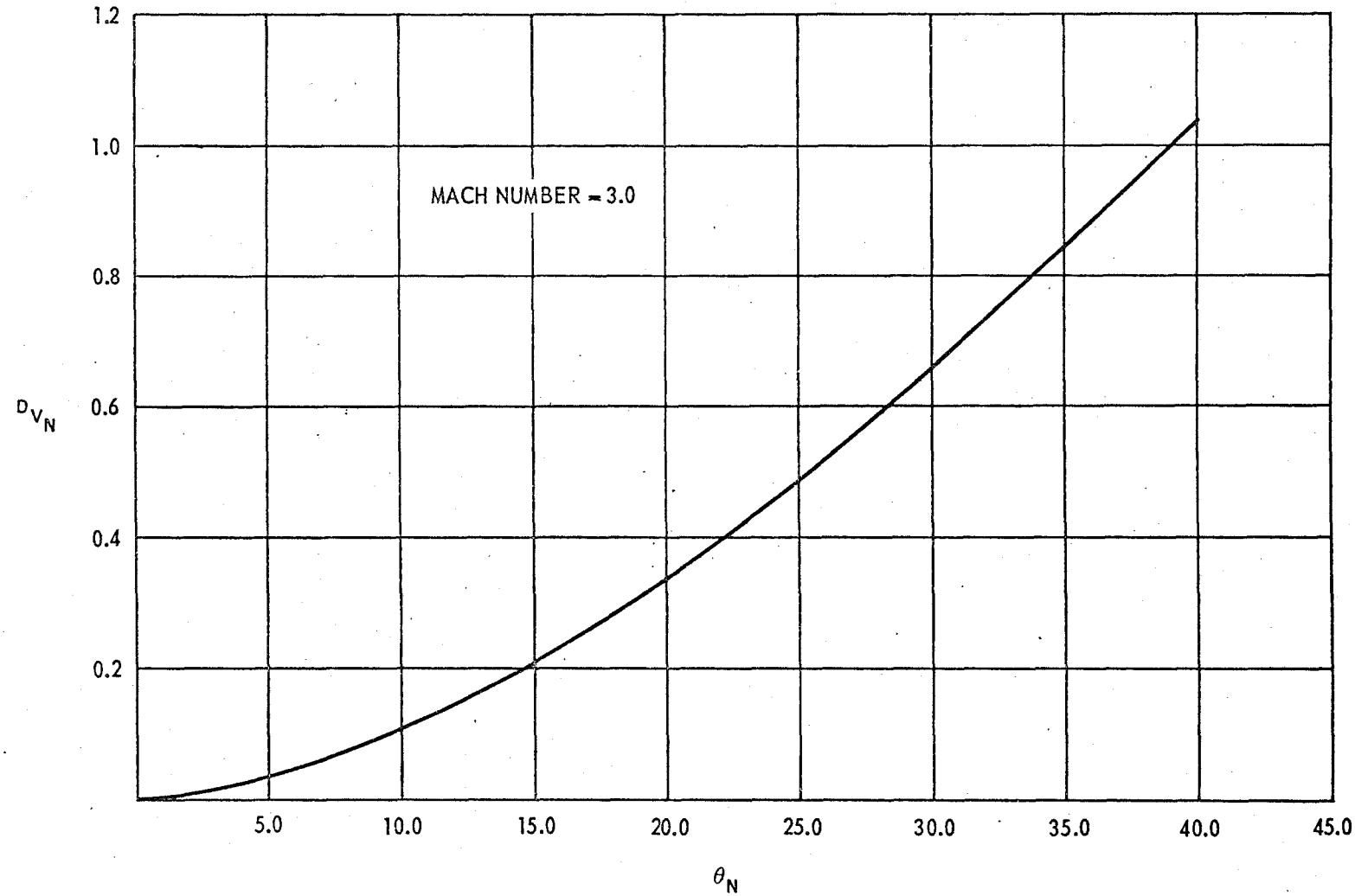

Figure 15 – Wave Drag of a Pointed Conical Nose (from Reference 6)

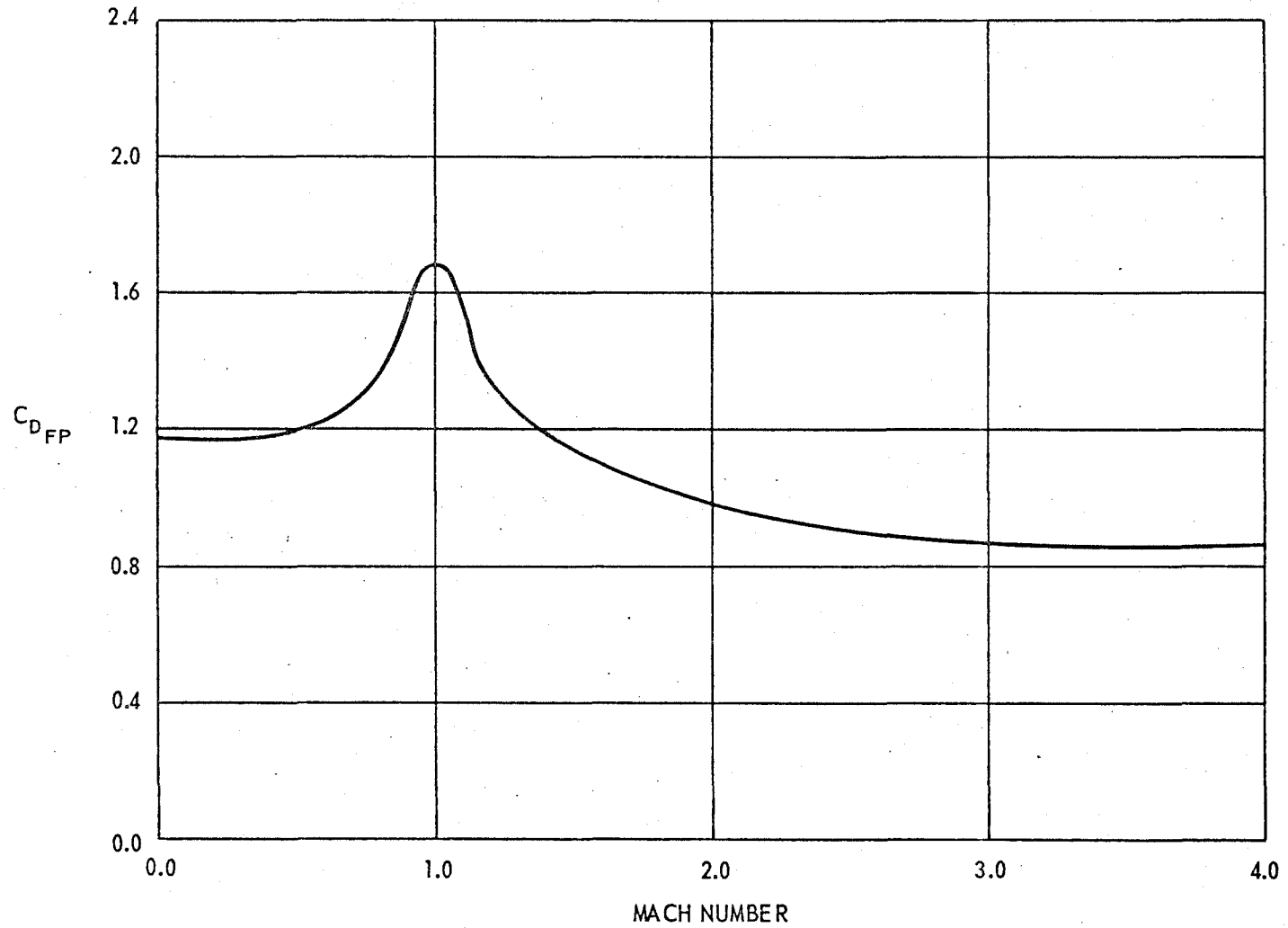

Figure 16 – Drag Coefficient for a Flat Plate Normal to the Flow

Figure 17 – Lifting Surface Center of Pressure as a Function of Effective Aspect Ratio (from Reference 1)

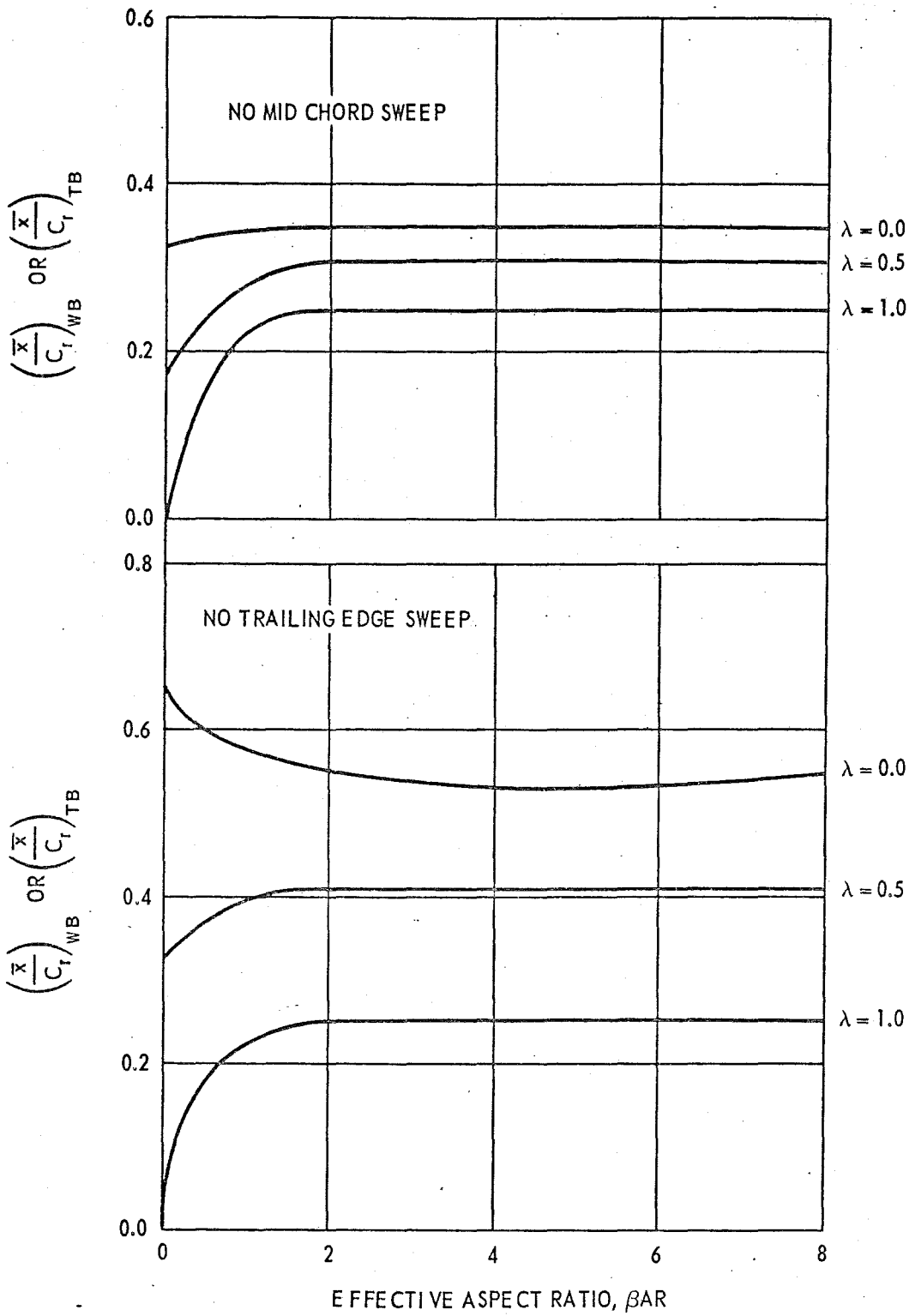

Figure 17a – $M \leq 1.0$

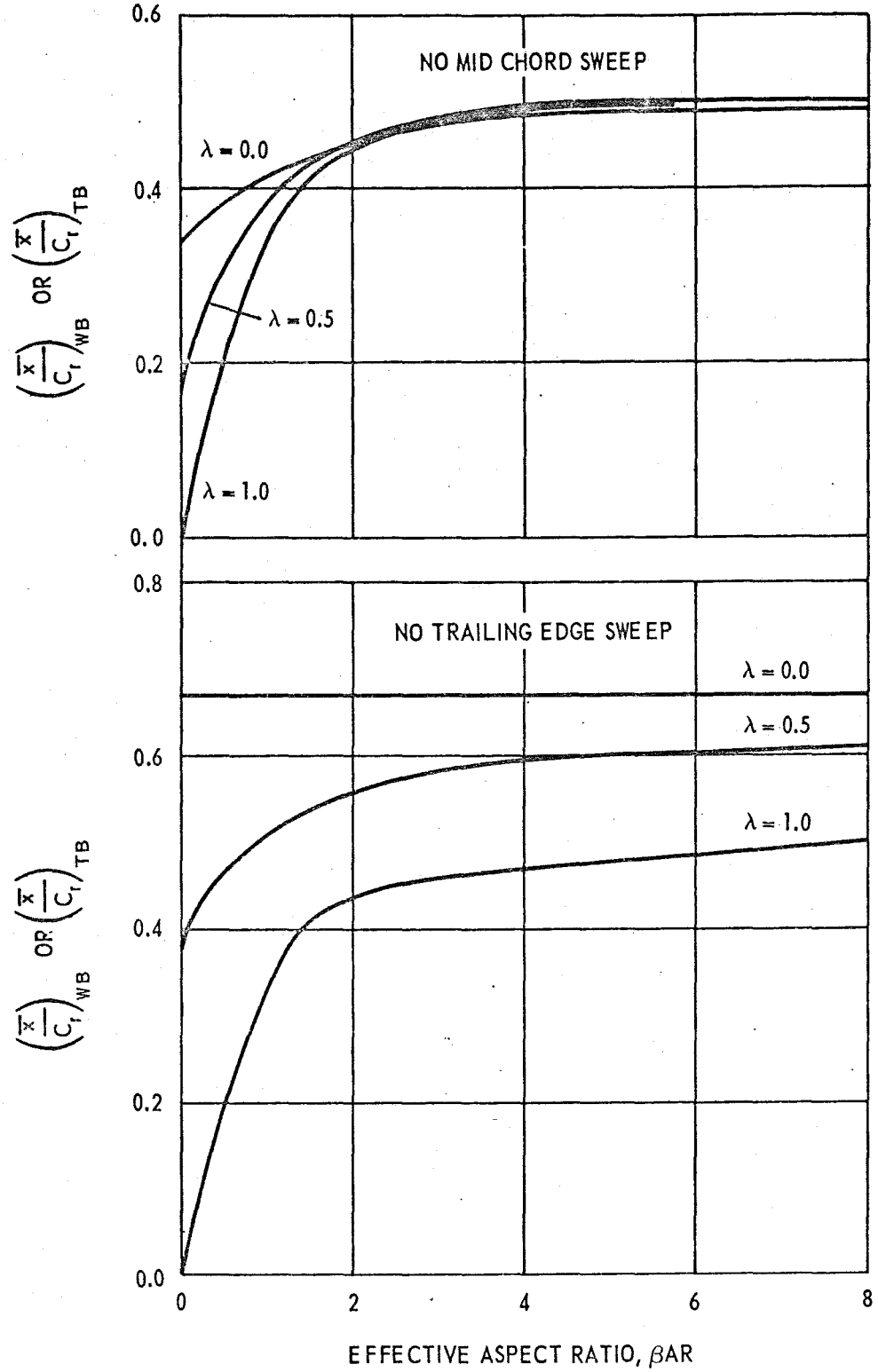

Figure 17b — M > 1.0

Figure 18 – Subsonic Center of Pressure Location of the Lift on the Body in the Presence of Wings or Tails (from Reference 1)

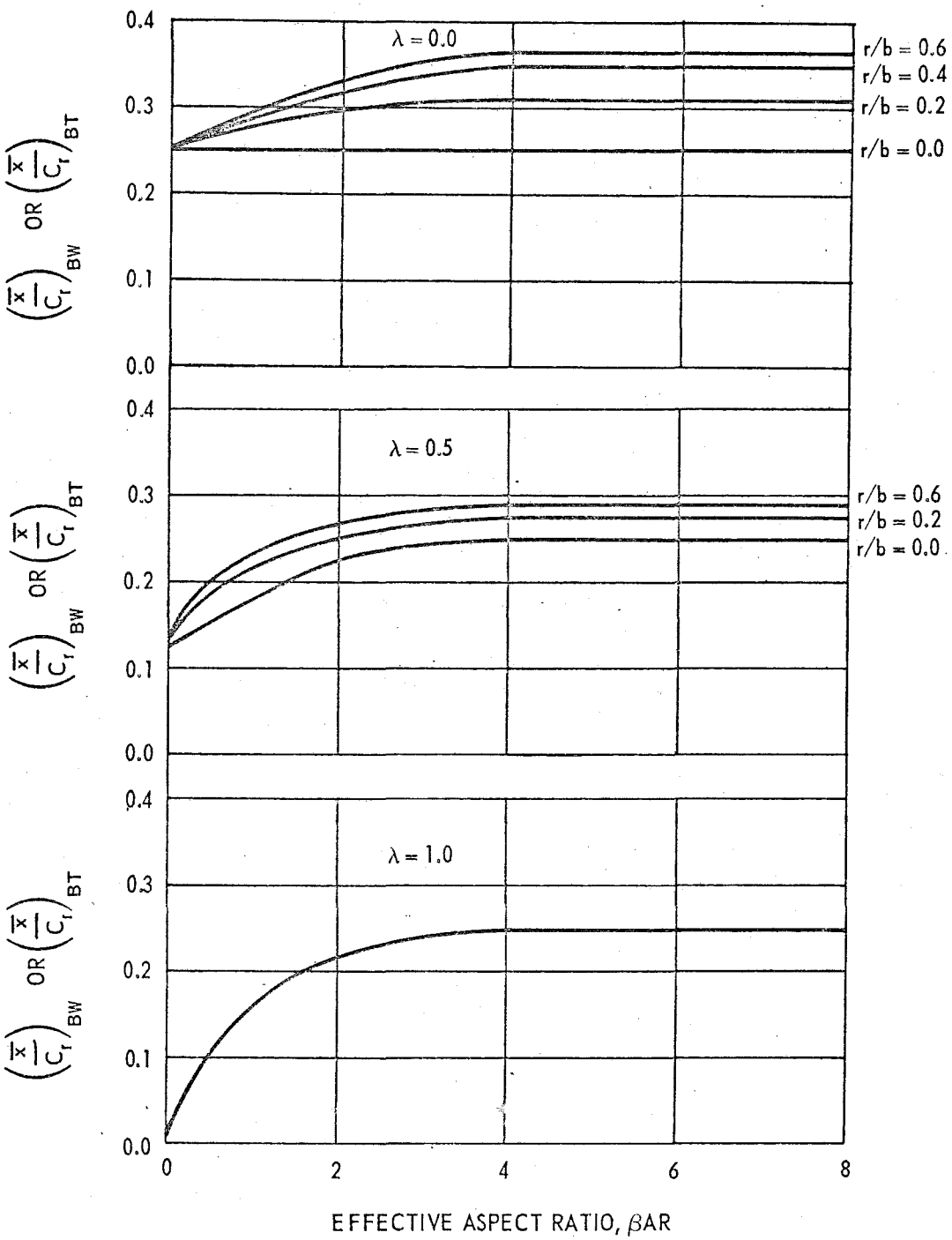

Figure 18a – No Mid Chord Sweep

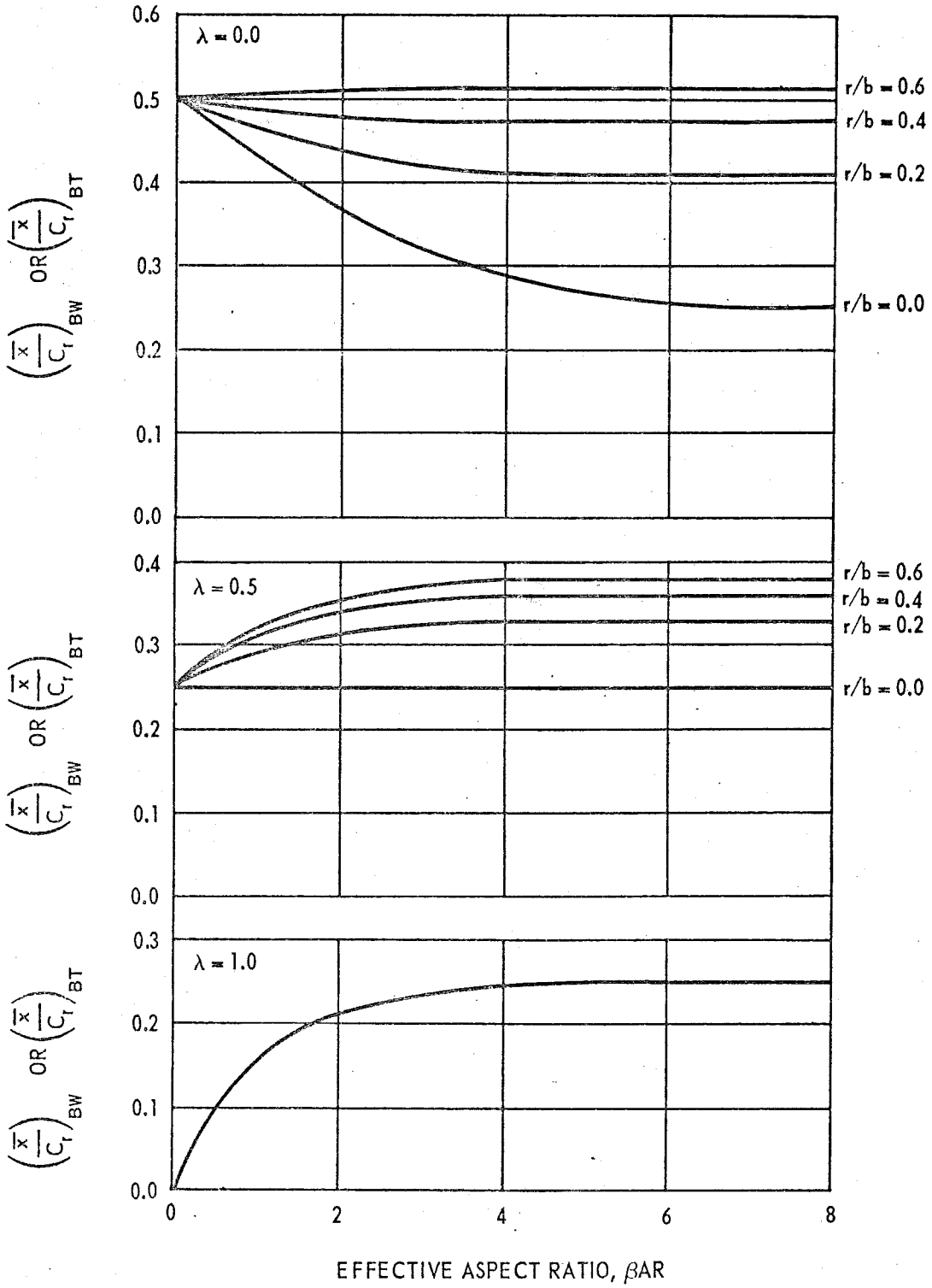

Figure 18b – No Trailing Edge Sweep

Figure 19 – Supersonic Center of Pressure Location of Lift on the Body in the Presence of Wings or Tails for $\beta AR(1 + \lambda)(1 + 1/m\beta) \leq 4.0$ (from Reference 1)

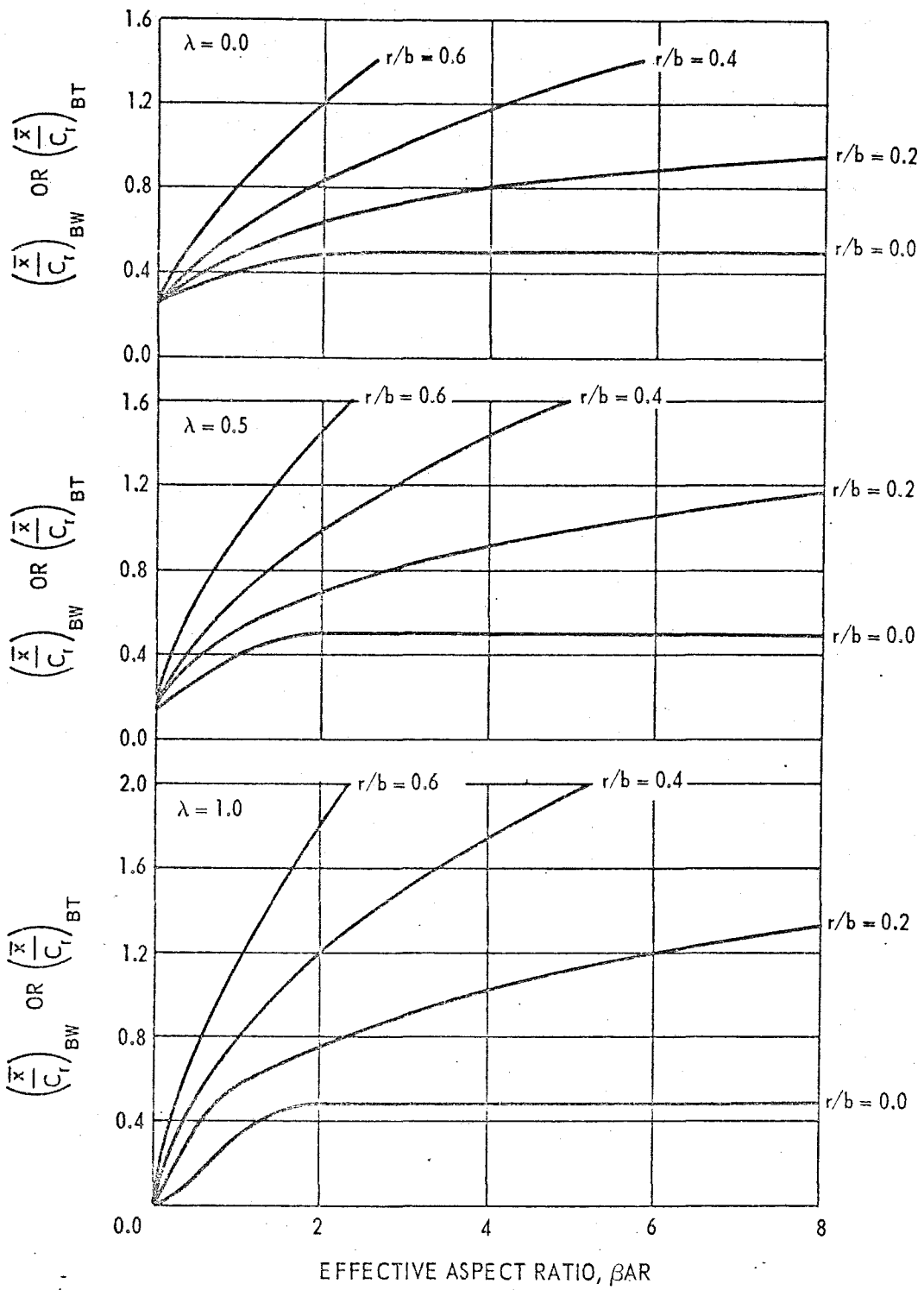

Figure 19a – No Mid Chord Sweep

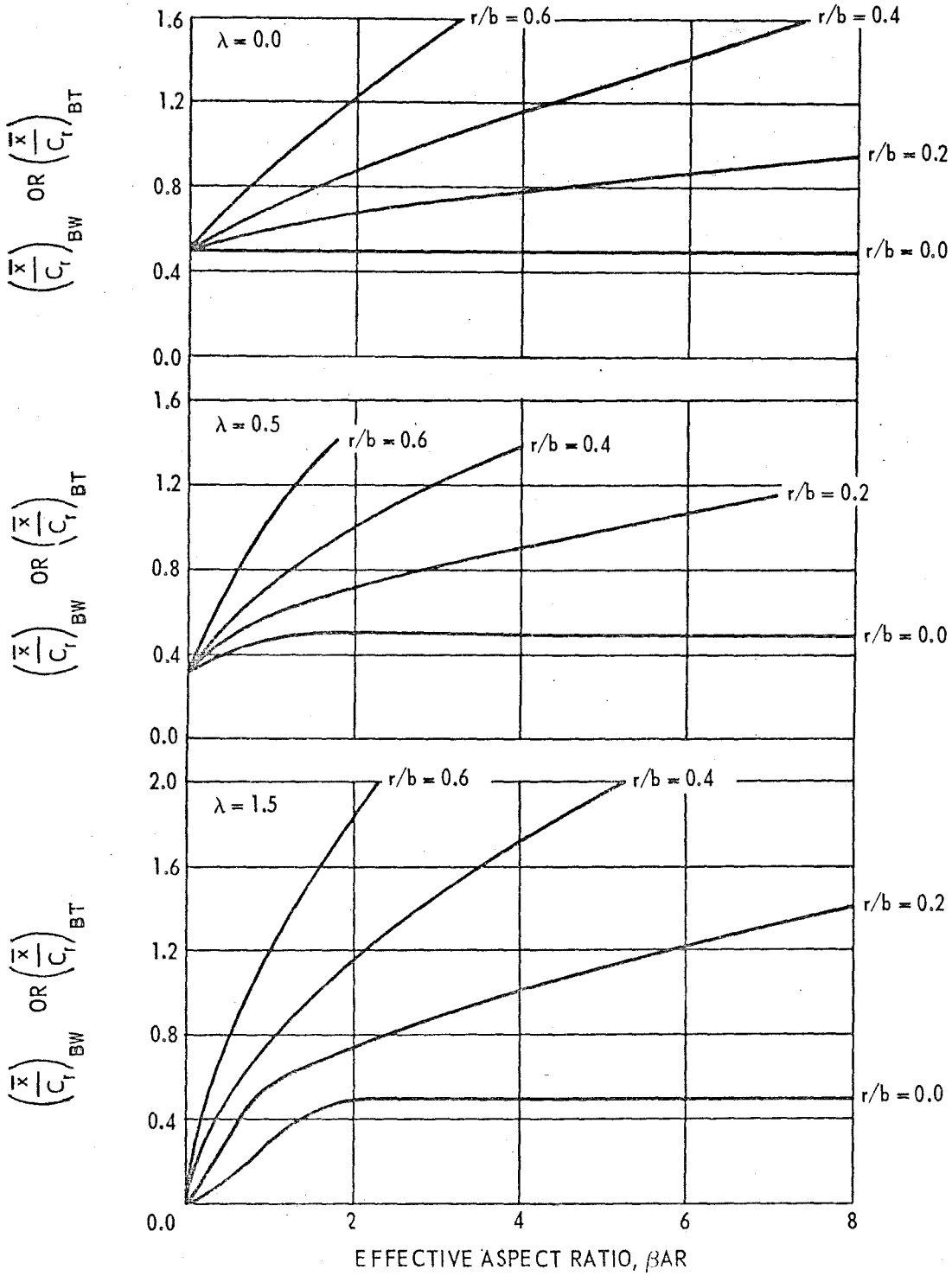

Figure 19b – No Trailing Edge Sweep

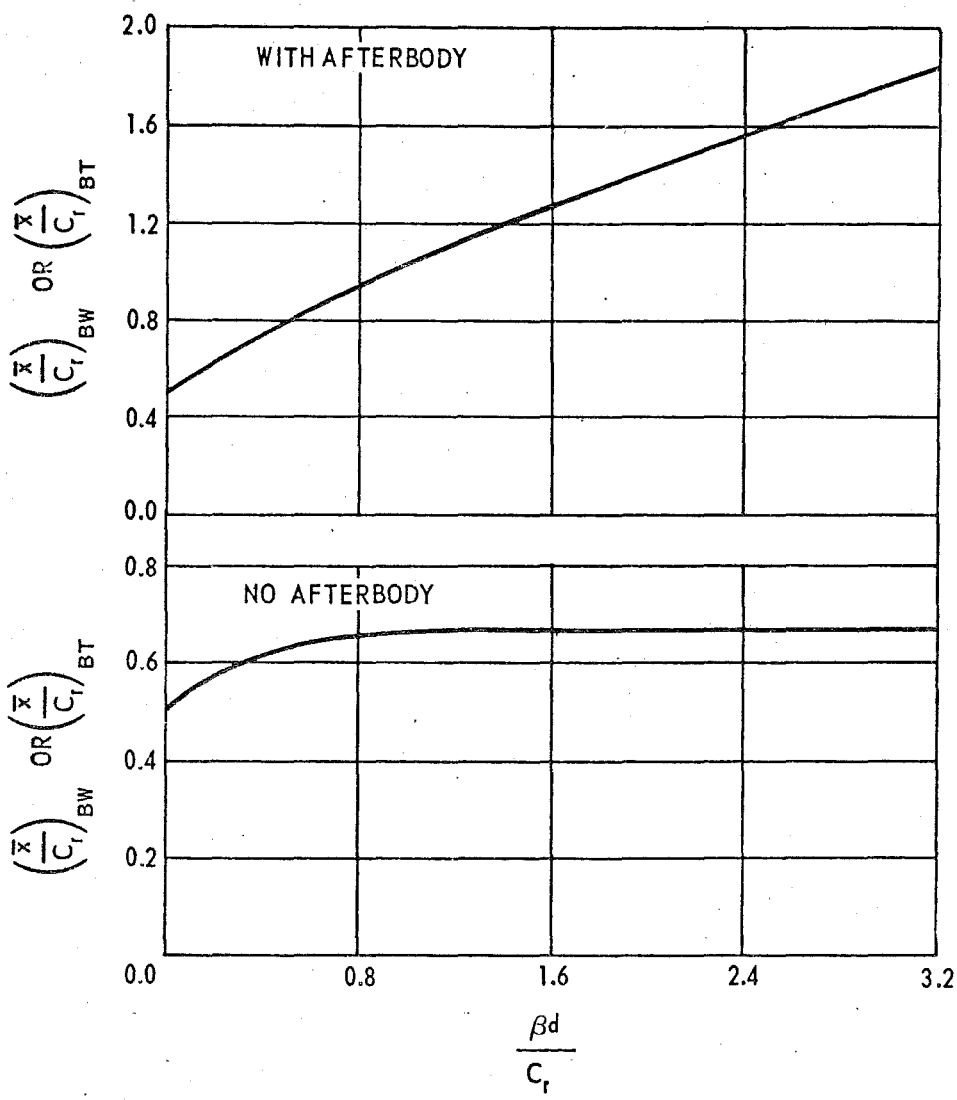

Figure 20 – Supersonic Center of Pressure Location of Lift on the Body in the Presence of Wings or Tails for $\beta AR(1 + \lambda)(1 + 1/m\beta) > 4.0$ (from Reference 1)

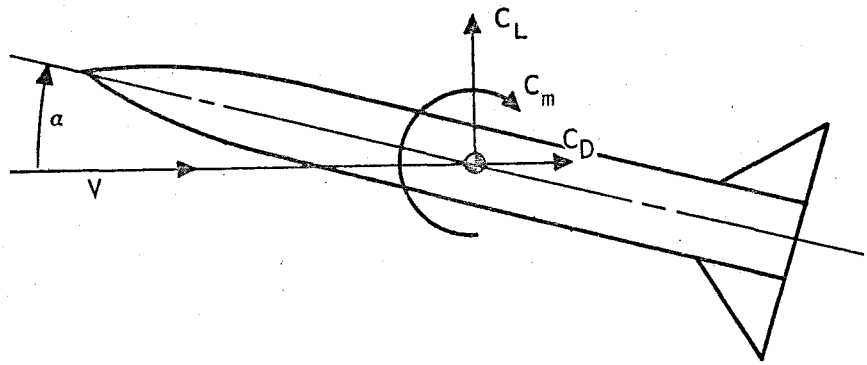

Figure 21a – Stability Axes

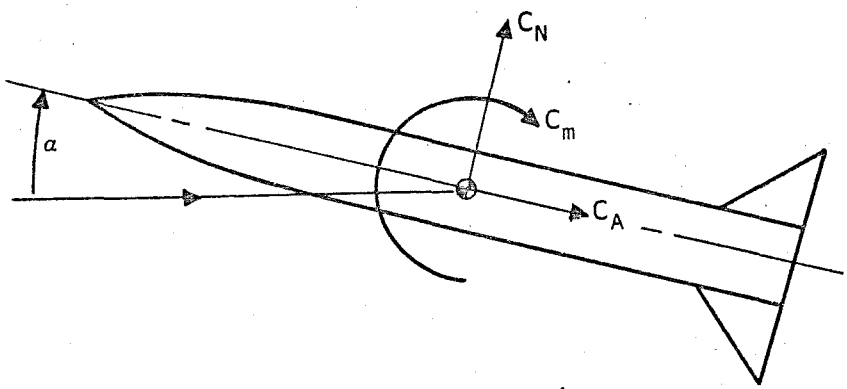

Figure 21b – Body Axes

Figure 21 – Missile Axis Systems

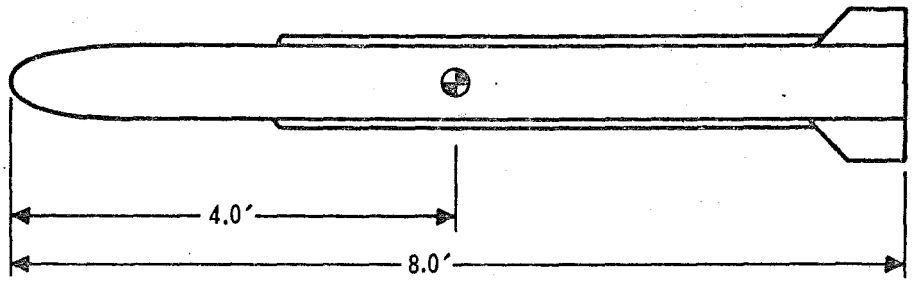

CONFIGURATION 1

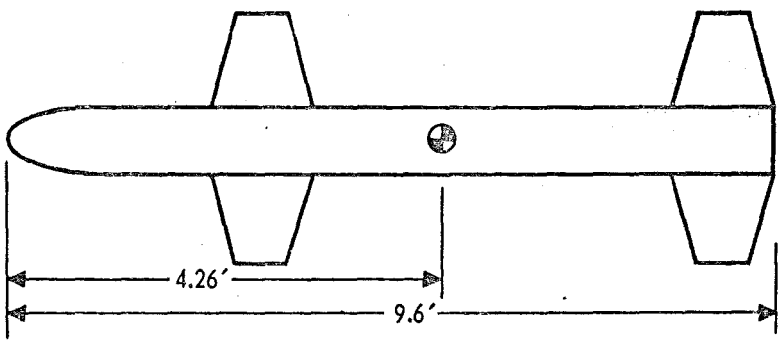

CONFIGURATION 2

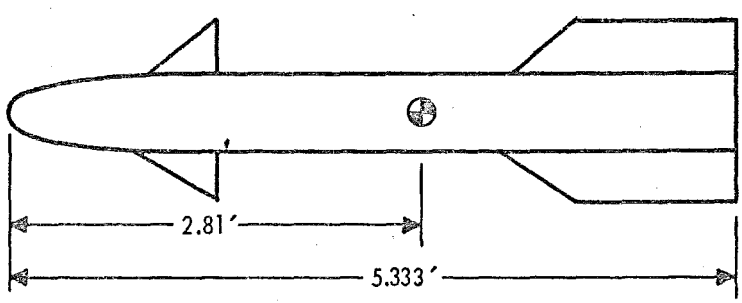

CONFIGURATION 3

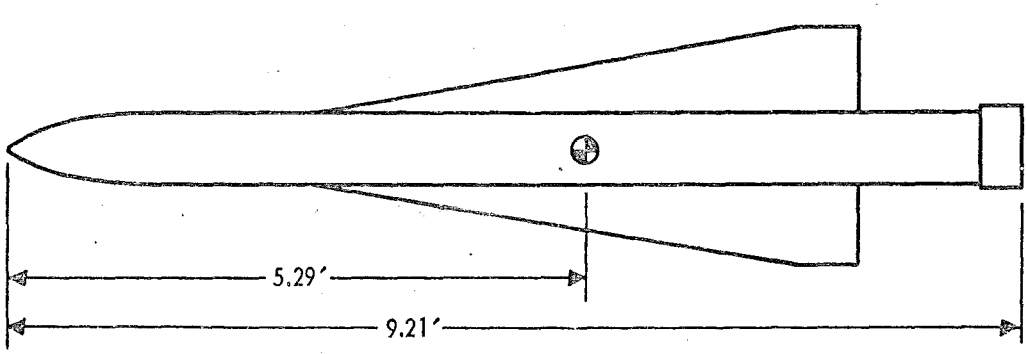

CONFIGURATION 4

Figure 22 – Configurations Used to Compare Theory with Experiment

Figure 23 – Comparison of Experimental Data with Theoretical Results for Configuration 1

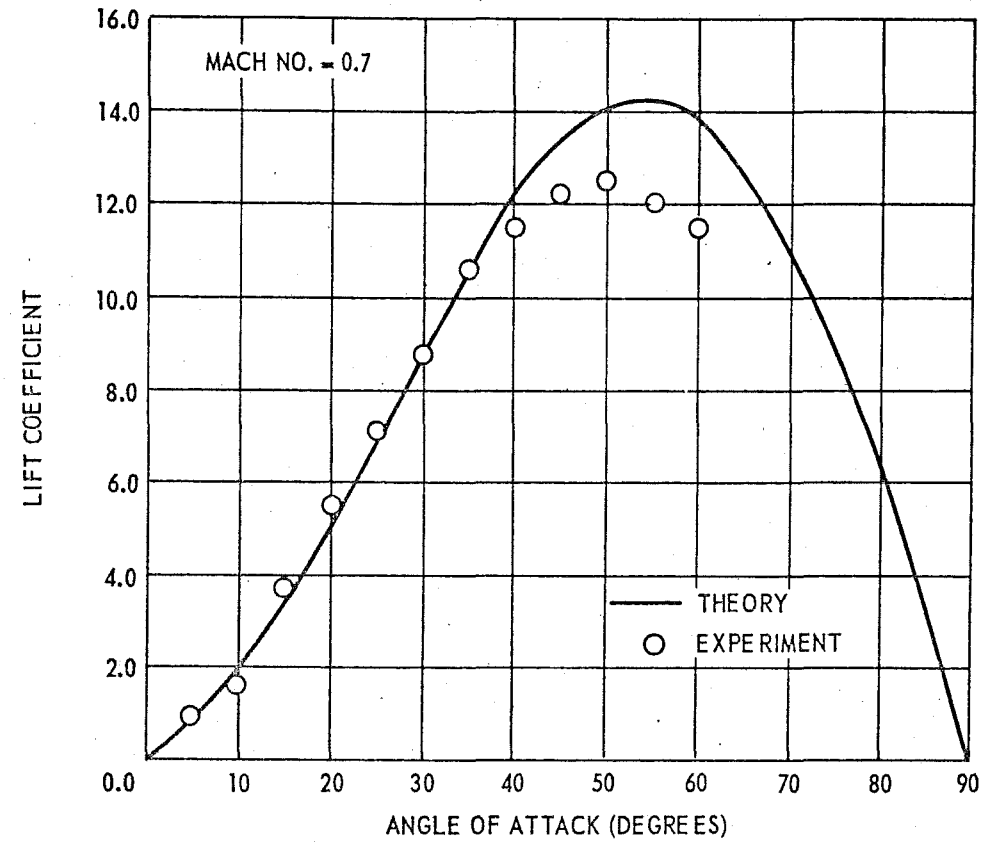

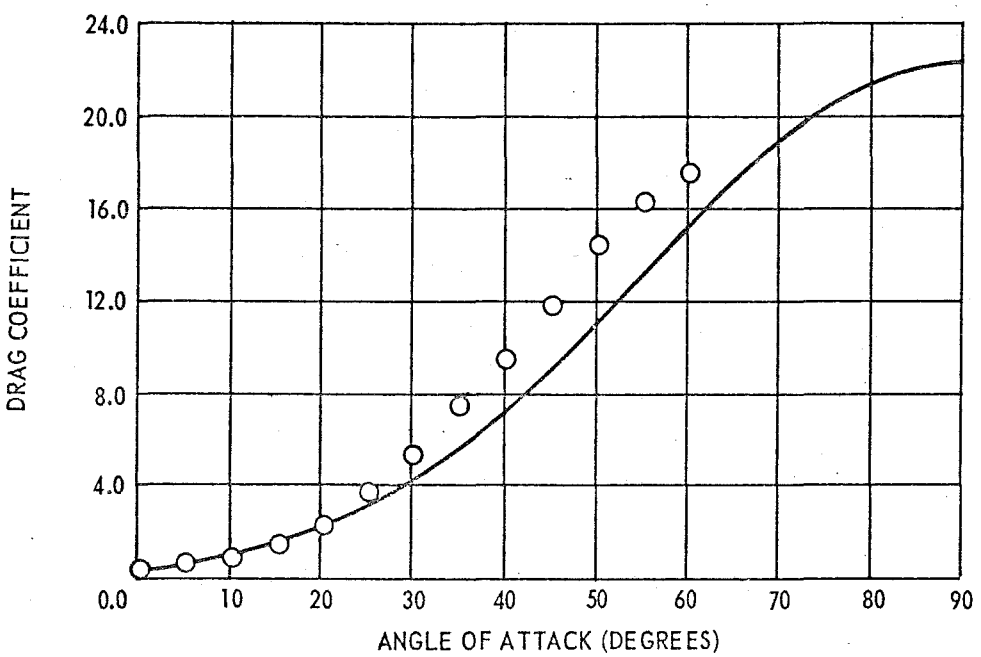

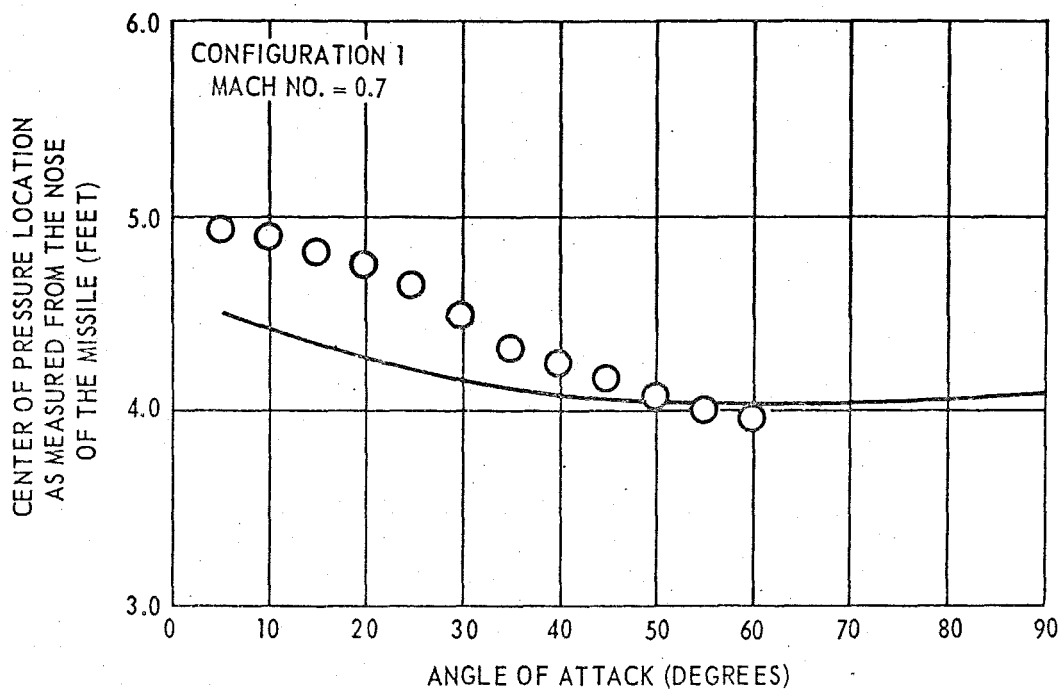

Figure 23 (Continued)

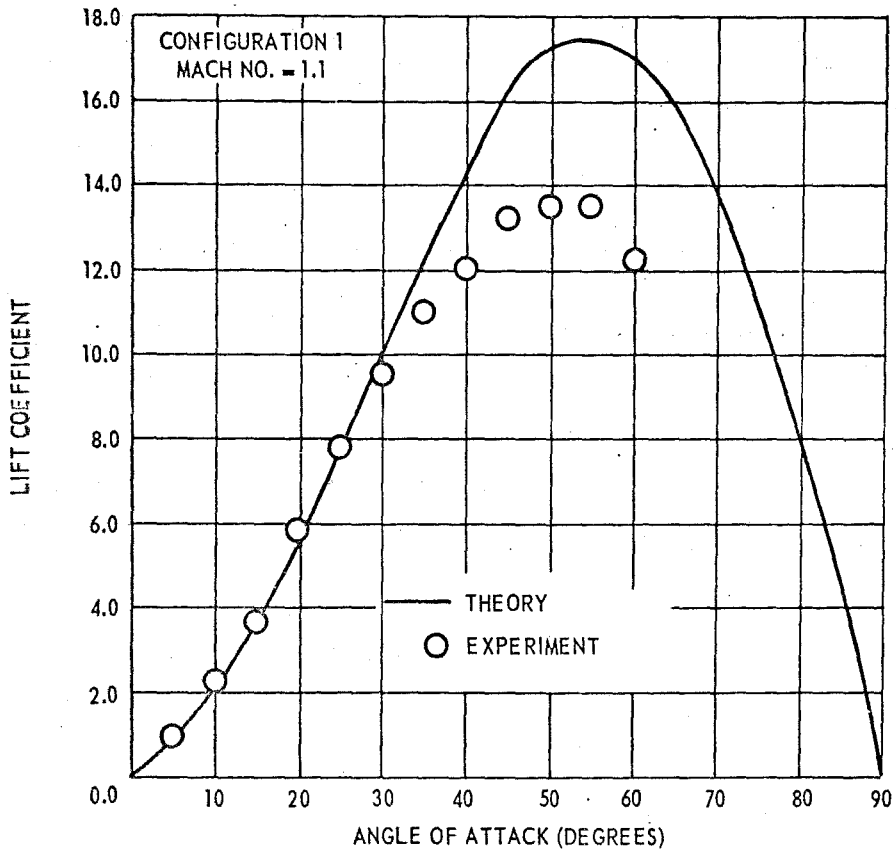

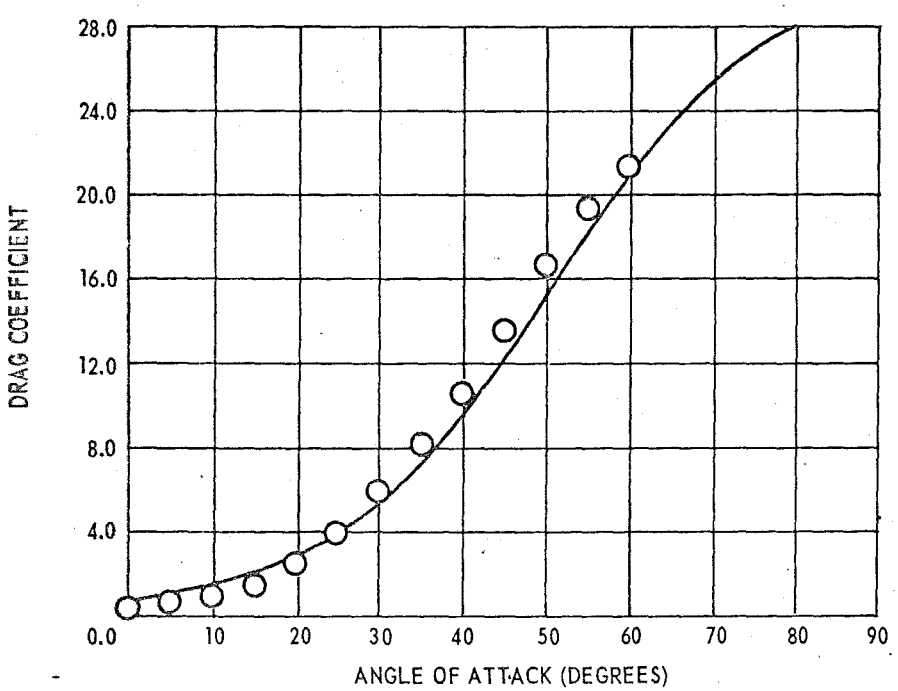

Figure 23 (Continued)

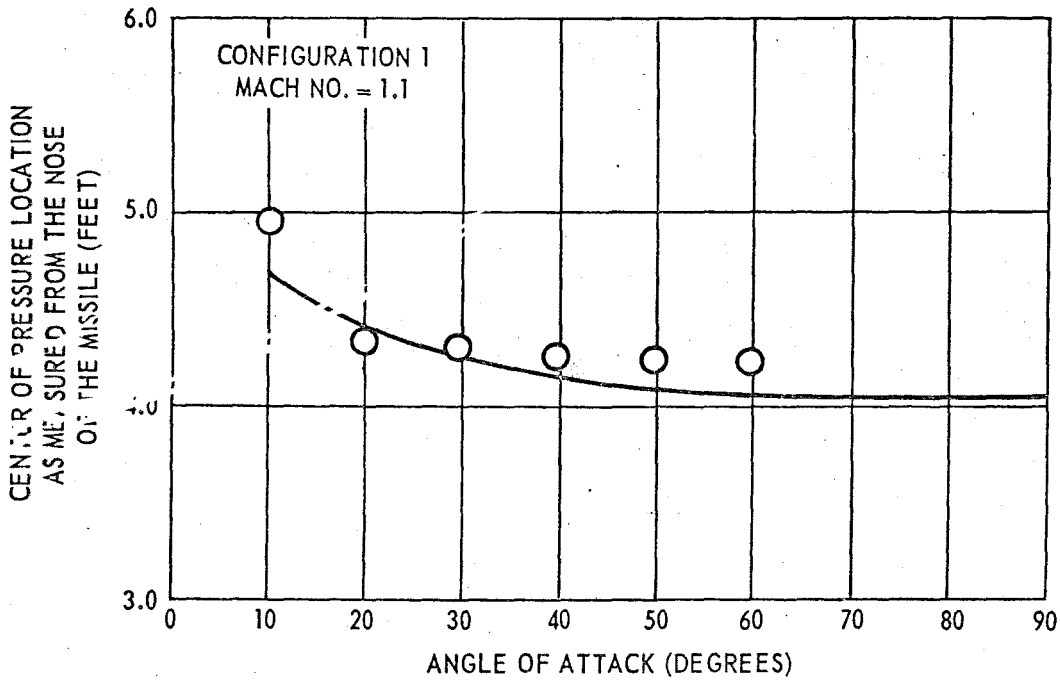

Figure 23 (Continued)

Figure 24 – Comparison of Experimental Data with Theoretical Results for Configuration 2

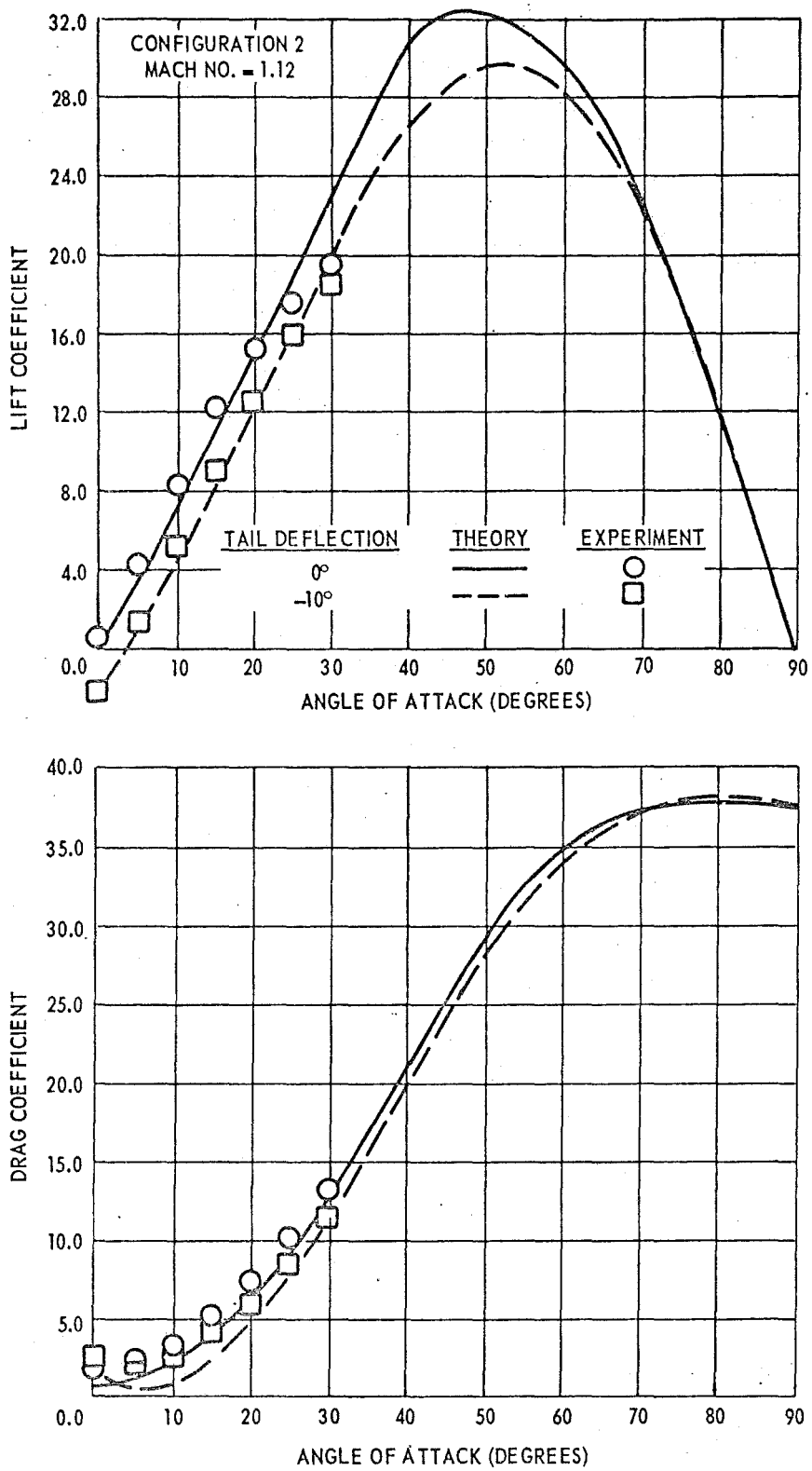

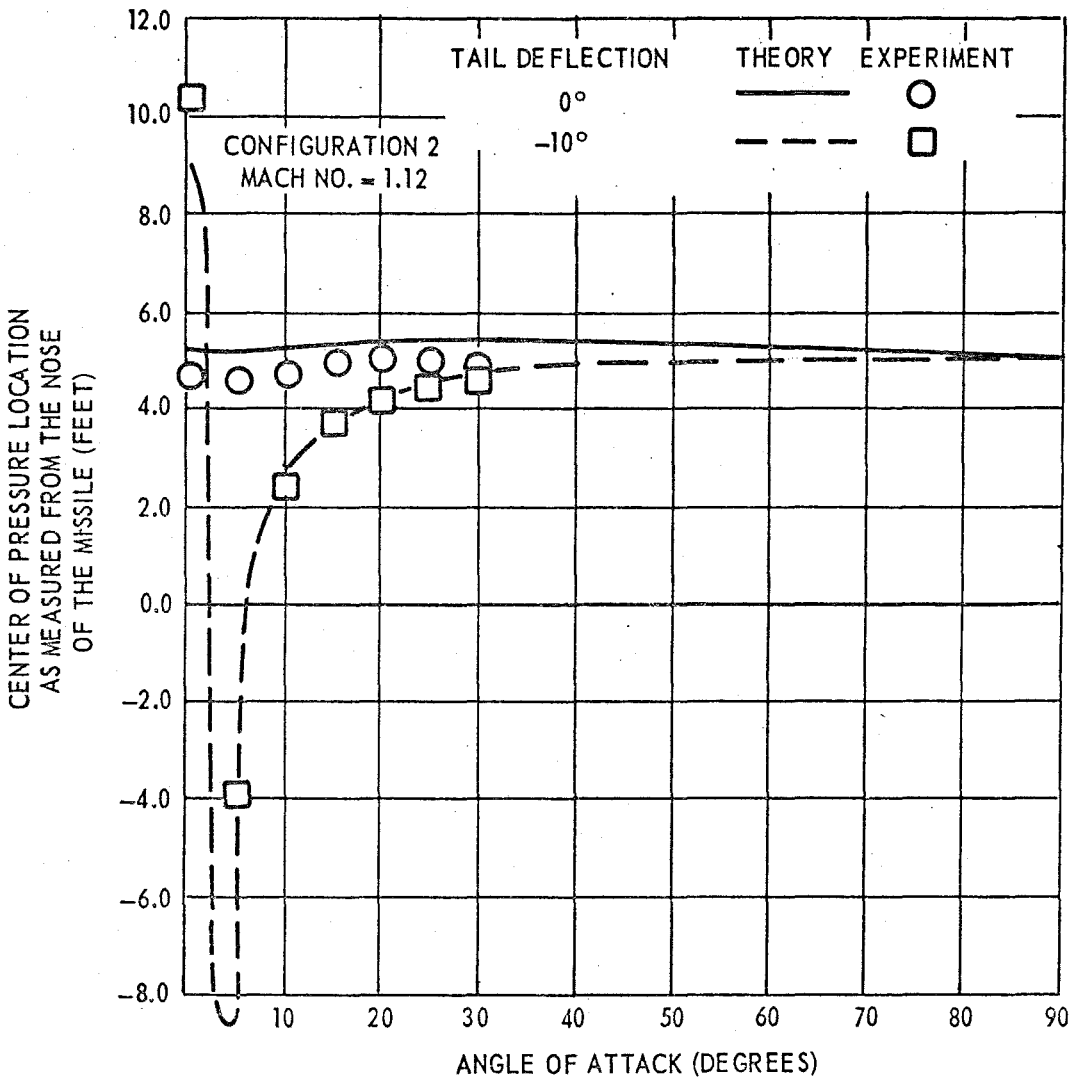

Figure 24 (Continued)

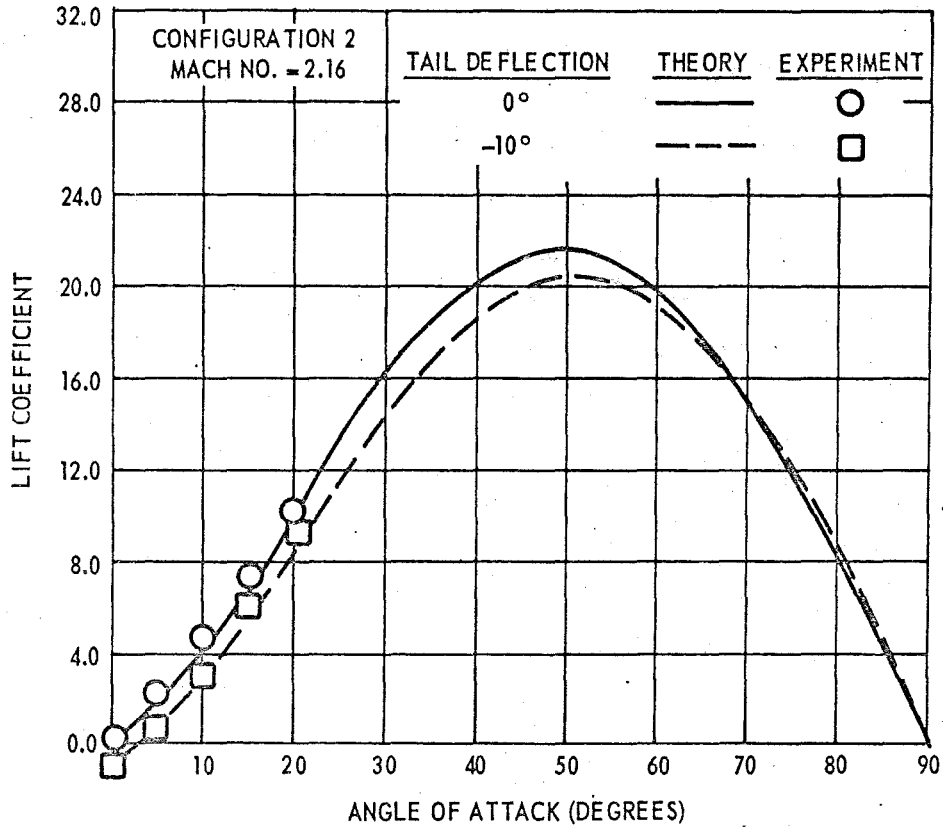

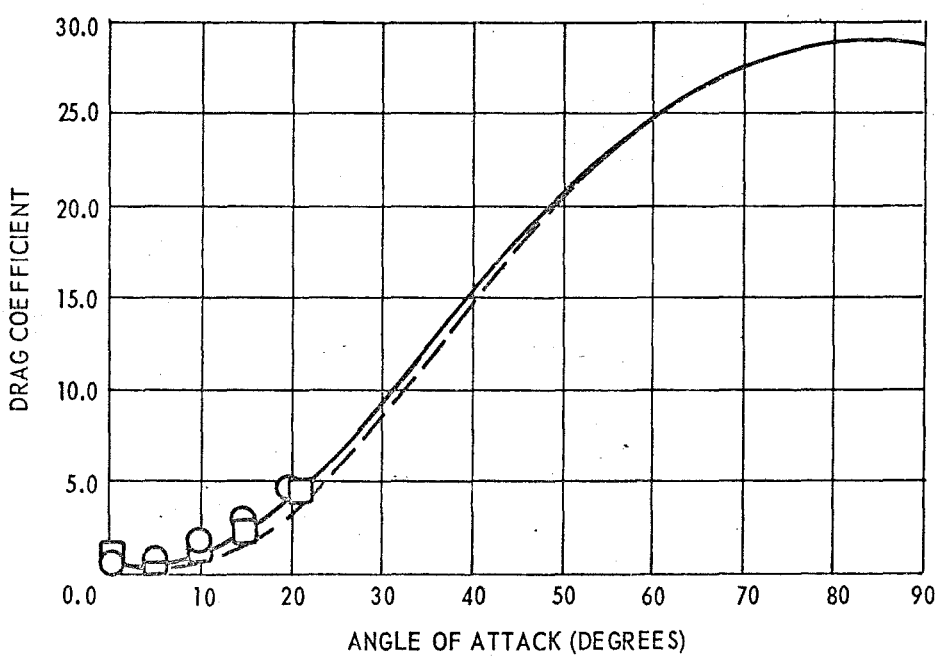

Figure 24 (Continued)

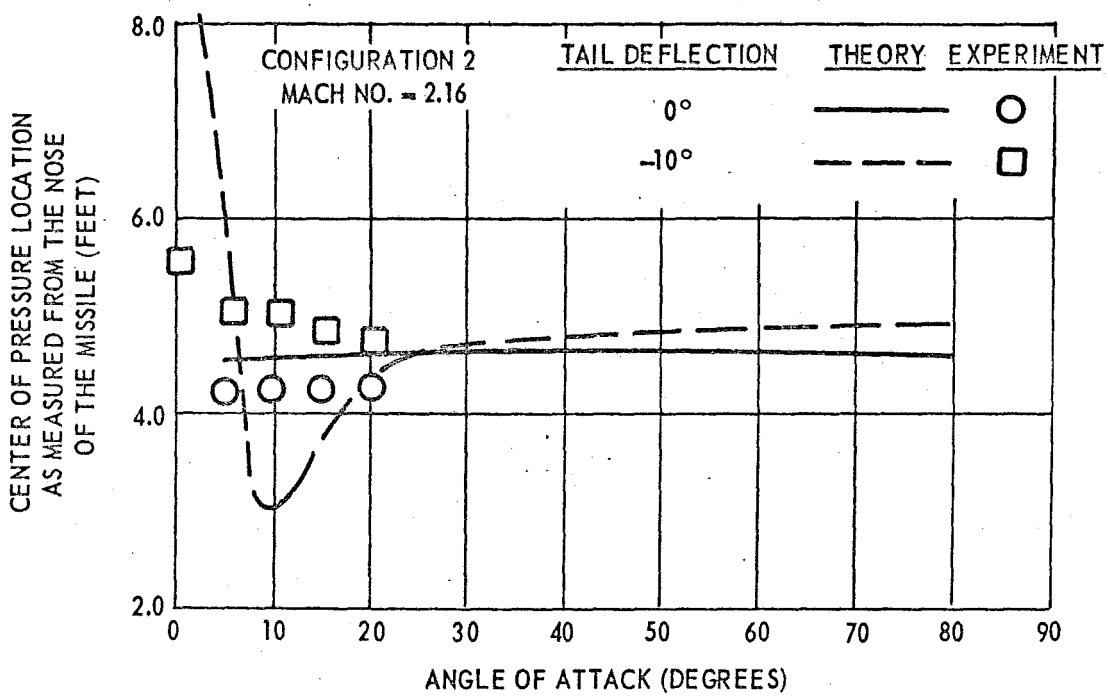

Figure 24 (Continued)

Figure 25 – Comparison of Experimental Data with Theoretical Results for Configuration 3

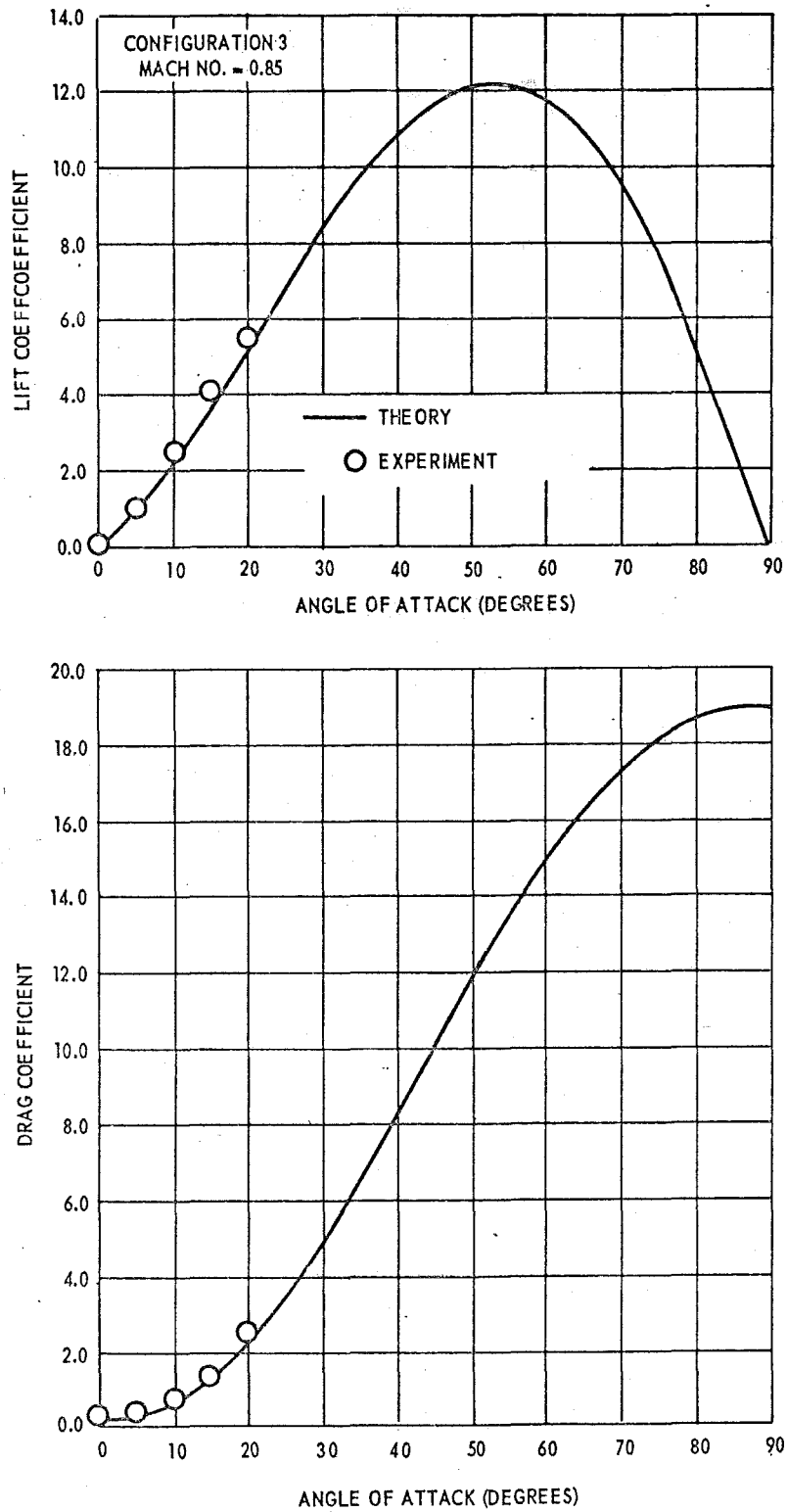

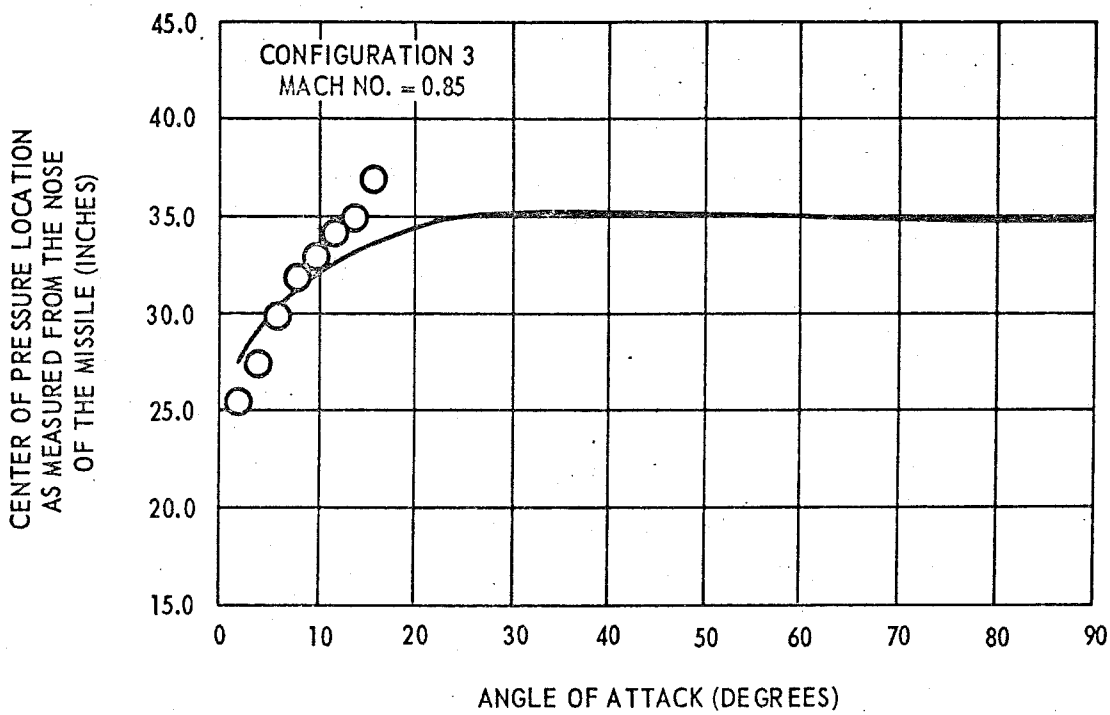

Figure 25 (Continued)

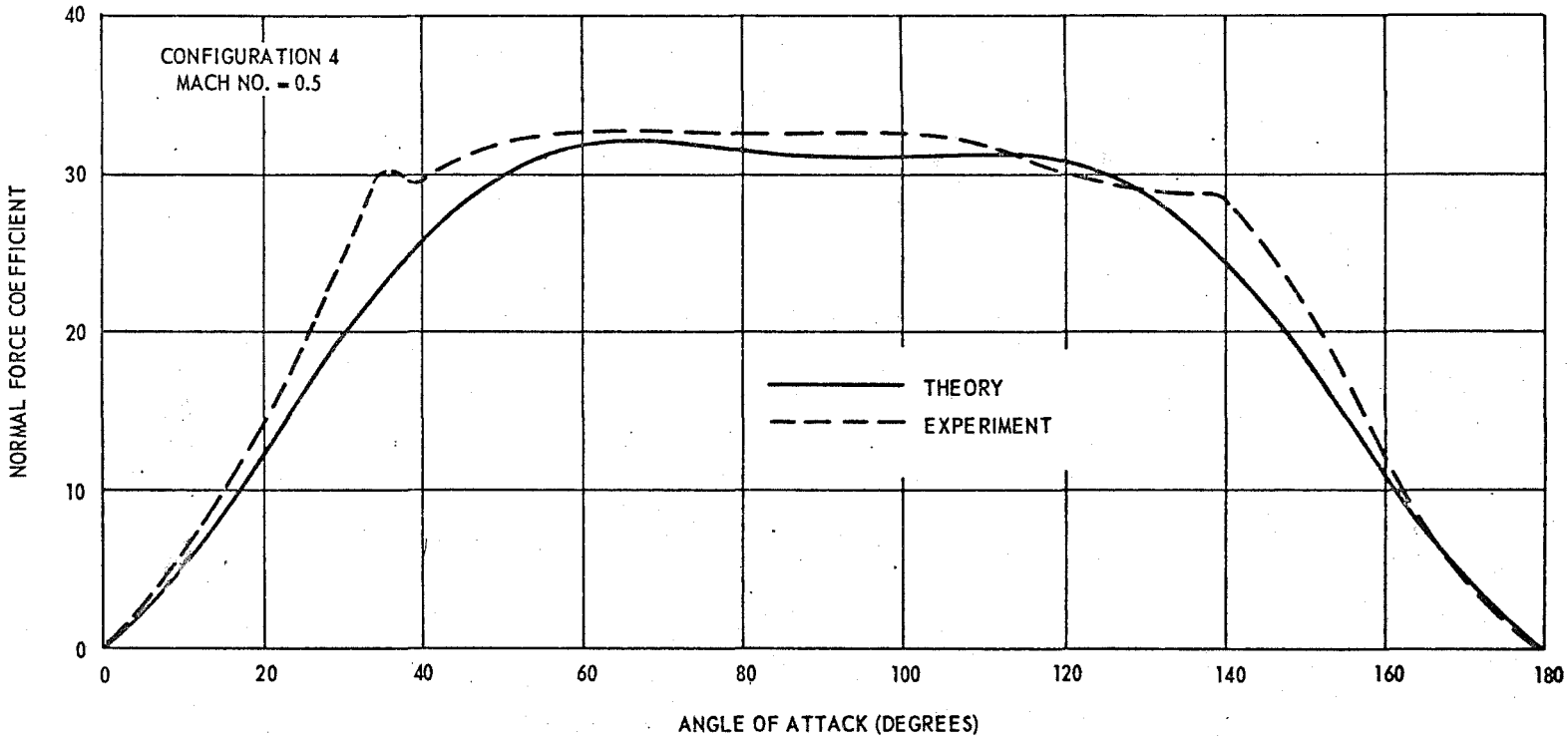

Figure 26 – Comparison of Experimental Data with Theoretical Results for Configuration 4

Table 1

COMPUTER PROGRAM LISTING

```
      DIMENSION XVXM(16),XDT(16),XAL(48)
      COMMON XVXM,XDT,XAL
      COMMON CN,CA,CNB,CNW,CNT,CNW2,CLW,CLT,CLW2,CLI,CLWB,CLVISW,CLIT,
     1       CLIW,CNTD,CAB,XCP2,XCG2,XCPB,XCPT,XCPW,XCPW2,XCG,XCPTV,
     2       XLAMT4
      COMMON LLKK,ISWPW,ISWPT,ISWPW2,IAFBW,IAFBT,IAFBW2,IL,LLLL,IJ,J,
     1       II,NBODY,IZZY,ICSC,INOSE,NM,NMLK,IDT,IM,IAL,ISWP1,IAFB
      COMMON XLAMW,XLAMT,XLAMW2,XMACW,XMACT,XMACW2,CLAMW,CLAMT,CLAMW2,
     1       BW,BT,BW2,CROOTW,CROOTT,CROOTW2,SW,ST,SW2,XWING,XTAIL,XWING2
     2       ,XL,D,D1,XLN,AREA,XREF,SSUBS,XLOB,ZF,ART,ARW,ARW2,XLNOSE
      COMMON COLAM,BCOLAM,CROOT,R1,CLAL1,XLAM1,BAR,RATIO,XKTB,XKBT,
     1       XKWB,XKBW,XBCRBW,XKWBW,XKWBT,XKWBW2,XKBWW,XKBWT,XKBWW2,
     2       XCPBW,XCPBT,XCPBW2,XCPWB,XCPTB,XCPWB2,XKWBI,ODC,ODCW,ODCT,
     3       ODCW2,CLALW,CLALT,CLALW2,REFT,BETA,AL,TONST,HONST,HT,XKTBI,
     4       VXM,VXMR1,DELTA,XKCRWB,XBCRWB,XMAC,XLAMW4,XLAM24,XLAM2,
     5       XLAM4,TOVC,TOVCT,TOVCW2,TOVCW,EXS,STTOT,SWTOT,SW2TOT,RE,
     6       CDO,CDOW,CDOT,CDOB,CDOW2,CLBW,CLWB2,CLBW2,CLTB,CLBT,CLTD,
     7       CLTDB,CLBDT,CLVIST,CLVIW2,CMB,CDOWBT
      COMMON DCDOSW,DCDOST,DCDOS2,DCDOW,DCDOT,DCDOW2
      COMMON CDALZ
       IL = 0
3040 FORMAT(2I5,7F10.5)
3050 FORMAT(6I5)
3020 FORMAT(7F10.3)
3010 FORMAT(10A6)
3110 FORMAT(1H1,10A6)
3120 FORMAT(6X,2HHT, 9X,2HD ,8X,2HXL,6X,6HXLNOSE,5X,3HXCG,6X,4HAREA,6X,
     14HXREF)
3021 FORMAT(//,5X,5HTOVCW,5X,6HTOVCW2,5X,5HTOVCT)
3140  FORMAT ( 3X, I5,  5X, I5,  4X, 7F15.6,//)
3150 FORMAT(4X,I5,5X,I5,5X,I5,5X,I5,6X,I5,5X,I5)
3240  FORMAT ( 6X,5HISWPW,  5X,5HIAFBW, 10X, 5HXLAMW, 10X, 5HCLAMW,
     1 10X,5H BW  ,9X,6HCROOTW,10X,5H SW  ,10X,5HXMACW,10X,5HXWING,/)
3244  FORMAT ( 6X,6HISWPW2, 4X,6HIAFBW2, 9X, 6HXLAMW2, 9X, 6HCLAMW2,
     1 10X,5H BW2 ,9X,6HCROOW2,10X,5H SW2 ,9X,6HXMACW2,9X,6HXWING2,/)
3248 FORMAT ( 6X,5HISWPT,  5X,5HIAFBT, 10X, 5HXLAMT, 10X, 5HCLAMT,
     1 10X,5H BT  ,9X,6HCROOTT,10X,5H ST  ,10X,5HXMACT,10X,5HXTAIL,/)
3241 FORMAT(//,6X,5HICSC ,5X,5HINOSE,5X,5HNDELT,5X,5HNMACH,5X,5HNALPH,
     15X,5HNBODY)
3333 READ 3010, TITL1,TITL2,TITL3,TITL4,TITL5,TITL6,TITL7,TITL8,TITL9,
     1TITLO
      READ 3050, ICSC,INOSE,IDT,IM,IAL,NBODY
      READ 3040, ISWPW,IAFBW,XLAMW,CLAMW,BW,CROOTW,SW,XMACW,XWING
      READ 3040, ISWPW2,IAFBW2,XLAMW2,CLAMW2,BW2,CROOW2,SW2,XMACW2,XWIN
     1G2
      READ 3040, ISWPT,IAFBT,XLAMT,CLAMT,BT,CROOTT,ST,XMACT,XTAIL
      READ 3020, HT,D,XL,XLNOSE,XCG,AREA,XREF
      READ 3020, TOVCW,TOVCW2,TOVCT
```

```
      PRINT 3110, TITL1,TITL2,TITL3,TITL4,TITL5,TITL6,TITL7,TITL8,TITL9,
     1TITLO
      PRINT 3241
      PRINT 3150, ICSC,INOSE,IDT,IM,IAL,NBODY
      PRINT 3240
      PRINT 3140, ISWPW,IAFBW,XLAMW,CLAMW,BW,CROOTW,SW,XMACW,XWING
      PRINT 3244
      PRINT 3140, ISWPW2,IAFBW2,XLAMW2,CLAMW2,BW2,CROOW2,SW2,XMACW2,
     1XWING2
      PRINT 3248
      PRINT 3140, ISWPT,IAFBT,XLAMT,CLAMT,BT,CROOTT,ST,XMACT,XTAIL
      PRINT 3120
      PRINT 3020, HT,D,XL,XLNOSE,XCG,AREA,XREF
      PRINT 3021
      PRINT 3020, TOVCW,TOVCW2,TOVCT
       IL = 1  + IL
      LLKK=0
      LLLL=0
       XCG2 = XCG
       IZZY = 0
      CALL GEOSUB
      READ 4000, [XDT[M],M=1,IDT]
      READ 4000, [XVXM[N],N=1,IM]
      READ 4000, [XAL[NA],NA=1,IAL]
      RE=REFT*VXM
      VXM=XVXM[1]
      DO 6002 IJ=1,IM
      DELTA1=XDT[1]
      DO 6001 II=1,IDT
      ALPHA=XAL[1]
4000  FORMAT[16F5.1]
5000  FORMAT[1H1,4HVXM=,F5.2,2X,6HDELTA=,F6.2,/]
5001  FORMAT[2X,2HAL,3X,5HCLTOT,2X,5HCDTOT,2X,4HCLWT,3X,4HCLTT,3X,3HCLB,
     14X,3HCLI,4X,3HCNW,4X,3HCNT,4X,4HCNTD,3X,3HCNB,5X,2HCN,5X,2HCA,4X,
     24HXCPW,3X,4HXCPT,3X,4HXCPB,3X,4HXCP2,4X,2HCM,/]
8200  PRINT 5000, VXM,DELTA1
      PRINT 5001
      DELTA=DELTA1/57.29578+.000000001
      DO 6000 J=1,IAL
      AL=ALPHA/57.29578+.00000001
    1 VXMR1=VXM
      IZZY=IZZY+1
       IF [IZZY - 4] 6666,6666,1111
6666  VXM=.6
1111  CALL CLASUB
      IF[LLLL-1] 900,942,980
 900  IF[IZZY-4] 6009,6009,925
 925   CALL CATSUB
6009  XLAM14=ATAN[[.5*[B1-D]*1./C0LAM+.25*XLAM1*CROOT-.25*CROOT]/
     1[.5*[B1-D]]]
      RE=REFT*VXM*XMAC
      IF [RE-1.E06] 6010,6020,6020
```

```
6C1C AA=.0835
     XNN=-.211
      GO TO 6070
6C2C IF (RE-1.E07) 6030,6040,6040
6C3C AA=.052
     XNN=-.177
      GO TO 6070
6C4C IF (RE-1.E08) 6050,6060,6060
6C5C AA=.0333
     XNN=-.1488
      GO TO 6070
6C6C AA=.0221
     XNN=-.127
6C7C CF=AA*RE**XNN
     CDO=4.*CF*(1.+2.*TOVC+100.*TOVC**4.)
     EXS=(D*D)/(8.*COLAM)
     IF (ISWP1-1) 6080,6080,6090
6C8C EXS=2.*EXS
6C9C EXS=(CROOT*D/2.+EXS)*2.
     IF (IZZY-4) 6091,6091,6092
6C91 IF (IZZY-3) 6093,6094,6095
6C92 IF (AL)  2401,2402,2402
2401 DDC=-DDC
2402 LLKK=LLKK+1
     IF (LLKK-2) 2403,2404,2420
2403 IF (SW) 2410,2410,2420
2410 LLKK=LLKK+1
2404 IF (SW2) 2411,2411,2420
2411 LLKK=LLKK+1
2420 IF (LLKK-2) 930,943,950
 930 XKWBW=XKWB
     XKBWW=XKBW
     XCPWB=XWING+XBCRWB*CROOT
     XCPBW=XWING+XBCRBW*CROOT
     DDCW=DDC
 960 CLW=SIN(AL)*(XKWBW+XKBWW)*CLALW*SW*COS(AL)/AREA
     CLWB=SIN(AL)*XKWBW*CLALW*SW*COS(AL)/AREA
     CLBW=CLW-CLWB
     CLVISW=    (SIN(AL)*SIN(AL)*SW*COS(AL)/AREA)*DDCW
     CLW=CLW+CLVISW
6C93 CDOW=CDO*(SW+EXS)/AREA
     XLAMW4=XLAM14
     TOVCW=TOVC
     SWTOT=SW+EXS
     IZZY=IZZY+1
     IF(SW2) 942,942,511
 511 COLAM=COS(CLAMW2)/SIN(CLAMW2)
     BCOLAM=BETA*COLAM
     CROOT=CROOW2
     B1=BW2
     IAFB=IAFBW2
     CLAL1=CLALW2
     XLAM1=XLAMW2
     TOVC=TOVCW2
     XMAC=XMACW2
     ISWP1=ISWPW2
```

```
      BAR=BETA*ARW2
      RATIO=CR00T/(BETA*D)
      IF(IZZY-4) 6009,6009,925
  943 XKWBW2=XKWB
      XKBWW2=XKBW
      XCPWB2=XWING2+XBCRWB*CR00T
      XCPBW2=XWING2+XBCRBW*CR00T
      ODCW2=ODC
  944 CLW2=SIN(AL)*((XKWBW2+XKBWW2)*CLALW2*SW2*COS(AL)/AREA
      CLWB2=SIN(AL)*XKWBW2*CLALW2*SW2*COS(AL)/AREA
      CLBW2=CLW2-CLWB2
      CLVIW2=(SIN(AL)*SIN(AL)*SW2*COS(AL)/AREA)*ODCW2
      CLW2=CLW2+CLVIW2
 6094 CDOW2=CD0*(SW2+EXS)/AREA
      XLAM24=XLAM14
      XLAM2=XLAM14
      SW2TOT=SW2+EXS
  942  IZZY = IZZY + 1
      LLKK=LLKK+2
       IF (ST) 980,980,940
  940 COLAM=COS(CLAMT)/SIN(CLAMT)
      ART=(BT-D)**2/ST
      BCOLAM=BETA*COLAM
      CR00T=CR00TT
      B1=BT
      BAR=BETA*ART
      CLAL1=CLALT
      IAFB=IAFBT
      XMAC=XMACT
      TOVC=TOVCT
      ISWP1=ISWPT
      XLAM1=XLAMT
      RATIO=CR00T/(BETA*D)
      IF (IZZY-4) 6009,6009,925
  950 XKWBT=XKWB
      XKBWT=XKBW
      XCPBT=XTAIL+XBCRBW*CR00T
      ODCT=ODC
  951 CLT=((XKWBT+XKBWT)*SIN(AL))*CLALT*ST*COS(AL)/AREA
      CLTB=SIN(AL)*XKWBT*CLALT*ST*COS(AL)/AREA
      CLBT=CLT-CLTB
      CLTDB=XKTB*CLALT*SIN(DELTA)*ST*COS(AL+DELTA)/AREA
      CLTD=(XKTB+XKBT)*CLALT*SIN(DELTA)*ST*COS(AL+DELTA)/AREA
      CLBDT=CLTD-CLTDB
      CLVIST=((SIN(AL+DELTA)*SIN(AL+DELTA))*ST*COS(AL+DELTA)/AREA)*ODCT
      CLT=CLT+CLVIST
 6095 CD0T=CD0*(ST+EXS)/AREA
      STTOT=ST+EXS
      XLAMT4=XLAM14
      IF (IZZY-4) 1610,1610,6098
 6098 XCPTB=XTAIL+((XKWBT*SIN(AL)*XBCRWB+XKTB*SIN(DELTA)*XBCRWB)/
     1(XKWBT*SIN(AL)+XKTB*SIN(DELTA)))*CR00TT
  980  IF (IZZY - 4) 1610, 1610, 1710
 1710  XLOD = XL/D
      ZXM=VXM*ABS(SIN(AL))
      IF (ZXM-.8) 1310,1350,1350
 1310 CDC=2.4*SQRT(1.5129-1.5129*ZXM*ZXM)
      GO TO 1391
```

```
1350 IF (ZXM-1.15) 1380,1370,1370
1380 CDC=1.6+SQRT(.0344-(ZXM-.975)**2)
     GO TO 1391
1370 IF (ZXM-3.) 1360,1381,1381
1360 CDC=1.9-SQRT(.361-.09*(ZXM-3.)**2)
     GO TO 1391
1381 CDC=1.3
1391 ETA=(0.000475*(XLOB**3))-(0.00173*(XLOB**2))+(0.0298*XLOB)+0.5146
     IF (VXM-.5) 1395,1395,1392
1392 IF (VXM-1.4) 1393,1394,1394
1393 ETA=ETA+(1.-ETA)*(VXM-.5)*1.1111111111111
     GO TO 1395
1394 ETA=1.
1395 IF (XLOB-10.) 1320,1330,1340
1320 XK2K1=-0.0054*(XLOB**2)+0.104*XLOB+0.437
     GO TO 1600
1330 XK2K1=0.939
     GO TO 1600
1340 XK2K1=0.939+(0.001525*(XLOB-10.0))
1600 ALP=AL
     IF(AL) 1602,1601,1601
1602 CDC=-CDC
1601 CMB=(XK2K1*SIN(2.*ALP)*COS(ALP/2.))*3.14159*D*D/(4.*AREA)
    1+ETA*CDC*((XL*D)/AREA)*((SIN(ALP))**2)
     XCG=XCG/D
     CMB1=(XK2K1*XCG*SIN(2.*ALP)*COS(ALP/2.))*3.14159*D*D*D/
    1(4.*AREA*XREF)
     CMB2=(ETA*CDC*((XL*D)/AREA)*((XCG-(XL/2.))/D)*((SIN(ALP)**2)))
    1*D/XREF
     CMB=CMB1+CMB2
1610 RE=REFT*VXM*XL
     IF (RE-1.E06) 1611,1612,1612
1611 AA=.0835
     XN=-.211
     GO TO 1617
1612 IF (RE-1.E07) 1613,1614,1614
1613 AA=.052
     XN=-.177
     GO TO 1617
1614 IF (RE-1.E08) 1615,1616,1616
1615 AA=.033
     XN=-.1488
     GO TO 1617
1616 AA=.0221
     XN=-.127
1617 CFBOD=AA*RE**XN
     CDBB=1.02*CFBOD*(1.+1.5/(XLOB**1.5)+7./(XLOB**3.))*SSUBS/AREA
     IF (IZZY-4) 1618,1618,1619
1618 VXM=1.1999999
     IF (SW) 1620,1620,1621
1620 CDBW=0.
1621 IF (SW2) 1622,1622,1623
1622 CDBW2=0.
1623 IF (ST) 1624,1624,1625
1624 CDBT=0.
1625 CDBST=CDBW+CDBW2+CDBT+CDBB
```

```
      GO TO 1639
1619  IF (VXM-1.2) 1631,1631,1632
1631  IF (VXM-.8) 1638,1638,1639
1638  CDALZ=CD0B
      CD0WBT=CD0B+CD0W+CD0T+CD0W2
      GO TO 1663
1639   IF (SW) 1700,1700,1701
1700   DCD0SW = 0.0
       SWT0T=0.0
       CD0W = 0.0
       GO TO 1702
1701   XXM = VXM*SQRT(COS(XLAMW4))
      SQMITC=SQRT(ABS((XXM*XXM)-1.0))/(T0VCW**0.33333)
      ATC=ARW*(T0VCW**.333333)
      IZT=1
1640  IF (ATC-1.5) 1641,1642,1642
1642  IF (VXM-1.) 1643,1643,1644
1643  FUNCT=3.3081-1.88779*SQMITC+11.0916*SQMITC*SQMITC-18.6087*
     1SQMITC**3+7.4633*SQMITC**4
      GO TO 1650
1644  FUNCT=3.4
      GO TO 1650
1641  IF (ATC-.5) 1645,1645,1646
1646  IF (VXM-1.) 1647,1647,1648
1647  FUNCT=2.47917-1.42798*SQMITC-.324405*SQMITC*SQMITC
      GO TO 1650
1648  FUNCT=2.5*ATC
      GO TO 1650
1645  IF (VXM-1.) 1649,1649,1651
1649  FUNCT=.5325-.47202*SQMITC+.08631*SQMITC*SQMITC
      GO TO 1650
1651  FUNCT=.55917+.33333*SQMITC-.071429*SQMITC*SQMITC
1650  IF (IZT-2) 1652,1653,1654
1652  DCD0SW=FUNCT*(T0VCW**1.66667)*((COS(XLAMW4))**2.5)
      DCD0W=DCD0SW
1702   IF (SW2) 1703,1703,1704
1703   DCD0S2 = 0.0
       SW2T0T = 0.0
       CD0W2= 0.0
       GO TO 1705
1704   IZT = 2
      XXM=VXM*SQRT(COS(XLAM24))
      SQMITC=SQRT(ABS((XXM*XXM)-1.))/(T0VCW2**0.33333)
      ATC=ARW2*(T0VCW2**.33333)
      GO TO 1640
1653  DCD0S2=FUNCT*(T0VCW2**1.66667)*((COS(XLAM24))**2.5)
      DCD0W2=DCD0S2
1705   IF (ST ) 1706,1706,1707
1706   DCD0ST = 0.0
      STT0T=0.0
       CD0T = 0.0
       GO TO 1708
1707   IZT = 3
      XXM=VXM*SQRT(COS(XLAMT4))
      SQMITC=SQRT(ABS((XXM*XXM)-1.))/(T0VCT**0.33333)
      ATC=ART*(T0VCT**.33333)
      GO TO 1640
```

```
1654 DCD0ST=FUNCT*[T0VCT**1.66667]*[[C0S[XLAMT4]]**2.5]
     DCD0T=DCD0ST
1708  C0VC = 1.31213-0.36633*VXM+.06038*VXM**2-.00601*VXM**3+.000275*
    1VXM**4
      CDFPTR=1.02*CFB0D*C0VC*SSUBS/AREA
       CDPPTR=CD0B-1.02*CFB0D*SSUBS/AREA
      IF[VXM-1.0] 1709,1709,1711
1711 CDPPTR=[CDPPTR/0.2]*[1.2-VXM]
1709 FR=XLN0SE/D
      CDWN1=0.000407*[FR**8]-0.0102*[FR**7]+0.108*[FR**6]-0.616*[FR**5]
    1+2.074*[FR**4]-4.183*[FR**3]+4.891*[FR**2]-3.017*FR+0.7795
      CDWN2=0.000172*[FR**8]-0.00453*[FR**7]+0.050*[FR**6]-0.304*[FR**5]
    1+1.096*[FR**4]-2.406*[FR**3]+3.160*[FR**2]-2.391*[FR]+1.000
      CDWN3=.000125*[FR**8]-.00370*[FR**7]+.0447*[FR**6]-.288*[FR**5]
    1+1.076*[FR**4]-2.385*[FR**3]+3.141*[FR**2]-2.529*FR+1.300
      IF[VXM-0.8] 1664,1661,1662
1661 CDPTR=CDWN1
      GO TO 1658
1662 IF[VXM-1.0] 1655,1665,1666
1665 CDPTR=CDWN2
      GO TO 1658
1655 CDPTR=[[CDWN2-CDWN1]/0.2]*[VXM-0.8]+CDWN1
      GO TO 1658
1666 IF[VXM-1.2] 1667,1668,1664
1668 CDPTR=CDWN3
      GO TO 1658
1667 CDPTR=[[CDWN3-CDWN2]/0.2]*[VXM-1.0]+CDWN2
      GO TO 1658
1664 CDPTR=0.0
1658 CD0B=CDFPTR+CDPPTR+CDPTR*VXM*3.14159*D*D/[4.*AREA]
      CDALZ=CD0B
      CD0T=1.1*[DCD0ST*[STT0T/AREA]+CD0T]
      CD0W=1.1*[DCD0SW*[SWT0T/AREA]+CD0W]
      CD0W2=1.1*[CD0W2+DCD0S2*[SWT0T/AREA]]
      CD0WBT=1.1*[CD0W+DCD0SW*[SWT0T/AREA]+CD0W2+DCD0S2*[SW2T0T/AREA]
    1+CD0T+DCD0ST*[STT0T/AREA]+CD0B]
      IF [IZZY-4] 1659,1659,1663
1659 T0NST=CD0WBT
      H0NST=H0NST+ZF*[T0NST-H0NST]
      VXM=VXMR1
       IZZY = IZZY + 1
      GO TO 1
1632 CD0WBT=[[H0NST-T0NST]/[SQRT[3.]-SQRT[1.2]]]*SQRT[VXM]+T0NST
    1+[H0NST-T0NST]/[1.-SQRT[3.]/SQRT[1.2]]
      CD0T=1.1*[DCD0T *[STT0T/AREA]+CD0T]
      CD0W=1.1*[DCD0W *[SWT0T/AREA]+CD0W]
      CD0W2=1.1*[CD0W2+DCD0W2*[SWT0T/AREA]]
      CD0B=CD0WBT-CD0T-CD0W-CD0W2
      CDALZ=CD0B
1663 CDB=XK2K1*SIN[2.*AL]*SIN[AL/2.]*3.14159*D*D/[4.*AREA]+ETA*CDC*XL
    1*D*[[SIN[AL]]**3]/AREA
      CLB=XK2K1*[SIN[2.*AL]]*C0S[AL/2.]*3.14159*D*D/[4.*AREA]+ETA*CDC*XL
    1*D*[[SIN[AL]]**2]*C0S[AL]/AREA-CDALZ*C0S[AL]*C0S[AL]*SIN[AL]
      CA5=CD0WBT
      IF[AL] 1603,1604,1603
```

```
1604 XCPB=0.0
     GO TO 1605
1603 XCPB=[[XCG/XREF]-[CMB/CNB]]*XREF
1605 IF [SW] 1607,1607,1606
1606 IF [ST] 2973,2973,1608
1607 IF [ST] 1990,1990,2974
1608 R=D/2.
      IF [ICSC - 1] 1970,1970,1971
1971 XB1=BW/2.
     XB2=BT/2.
     TT=D/BT
     HW1=-0.5*CR00TT*ABS[SIN[DELTA]]+[XCPWB-XTAIL-CR00TT]*ABS[SIN[AL]]
     XLAM1=XLAMW
     GO TO 1969
1970 XB1=BT/2.
     XB2=BW/2.
     TT=D/BW
     HW1=[XCPTB-XWING-CR00TW]*ABS[SIN[AL]]
     XLAM1=XLAMT
1969 FTRT=[[XB2-R]/[2.*[1.-TT]]]*[[3.14159/4.]-[[3.14159*TT**2]/4.]-TT+
    1[[[1.+TT**2]**2]/[2.*[1.-TT**2]]]*ARSIN[[1.-TT**2]/[1.+TT**2]]]
     FW=FTRT+R
     FI1=[FW*R**2]/[[FW**2]+[HW1**2]]
     HI1=[HW1*R**2]/[[FW**2]+[HW1**2]]
     ZC=FW
     ZD=HW1
     ZLT=0.0
     DO 1800 I=1,4
     ZL1=[[XB1-[XLAM1*R]]-[ZC*[1.-XLAM1]]]/[2.*[XB1-R]]
     ZL2=ALOG[[[ZD**2]+[[ZC-XB1]**2]]/[[ZD**2]+[[ZC-R]**2]]]
     ZL3=[[1.-XLAM1]/[XB1-R]]*[[XB1-R]+[ZD*[ATAN[[ZC-XB1]/ZD]-ATAN[[ZC-
    1R]/ZD]]]]
     ZL=[ZL1*ZL2]-ZL3
     IF[I-2] 1810,1820,1820
1810 ZC=-ZC
     GO TO 1850
1820 IF[I-3] 1830,1840,1850
1830 ZL=-ZL
     ZC=FI1
     ZD=HI1
     GO TO 1850
1840 ZL=-ZL
     ZC=-FI1
1850 ZLT=ZLT+ZL
1800 CONTINUE
     IF[ICSC-1] 2970,2970,2971
2970 ART=[BT-D]**2/ST
     XBT=BT/2.
     CLI=[CLALW*CLALT*XKWBI*SIN[AL]*SW*2.*ZLT*[XBT-R]]/[2.*3.14159*ART*
    1FTRT*AREA*[1.+XLAMT]]
     CLI=CLI*COS[AL]
     CLT=CLT+CLI
     CLIT=CLI
     CLIW=0.
     XCPTV=XCPTB
     GO TO 2972
```

```
2971 ARW=(BW-D)**2/SW
     XBW=BW/2.
     CLI=(CLALW*CLALT*(XKWBI*SIN(AL)+XKTBI*SIN(DELTA))*ST*2.*ZLT*(XBW-
    1R))/(2.*3.14159*ARW*FTRT*AREA*(1.+XLAMW))
     CLI=CLI*COS(AL)
     CLW=CLW+CLI
     CLIW=CLI
     CLIT=0.
     XCPTV=XCPWB
     GO TO 2972
2973 CLT=0.
     CLALT=0.
     CLTD=0.
     CDTD=0.
     CLBT=0.
     CLBDT=0.
     CLTB=0.
     CLTDB=0.
     CLVIST=0.
     CLIT=0.
     CLIW=0.
     CLI=0.
     GO TO 2972
2974 CLW=0.
     CLALW=0.
     CLBW=0.
     CLWB=0.
     CLVISW=0.
     CLIW=0.
     CLIT=0.
     CLI=0.
2972 IF (SW2) 700,700,701
 700 CLW2=0.
     CLALW2=0.
     CLBW2=0.
     CLWB2=0.
     CLVIW2=0.
 701 ALPHA=AL
     IF(VXM-0.5) 1975,1976,1976
1975 XK=1.17
     GO TO 1973
1976 IF(VXM-1.) 1977,1978,1978
1977 XK=2.0-SQRT(0.764-(VXM-0.126)**2)
     GO TO 1973
1978 IF(VXM-2.0) 1979,1979,1980
1979 XK=2.0-SQRT(1.298-(VXM-2.13 )**2)
     GO TO 1973
1980 XK=0.87
1973 CDT=XK*ABS(SIN(AL))*ST/AREA
     CDW=XK*ABS(SIN(AL))*SW/AREA
     CDW2=XK*ABS(SIN(AL))*SW2/AREA
     CDD=XK*ABS(SIN(AL+DELTA))*ST/AREA
     CDTD=CDD-CDT
     CATD=CDTD*COS(AL)-CLTD*SIN(AL)
     CNTD=CLTD*COS(AL)+CDTD*SIN(AL)
     CNT=CLT*COS(ALPHA)+CDT*SIN(ALPHA)
     CAT=CDT*COS(ALPHA)-CLT*SIN(ALPHA)
     CAW2=CDW2*COS(AL)-CLW2*SIN(AL)
```

```
      CAW=CDW*COS(ALPHA)-CLW*SIN(ALPHA)
      CNW=CLW*COS(ALPHA)+CDW*SIN(ALPHA)
      CNW2=CLW2*COS(AL)+CDW2*SIN(AL)
      CAB=CDB*COS(AL)-CLB*SIN(AL)
      CA5=CAT+CAW+CAW2+CATD+CAB
      GO TO 1991
 1990 CN=CNB
      XCP2=XCPB
      CA=CA5
      CLTOT=CLB
      CDTOT=CDB+CA*COS(AL)*COS(AL)
      CLALT=0.
      CLALW=0.
      CDT=0.
      CDD=0.0
      CDW=0.
      CATD=0.
      CNTD=0.
      CNT=0.
      CAT=0.
      CAW=0.
      CNW=0.
      CLW=0.
      CLT=0.
      CLI=0.
      CLTT=0.
      CLWT=0.
      CLALW2=0.
      CPW2=0.
      CAW2=0.
      CNTT=0.
      CNWT=0.
CNWT2=0.
      CNW2=0.
      CLW2=0.
      CLW2T=0.
      XCPW2=0.
      XCPT=0.
      XCPW=0.
      GO TO 1992
 1991 CN=CNB+CNW+CNT+CNTD+CNW2
      CLTT=CLBT+CLTB+CLBDT+CLTDB+CLIT+CLVIST
      CLWT=CLBW+CLWB+CLIW+CLVISW+CLBW2+CLWB2+CLVIW2
      CNTT=(CLIT+CLTB+CLBT+CLVIST)*COS(AL)+CDT*SIN(AL)+CLTDB+CLBDT
      CNWT=(CLIW+CLWB+CLBW+CLVISW)*COS(AL)+CDW*SIN(AL)
      CNWT2=( CLWB2+CLBW2+CLVIW2)*COS(AL)+CDW2*SIN(AL)
      CLTOT=CLTT+CLWT+CLB
      CDTOT=CDB+CDW+CDD+CDW2+CDBWBT
      CA=CDTOT*COS(AL)-CLTOT*SIN(AL)
       IF (ST) 9901,9901,9902
9902 XCPT=((CLTB*COS(AL)+CDD*SIN(AL))*XCPTB+CLBT*COS(AL)*XCPBT+CLTDB*
     1XCPTB+CLBDT*XCPBT+CLIT*COS(AL)*XCPTB+CLVIST*COS(AL)*XCPTB)/CNTT
9901 IF (SW) 9903,9903,9904
9904 XCPW=((CLWB*COS(AL)+CDW*SIN(AL))*XCPWB+CLBW*COS(AL)*XCPBW+CLIW*
     1COS(AL)*XCPWB+CLVISW*COS(AL)*XCPWB)/CNWT
       IF (SW2) 9903, 9903, 1993
```

```
1993 XCPW2=[[CLWB2*COS[AL]+CDW2*SIN[AL]]*XCPWB2+CLBW2*COS[AL]*XCPBW2
    1+CLVIW2*COS[AL]*XCPWB2]/CNWT2
9903 IF [SW2] 1994,1994,1995
1994 XCPW2=0.
     CNWT2=0.
     IF [SW] 1997,1997,1995
1995 XCPW=[[XCPW        ]*CNWT+[XCPW2        ]*CNWT2]/[CNWT+CNWT2]
     CNWT=CNWT+CNWT2
     IF [SW] 1997,1997,1998
1997 XCPW=0.
1998 IF [ST] 1999,1999,1996
1999 XCPT=0.
1996 XCP2=[CNB*XCPB+XCPT*CNTT+XCPW*CNWT]/[CNB+CNTT+CNWT]
1992 CM=CN*[XCG2-XCP2]/XREF
7001 AL1=AL*57.29578
8700 PRINT 5002, AL1,CLT0T,CDT0T,CLWT,CLTT,CLB,CLI,CNWT,CNTT,CNTD,CNB,
    1CN,CA,XCPW,XCPT,XCPB,XCP2,CM
5002 FORMAT [1X,F4.0,17[1X,F6.2]]
     ALPHA=XAL[J+1]
6000 CONTINUE
     PRINT 9400, CLALT,CLALW,CLALW2
9400 FORMAT[//,2X,6HCLALT=,F6.3,5X,6HCLALW=,F6.3,5X,7HCLALW2=,F6.3]
     DELTA1=XDT[II+1]
6001 CONTINUE
     VXM=XVXM[IJ+1]
6002 CONTINUE
     IF[NBODY-IL] 3334,3334,3333
3334 CONTINUE
     STOP
     END
```

```
      SUBROUTINE GEOSUB
      DIMENSION XVXM(16),XDT(16),XAL(48)
      COMMON XVXM,XDT,XAL
      COMMON CN,CA,CNB,CNW,CNT,CNW2,CLW,CLT,CLW2,CLI,CLWB,CLVISW,CLIT,
     1       CLIW,CNTD,CAB,XCP2,XCG2,XCPB,XCPT,XCPW,XCPW2,XCG,XCPTV,
     2       XLAMT4
      COMMON LLKK,ISWPW,ISWPT,ISWPW2,IAFBW,IAFBT,IAFBW2,IL,LLLL,IJ,J,
     1       II,NBODY,IZZY,ICSC,INOSE,NM,NMLK,IDT,IM,IAL,ISWP1,IAFB
      COMMON XLAMW,XLAMT,XLAMW2,XMACW,XMACT,XMACW2,CLAMW,CLAMT,CLAMW2,
     1       BW,BT,BW2,CROOTW,CROOTT,CROOW2,SW,ST,SW2,XWING,XTAIL,XWING2
     2       ,XL,D,D1,XLN,AREA,XREF,SSUBS,XLOB,ZF,ART,ARW,ARW2,XLNOSE
      COMMON COLAM,BCOLAM,CROOT,B1,CLAL1,XLAM1,BAR,RATIO,XKTB,XKBT,
     1       XKWB,XKBW,XBCRBW,XKWBW,XKWBT,XKWBW2,XKBWW,XKBWT,XKBWW2,
     2       XCPBW,XCPBT,XCPBW2,XCPWB,XCPTB,XCPWB2,XKWBI,BDC,BDCW,BDCT,
     3       BDCW2,CLALW,CLALT,CLALW2,REFT,BETA,AL,TONST,HONST,HT,XKTBI,
     4       VXM,VXMR1,DELTA,XKCRWB,XBCRWB,XMAC,XLAMW4,XLAM24,XLAM2,
     5       XLAM4,TOVC,TOVCT,TOVCW2,TOVCW,EXS,STTOT,SWTOT,SW2TOT,RE,
     6       CDO,CDOW,CDOT,CDOB,CDOW2,CLBW,CLWB2,CLBW2,CLTB,CLBT,CLTD,
     7       CLTDB,CLBDT,CLVIST,CLVIW2,CMB,CDOWBT
      COMMON DCDOSW,DCDOST,DCDOS2,DCDOW,DCDOT,DCDOW2
      COMMON CDALZ
       DRAT = XLNOSE/D
       D1=D
       XLOB = XL/D
      IF(CLAMW-5.) 10,10,20
   10 CLAMW=5.
   20 IF(CLAMW2-5.) 30,30,40
   30 CLAMW2=5.
   40 IF(CLAMT-5.) 50,50,60
   50 CLAMT=5.
   60 CONTINUE
      CLAMW=CLAMW/57.29578
      CLAMT=CLAMT/57.29578
      CLAMW2=CLAMW2/57.29578
      IF (INOSE-1) 1571,1572,1571
 1572 SS1=8.+3.*(DRAT-2.5)
      GO TO 1579
 1571 IF (INOSE-2) 1573,1574,1573
 1574 SS1=4.+8.*(DRAT-1.5)/3.
      GO TO 1579
 1573 IF(INOSE-3) 1579,1576,1579
 1576 SS1=4.+2.*(DRAT-1.87)
 1579 SSUBS=SS1*(3.14159*D*D/4.)+3.14159*D*(XL-XLNOSE)
      IF (DRAT-.6) 1580,1580,1581
 1580 ZF=1.
      GO TO 1594
 1581 ZF=1.522*EXP(-.7*DRAT)
 1594 Z=HT*0.001
      IF(HT-35332.0) 1595,1595,1596
 1595 T=519.-HT/280.
       PS=(1.91-0.01315*Z)**5.256
      GO TO 1597
 1596 T=393.
      B=1.69-0.00478*Z
      PS=6.49*EXP(B)
```

```
1597 C=49.1*SQRT(T)
     PS=PS*70.9
     RHO=PS/(1715.*T)
     XMU=2.270*(T**1.5)/((T+198.6)*(10.**8))
     REFT=(C*RHO)/XMU
     RETURN
     END
```

```
      SUBROUTINE CLASUB
      DIMENSION XVXM(16),XDT(16),XAL(48)
      COMMON XVXM,XDT,XAL
      COMMON CN,CA,CNB,CNW,CNT,CNW2,CLW,CLT,CLW2,CLI,CLWB,CLVISW,CLIT,
     1       CLIW,CNTD,CAB,XCP2,XCG2,XCPB,XCPT,XCPW,XCPW2,XCG,XCPTV,
     2       XLAMT4
      COMMON LLKK,ISWPW,ISWPT,ISWPW2,IAFBW,IAFBT,IAFBW2,IL,LLLL,IJ,J,
     1       II,NBODY,IZZY,ICSC,INOSE,NM,NMLK,IDT,IM,IAL,ISWP1,IAFB
      COMMON XLAMW,XLAMT,XLAMW2,XMACW,XMACT,XMACW2,CLAMW,CLAMT,CLAMW2,
     1       BW,BT,BW2,CROOTW,CROOTT,CROOW2,SW,ST,SW2,XWING,XTAIL,XWING2
     2       ,XL,D,D1,XLN,AREA,XREF,SSUBS,XLOB,ZF,ART,ARW,ARW2,XLNOSE
      COMMON COLAM,BCOLAM,CROOT,B1,CLAL1,XLAM1,BAR,RATIO,XKTB,XKBT,
     1       XKWB,XKBW,XBCRBW,XKWBW,XKWBT,XKWBW2,XKBWW,XKBWT,XKBWW2,
     2       XCPBW,XCPBT,XCPBW2,XCPWB,XCPTB,XCPWB2,XKWBI,ODC,ODCW,ODCT,
     3       ODCW2,CLALW,CLALT,CLALW2,REFT,BETA,AL,TONST,HONST,HT,XKTBI,
     4       VXM,VXMR1,DELTA,XKCRWB,XBCRWB,XMAC,XLAMW4,XLAM24,XLAM2,
     5       XLAM4,TOVC,TOVCT,TOVCW2,TOVCW,EXS,STTOT,SWTOT,SW2TOT,RE,
     6       CDO,CDOW,CDOT,CDOB,CDOW2,CLBW,CLWB2,CLBW2,CLTB,CLBT,CLTD,
     7       CLTDB,CLBDT,CLVIST,CLVIW2,CMB,CDOWBT
      COMMON DCDOSW,DCDOST,DCDOS2,DCDOW,DCDOT,DCDOW2
      COMMON CDALZ
      IF(VXM-1.)2,2,3
    2 BETA=SQRT(1.-VXM**2)
      GO TO 4
    3 BETA=SQRT(VXM**2-1.)
    4 IF(IZZY-4)902,902,1111
 1111 IF(VXM-1.)41,42,41
   42 BETA=0.CC00001
   41 KFIN=0
      KFIN=KFIN+1
       IF (SW) 504,504,411
  411 ARW = (BW - D)**2/SW
      BAR=BETA*ARW
      ISWP=ISWPW
      XLAM=XLAMW
      AR=ARW
  505 IF (ISWP-1) 5,5,200
    5 IF (XLAM-.25) 60,10,10
   10 IF(VXM-1.0) 20,20,30
   20 CLAR=-.1833*BAR+1.6
      GO TO 370
   30 IF(BAR-1.) 50,40,40
   40 CLAR=1.508*(1.26)**(2.-BAR)
      GO TO 370
   50 CLAR=.3*BAR+1.6
      GO TO 370
   60 IF(VXM-1.) 70,70,80
   70 CLAR=-.1667*BAR+1.575
      GO TO 370
   80 IF(BAR-1.) 90,90,100
   90 CLAR=.1667*BAR+1.575
      GO TO 370
  100 IF(BAR-2.) 110,110,120
  110 CLAR=1.7417
      GO TO 370
```

← sel-Bo Wing 1.

```
120 CLAR=1.428*[1.22]**[2.*BAR]
    GO TO 370
200 IF [XLAM=.1] 210,260,260
210 IF[VXM=1.] 220,220,230
220 CLAR=-.2077*BAR+1.575
    GO TO 370
230 IF[BAR=.25] 240,240,250
240 CLAR=.2077*BAR+1.575
    GO TO 370
250 IF[BAR=4.] 251,251,252
251 CLAR=-.1668*BAR+1.667
    GO TO 370
252 CLAR=1.587*[1.26]**[2.*BAR]
    GO TO 370
260 IF [XLAM=.3] 270,320,320
270 IF[VXM=1.] 280,280,290
280 CLAR=-.2065*BAR+1.6
    GO TO 370
290 IF[BAR=0.75] 300,300,310
300 CLAR=.2065*BAR+1.6
    GO TO 370
310 IF[BAR=2.5] 311,311,312
311 CLAR=-.217*BAR+2.293
    GO TO 370
312 CLAR=1.543*[1.26]**[2.*BAR]
    GO TO 370
320 IF[VXM=1.] 330,330,340
330 CLAR=-.225*BAR+1.675
    GO TO 370
340 IF[BAR=1.] 350,350,360
350 CLAR=.225*BAR+1.675
    GO TO 370
360 CLAR=1.508*[1.26]**[2.*BAR]
370 IF[AR-1.0] 800,800,810
800 ARR=1.0
    GO TO 820
810 ARR=1./[AR**[[AR-1.]/AR]]
820 CLAL=CLAR*ARR*AR
     IF [KFIN-2] 500,501,502
500 CLALW=CLAL
    GO TO 503
501  CLALW2=CLAL
    GO TO 503
502 CLALT=CLAL
503 IF [KFIN-2] 504,507,900
504 KFIN=KFIN+1
    IF [SW2] 507,507,506
506 AR=[BW2-D]**2/SW2
    BAR=BETA*AR
    ISWP=ISWPW2
    ARW2=AR
    XLAM=XLAMW2
    GO TO 505
```

set for wing 2 go back + start over

```
  507 KFIN=KFIN+1
      IF (ST) 509,509,508
  508 AR=(BT+D)**2/ST
      BAR=BETA*AR
      ART=AR
      ISWP=ISWPT
      XLAM=XLAMT
      GO TO 505
  509 IF (SW) 5100,5100,900
 5100 IF (SW2) 5110,5110,900
 5110 IF (ST) 980,980,900
  980 LLLL=2
      RETURN
  900 LLKK=0
  902  IZZY = IZZY + 1
      IF (SW) 510,510,901
  901 COLAM= COS(CLAMW)/(SIN(CLAMW))
      ARW=(BW+D)**2/SW
      BCOLAM=BETA*COLAM
      CROOT=CROOTW
      B1=BW
      IAFB=IAFBW
      XMAC=XMACW
      TOVC=TOVCW
      CLAL1=CLALW
      XLAM1=XLAMW
      ISWP1=ISWPW
      BAR=BETA*ARW
      RATIO=CROOT/(BETA*D)
      LLLL=0
      RETURN
  510  IZZY = IZZY + 1
       IF (SW2) 942,942,511
  942 LLLL=1
      RETURN
  511 COLAM=COS(CLAMW2)/(SIN(CLAMW2))
      BCOLAM=BETA*COLAM
      CROOT=CROOTW2
      B1=BW2
      IAFB=IAFBW2
      CLAL1=CLALW2
      XLAM1=XLAMW2
      XMAC=XMACW2
      TOVC=TOVCW2
      ISWP1=ISWPW2
      ARW2=(BW2+D)**2/SW2
      BAR=BETA*ARW2
      RATIO=CROOT/(BETA*D)
      LLLL=0
      RETURN
      END
```

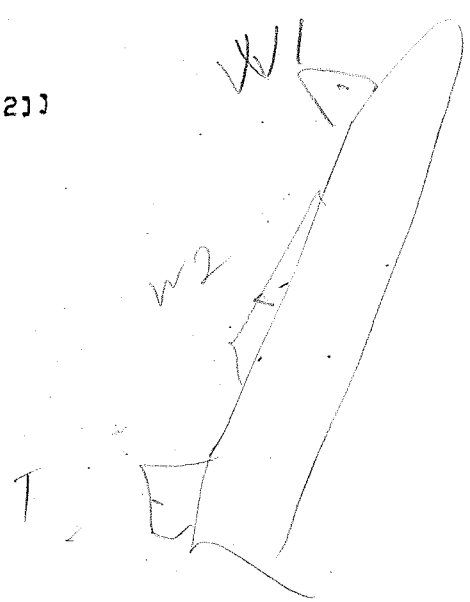

```
      SUBROUTINE CATSUB
      DIMENSION XVXM(16),XDT(16),XAL(48)
      COMMON XVXM,XDT,XAL
      COMMON CN,CA,CNB,CNW,CNT,CNW2,CLW,CLT,CLW2,CLI,CLWB,CLVISW,CLIT,
     1       CLIW,CNTD,CAB,XCP2,XCG2,XCPB,XCPT,XCPW,XCPW2,XCG,XCPTV,
     2       XLAMT4
      COMMON LLKK,ISWPW,ISWPT,ISWPW2,IAFBW,IAFBT,IAFBW2,IL,LLLL,IJ,J,
     1       II,NBODY,IZZY,ICSC,INOSE,NM,NMLK,IDT,IM,IAL,ISWP1,IAFB
      COMMON XLAMW,XLAMT,XLAMW2,XMACW,XMACT,XMACW2,CLAMW,CLAMT,CLAMW2,
     1       BW,BT,BW2,CROOTW,CROOTT,CROOW2,SW,ST,SW2,XWING,XTAIL,XWING2
     2       ,XL,D,D1,XLN,AREA,XREF,SSUBS,XLOB,ZF,ART,ARW,ARW2,XLNOSE
      COMMON COLAM,BCOLAM,CROOT,B1,CLAL1,XLAM1,BAR,RATIO,XKTB,XKBT,
     1       XKWB,XKBW,XBCRBW,XKWBW,XKWBT,XKWBW2,XKBWW,XKBWT,XKBOW2,
     2       XCPBW,XCPBT,XCPBW2,XCPWB,XCPTB,XCPWB2,XKWB1,BDC,BDCW,BDCT,
     3       BDCW2,CLALW,CLALT,CLALW2,REFT,BETA,AL,TONST,HONST,HT,XKTB1,
     4       VXM,VXMR1,DELTA,XKCRWB,XBCRWB,XMAC,XLAMW4,XLAM24,XLAM2,
     5       XLAM4,TOVC,TOVCT,TOVCW2,TOVCW,EXS,STTOT,SWTOT,SW2TOT,RE,
     6       CDO,CDOW,CDOT,CDOB,CDOW2,CLBW,CLWB2,CLBW2,CLTB,CLBT,CLTD,
     7       CLTDB,CLBDT,CLVIST,CLVIW2,CMB,CDOWBT
      COMMON DCDOSW,DCDOST,DCDOSP,DCDOW,DCDOT,DCDOW2
      COMMON CDALZ
      XKWB=(2./3.14159)*((1.+D**4/B1**4)*(.5*ATAN(.5*(B1/D-D/B1))+3.1415
     19/4.)-(D**2/B1**2)*((B1/D-D/B1)+2.*ATAN(D/B1)))/(1.-D/B1)**2
  926 XKTB1=((3.14159)**2*D**2*(B1/D+1.)**2)/(4.*B1**2)+(3.14159*D**2*(B
     11**2/D**2+1.)**2/(B1**2*(B1/D-1.)**2))*ARSIN((B1**2/D**2-1.)/(B1**
     22/D**2+1.))
      XKTB2=2.*3.14159*D*(B1/D+1.)/(B1*(B1/D-1.))-((B1**2/D**2+1.)**2/((
     1B1**2/D**2)*(B1/D-1.)**2))*(ARSIN((B1**2/D**2-1.)/(B1**2/D**2+1.))
     2)**2
      XKTB3=(4.*D*(B1/D+1.)/(B1*(B1/D-1.)))*ARSIN((B1**2/D**2-1.)/(B1**2
     1/D**2+1.))-(8./(B1/D-1.)**2)*ALOG((B1**2/D**2+1.)/(2.*B1/D))
      XKTB=(1./(3.14159)**2)*(XKTB1-XKTB2-XKTB3)
      IF (ICSC-1) 970,970,971
  970 IF (LLKK) 972,972,973
  972 XKWB1=D/B1+1.
      XKTB1=XKTB
      GO TO 973
  971 IF (LLKK-1) 973,973,972
  973 BAREF=BAR*(1.+XLAM1)*((1./(BETA*COLAM))+1.)
      IF (BAREF-4.) 928,928,929
  928 XKBW=(1.+D/B1)**2-XKWB
      GO TO 1000
  929 IF (IAFB) 9291,9292,9291
 9291 IF (BCOLAM-1.) 932,931,931
  931 XKBW1=(BCOLAM/(1.+BCOLAM))*(((((BCOLAM+1.)*(1./RATIO)+BCOLAM)/BCOLA
     1M)**2)*ARCOS((1.+(1.+BCOLAM)*(1./RATIO))/(BCOLAM*(BCOLAM+1.)*(1./
     2RATIO))))
      XKBW2=(SQRT(BCOLAM**2-1.)/(BCOLAM+1.))*(SQRT(1.+2.*BETA*D/CROOT)-
     11.)-(SQRT(BCOLAM**2-1.)/BCOLAM)*(BETA*D/CROOT)**2*ALOG((1.+CROOT/(
     2BETA*D))+SQRT((1.+CROOT/(BETA*D))-1.))-(BCOLAM/(1.+BCOLAM))*ARCOS
     3(1./BCOLAM)
      XKBW=(8.*BCOLAM/(3.14159*SQRT(BCOLAM**2-1.)*(1.+XLAM1)*(BETA*D/
     1CROOT)*(B1/D-1.)*(BETA*CLAL1)))*(XKBW1+XKBW2)
      GO TO 1000
```

```
 932 XKBW1=((BC0LAM+(1.+BC0LAM)*BETA*D/CR00T)/BC0LAM)**1.5+((BC0LAM+(1.
    1+BC0LAM)*BETA*D/CR00T)/BC0LAM)**.5-2.
     XKBW2=(((1.+BC0LAM)*BETA*D/CR00T)/BC0LAM)**2+0.5*(AL0G(1.+SQRT(BC0
    1LAM/(BC0LAM+(1.+BC0LAM)*BETA*D/CR00T)))-AL0G(1.-SQRT(BC0LAM/(BC0LA
    2M+(1.+BC0LAM)*BETA*D/CR00T))))
     XKBW=(16.*(BC0LAM/(1.+BC0LAM))**2/(3.14159*(1.+XLAM1)*(BETA*D/
    1CR00T)*(B1/D-1.)*(BETA*CLAL1)))*(XKBW1-XKBW2)
     G0 T0 1000
9292 IF(BC0LAM-1.) 9295,9294,9294
9294 IF(RATI0-1.) 9293,9311,9311
9293 RATI0=1.
     D=CR00T/BETA
9311 XKB1=(1.+C0LAM*BETA*RATI0)**2*ARC0S((BC0LAM+RATI0)/(1.+C0LAM*BETA
    1*RATI0))
     XKB2=BC0LAM**2*RATI0**2*ARC0S(1./BC0LAM)-BC0LAM*RATI0**2*SQRT(BC0L
    1AM**2-1.)*ARSIN(1./RATI0)
     XKB3=SQRT(BC0LAM**2-1.)*AL0G(RATI0+SQRT(RATI0**2-1.))
     XKBW=((8./(3.14159*SQRT(BC0LAM**2-1.)*BETA*CLAL1*(XLAM1+1.)*(B1/D1
    1-1.)))*(1./RATI0))*(XKB1-XKB2-XKB3)
     G0 T0 1000
9295 IF(RATI0-1.) 9296,9312,9312
9296 RATI0=1.
     D=CR00T/BETA
9312 XKB1=(1.+C0LAM*BETA*RATI0)*SQRT((RATI0-1.)*(C0LAM*BETA*RATI0+1.))
     XKB2=RATI0**2*(BC0LAM)**1.5-BC0LAM*RATI0**2*(BC0LAM+1.)*(ATAN(SQRT
    1(1./BC0LAM))-ATAN(SQRT((RATI0-1.)/(C0LAM*BETA*RATI0+1.))))
     XKB3=((BC0LAM+1.)/SQRT(BC0LAM))*0.5*(AL0G(1.+SQRT(BC0LAM*(RATI0-1.
    1)/(C0LAM*BETA*RATI0+1.)))-AL0G(1.-SQRT(BC0LAM*(RATI0-1.)/(C0LAM*
    2BETA*RATI0+1.))))
     XKBW=((16.*SQRT(BC0LAM)*(1./RATI0)/(BETA*CLAL1*(XLAM1+1.)*(B1/D1
    1-1.)*3.14159*(BC0LAM+1.)))))*(XKB1-XKB2-XKB3)
1CC0 XKBT=XKWB-XKTB
     D=D1
     IF(VXM-1.0) 2000,2000,2010
2000 IF(ISWP1-1  ) 2020,2020,2030
2020 IF(BAR-2.0) 2040,2050,2050
2040 XBCRWB=0.35-XLAM1*(0.35+17.885-SQRT(328.8782-(BAR-3.)**2))
     G0 T0 2080
2050 XBCRWB=0.35-0.1*XLAM1
     G0 T0 2080
2030 IF(BAR-2.0) 2060,2070,2070
2060 XCR1=SQRT(2029.5+(BAR-3.)**2)
     XBCRWB=((-44.5+XCR1)-XLAM1*(-44.5+XCR1+17.885-SQRT(328.8782-(BAR
    1-3.)**2)))
     G0 T0 2110
2070 XBCRWB=0.55-0.3*XLAM1
     G0 T0 2110
2080 IF(BAR-4.0) 2090,2100,2100
2090 XBCRBW=0.25-XLAM1*(32.125-SQRT(1032.02-(BAR-4.)**2))+(1.-XLAM1)*
    1AL0G(1.04+0.1*D/B1)*(-7.5+SQRT(72.25-(BAR-4.0)**2))
     G0 T0 2400
2100 XBCRBW=0.25+((1.-XLAM1)*AL0G(1.04+0.1*D/B1))
     G0 T0 2400
```

```
211C IF(BAR-4.0) 2120,2130,2130
212C XBCRBW=0.25+(1.-2.*XLAM1)*(32.125-SQRT(1032.02-(BAR-4.)**2))+
    1(1.-XLAM1)*ALOG(1.12+0.3*D/B1)*(-7.5+SQRT(72.25-(BAR-4.)**2))
     GO TO 2400
213C XBCRBW=0.25+(1.-XLAM1)*ALOG(1.12+0.3*D/B1)
     GO TO 2400
201C IF(ISWP1-1  ) 2140,2140,2150
214C IF(BAR-3.0) 2160,2170,2170
216C XBCRWB=-(9.235+25.*(1.-XLAM1))+SQRT((9.71+25.*(1.-XLAM1))**2-
    1(BAR-3.)**2)
     GO TO 2200
217C XBCRWB=0.005*BAR+0.46
     GO TO 2200
215C IF(BAR-3.) 2180,2190,2190
218C XBCRWB=0.675-XLAM1*(0.675+9.235-SQRT(94.1-(BAR-3.)**2))
     GO TO 2300
219C XBCRWB=0.005*BAR+0.46+0.2*(1.-XLAM1)
     GO TO 2300
220C BARLAM=BAR*(1.-XLAM1)*(1.+(1./BCOLAM))
     IF(BARLAM-4.0) 2210,2210,2220
221C IF(BAR-2.0) 2230,2240,2240
223C XBMID1 = ALOG(1.32 - 0.32*XLAM1)
2235 XBMID2=4.+(XBMID1**2)-((0.5+0.5139*(D/B1)*(1.17+XLAM1)*(1./(0.331
    1**(D/B1))))**2)
     XBMID3=2.*((XBMID1)-(0.5+0.5139*(D/B1)*(1.17+XLAM1)*(1./(0.331
    1**(D/B1))))
     XBMID=XBMID2/XBMID3
     XCMID=4.+(XBMID1-XBMID)**2
     XBCRBW=SQRT(XCMID-((BAR-2.)**2))+XBMID
     GO TO 2400
224C XBCRBW=0.5+0.25695*(D/B1)*(1./(0.331**(D/B1)))*BAR*(1.17+XLAM1)
     GO TO 2400
222C IF(IAFB) 2250,2250,2260
225C IF(RATIO-1.0) 2280,2280,2270
228C XBCRBW=0.67
     GO TO 2400
227C XBCRBW=-2.32+SQRT(8.9401-((1./RATIO)-1.)**2)
     GO TO 2400
226C XBCRBW=(0.429/RATIO)+0.5
     GO TO 2400
230C BARLAM=BAR*(1.-XLAM1)*(1.+(1./BCOLAM))
     IF(BARLAM-4.0) 2310,2310,2220
231C IF(BAR-2.0) 2320,2240,2240
232C XBMID1=ALOG(1.65-0.65*XLAM1)
     GO TO 2235
240C D=D1
     ARAT=BAR/BETA
     IF(ARAT-3.0) 20,20,21
  21 ARAT=3.0
  20 BDC=2.*(1.+XLAM1)**1.6*EXP(-.4*ARAT)
     IF(ARAT-1.0) 22,23,23
  23 BDC=BDC-0.25*(ARAT-1.0)
  22 CONTINUE
     RETURN
     END
```

TABLE 2

INPUT NOMENCLATURE*

AREA	arbitrary reference area, ft^2
BT	total tip-to-tip tail span including the missile body**
BW	total tip-to-tip wing span including the missile body
BW2	total tip-to-tip wing two span including the missile body
CLAMT	leading edge sweep angle of the tail***
CLAMW	leading edge sweep angle of the wing
CLAMW2	leading edge sweep angle of wing two
CROOTT	tail root chord
CROOTW	wing root chord
CROOTW2	wing two root chord
D	body diameter
HT	altitude in feet
IAFBT	afterbody constant for the tail 0 - no afterbody following the tail 1 - afterbody following the tail
IAFBW	afterbody constant for the wing 0 - no afterbody following the wing 1 - afterbody following the wing
IAFBW2	afterbody constant for wing two 0 - no afterbody following wing two 1 - afterbody following wing two
IAL	number of angles of attack
ICSC	control surface constant 1 - tail control 2 - wing control 3 - canard control
IDT	number of control surface deflection angles (must beat least one; if there is no control surface, IDT = 1, DELTA = 0.0)
IM	number of Mach numbers

TABLE 2

(continued)

INOSE	nose constant 1 - blunted ogive or cone 2 - pointed ogive 3 - pointed cone
ISWPT	sweep constant of tail 1 - unswept mid-chord 2 - unswept trailing edge
ISWPW	sweep constant of wing 1 - unswept mid-chord 2 - unswept trailing edge
ISWPW2	sweep constant of wing two 1 - unswept mid-chord 2 - unswept trailing edge
NBODY	number of configurations being run (a configuration is one complete data deck)
ST	exposed planform area of one pair of tail panels
SW	exposed planform area of one pair of wing panels
SW2	exposed planform area of one pair of wing two panels
TOVCT	thickness-to-chord ratio of the tail
TOVCW	thickness-to-chord ratio of the wing
TOVCW2	thickness-to-chord ratio of wing two
XAL	missile angle of attack (degrees)
XCG	missile center of gravity location as measured from the nose
XDT	control surface deflection angle (degrees)
XL	missile length
XLAMT	tip-to-root-chord ratio of the tail
XLAMW	tip-to-root-chord ratio of the wing
XLAMW2	tip-to-root-chord ratio of wing two
XLNOSE	length of the nose

TABLE 2

(continued)

XMACT	mean geometric chord of the tail
XMACW	mean geometric chord of the wing
XMACW2	mean geometric chord of wing two
XREF	arbitrary reference length
XTAIL	distance from the nose to the leading edge of the tail root chord
XVXM	missile flight Mach number
XWING	distance from the nose to the leading edge of the wing root chord
XWING2	distance from the nose to the leading edge of wing two root chord

* The control surface is defined as the tail regardless of the mode of control, and the fixed surface(s) is (are) always defined as the wing(s). See Figure 1.

** All linear dimensions are in feet.

***All angular dimensions are in degrees.

TABLE 3

PROGRAM INPUT FORMAT

1	Run Identification	Configuration Title and/or Number (1st 60 columns)								
2	Control Constants	ICSC (15)	INOSE (15)	IDT (15)	IM (15)	IAL (15)	NBODY (15)			
3	Wing Inputs	ISWPW (15)	IAFBW (15)	XLAMW (F10.5)	CLAMW (F10.5)	BW (F10.5)	CROOTW (F10.5)	SW (F10.5)	XMACW (F10.5)	XWING (F10.5)
4	Wing 2 Inputs	ISWPW2 (15)	IAFBW2 (15)	XLAMW2 (F10.5)	CLAMW2 (F10.5)	BW2 (F10.5)	CROOW2 (F10.5)	SW2 (F10.5)	XMACW2 (F10.5)	XWING2 (F10.5)
5	Tail Inputs	ISWPWT (15)	IAFBT (15)	XLAMT (F10.5)	CLAMT (F10.5)	BT (F10.5)	CROOTT (F10.5)	ST (F10.5)	XMACT (F10.5)	XTAIL (F10.5)
6	Miscellaneous Data	HT (F10.3)	D (F10.3)	XL (F10.3)	XLNOSE (F10.3)	XCG (F10.3)	AREA (F10.3)	XREF (F10.3)		
7	Miscellaneous Data	TOVCW (F10.3)	TOVCW2 (F10.3)	TOVCT (F10.3)						
8	Control Surface Deflection Angles	XDT (F5.1)	Any number of deflection angles up to 16 may be input.							
9	Missile Flight Mach Numbers	XVXM (F5.1)	Any number of Mach numbers up to 16 may be input.							
10	Missile Angles of Attack	XAL (F5.1)	Any number of angles of attack up to 48 may be input.							
11	Missile Angles of Attack	If this card is not required, leave out of data deck.								
12	Missile Angles of Attack	If this card is not required, leave out of data deck.								

TABLE 4

OUTPUT NOMENCLATURE

AL	missile angle of attack, degrees
CA	total axial force coefficient
CDTOT	total missile drag coefficient
CLALT	C_{L_α} of the tail
CLALW	C_{L_α} of the wing
CLALW2	C_{L_α} of wing two
CLB	body lift coefficient
CLI	lift loss due to downwash
CLTOT	total missile lift coefficient
CLTT	tail lift coefficient
CLWT	wing lift coefficient
CM	total pitching moment coefficient about the missile center of gravity
CN	total normal force coefficient
CNB	body normal force coefficient
CNT	tail normal force coefficient
CNTD	tail normal force coefficient due to control surface deflection
CNW	wing normal force coefficient
DELTA	control surface deflection angle, degrees
VXM	missile flight Mach number
XCPB	body center of pressure location as measured from the nose, feet
XCPT	tail center of pressure location as measured from the nose, feet

$CMB = CNB(XCG - XCPB)$

TABLE 4

(continued)

XCPW	wing center of pressure location as measured from the nose, feet
XCP2	total missile center of pressure location as measured from the nose, feet

XCP = XCG − XCP2

INITIAL DISTRIBUTION

Copy	
1	AIR 3033
1	AIR 320
1	AIR 360
1	AIR 5301
4	AIR 604
1	NWC 3013
1	NWC 30101
1	NWC 406
1	NWC 4063
1	NWC 4506
12	DDC

1 William Millard
Division 9324
Sandia Laboratories
Albuquerque, New Mexico 87115

1 Alvin Spector
Naval Air Development Center
Code AMFC-2
Warminster, Pennsylvania 18974

1 John Fiddler
Martin-Marietta Corp.
Orlando Division
Sand Lake Rd.
Mail Pt. 326
Orlando, Florida 32801

1 David N. Bixler
Missile Dynamics Division
Code 323
Naval Ordnance Laboratory
White Oak, Maryland 20910

1 R. A. Deep
U.S. Army Missile Command
Redstone Arsenal, Alabama 35809

1 Girard Rapp
Raytheon Company
Box 550
Bedford, Massachussettes 01730

1 Glen L. Martin
% Mr. Charles J. Dragowitz
Grumman Aerospace Corp.
South Oyster Bay Road
Bethpage, New York 11714

1 Terry Martin
NAVAIR 530142B

1 Frank J. Kranz
Hughes Aircraft
Missile Systems Division
Mail Station X-16
Canoga Park, California 91304

1 John G. Gebhard
Fluid Mechanics Department
Aerospace Corporation
P.O. Box 1308
San Bernadino, California 92402

1 Barry Clark
GBJ
Naval Weapons Laboratory
Dahlgren, Virginia

1 Wallace Sawyer
Mail Stop 413
Langley Research Center
Hampton, Virginia 23365

DOCUMENT CONTROL DATA - R & D

(Security classification of title, body of abstract and indexing annotation must be entered when the overall report is classified)

1 ORIGINATING ACTIVITY *(Corporate author)*
Aviation Department
Naval Ship Research and Development Center
Washington, D.C. 20034

2a. REPORT SECURITY CLASSIFICATION
UNCLASSIFIED

2b. GROUP

3 REPORT TITLE

A METHOD FOR PREDICTING THE STATIC AERODYNAMIC CHARACTERISTICS OF TYPICAL MISSILE CONFIGURATIONS FOR ANGLES OF ATTACK TO 180 DEGREES

4. DESCRIPTIVE NOTES *(Type of report and inclusive dates)*
Research and Development Report

5. AUTHOR(S) *(First name, middle initial, last name)*
Bernard F. Saffell, Jr., Millard L. Howard, and Eugene N. Brooks, Jr.

6. REPORT DATE
March 1971

7a. TOTAL NO. OF PAGES
99

7b. NO. OF REFS
14

8a. CONTRACT OR GRANT NO.

b. PROJECT NO. WW 16-25

c. Task 10501

d. NSRDC 1-651-106-01

9a. ORIGINATOR'S REPORT NUMBER(S)
Aero Report 1168

9b. OTHER REPORT NO(S) *(Any other numbers that may be assigned this report)*
Report 3645

10. DISTRIBUTION STATEMENT

Approved for public release; distribution unlimited

11. SUPPLEMENTARY NOTES

12. SPONSORING MILITARY ACTIVITY
Commander, Naval Air Systems Command
Navy Department
Washington, D.C. 20360

13. ABSTRACT

A method for predicting the static, longitudinal aerodynamic characteristics of typical missile configurations at zero roll angle (i.e., in a plus configuration) has been developed and programmed for use on the IBM 7090 digital computer. It can be applied throughout the subsonic, transonic, and supersonic speed regimes to slender bodies of revolution or to nose-cylinder body combinations with low aspect-ratio lifting surfaces. The aerodynamic characteristics can be computed for missile configurations operating at angles of attack up to 180 degrees. The effect of control surface deflections for all modes of aerodynamic control are taken into account by this method. The method is based on well-known linear, nonlinear crossflow and slender body theories with empirical modifications to provide the high angle of attack capability. Comparisons of the theory with experimental data are presented to demonstrate the accuracy of the method.

Security Classification

14. KEY WORDS	LINK A		LINK B		LINK C	
	ROLE	WT	ROLE	WT	ROLE	WT
Air-to-Air Missiles						
Aerodynamic Prediction Computer Program						
Control Surface Deflections						
Drag						
High Angle of Attack						
Lift						
Longitudinal Aerodynamics						
Missile Aerodynamics						
Pitching Moment						
Stability and Control						
Static Aerodynamics						